Structure-function analysis of pancreatic ATP-sensitive potassium channels

by

Yu-Wen Lin

A DISSERTATION

Presented to the Department of Physiology and Pharmacology
and the Oregon Health & Science University
School of Medicine
in partial fulfillment of
the requirements for the degree of
Doctor of Philosophy

March, 2006

School of Medicine

Oregon Health & Science University

CERTIFICATE OF APPROVAL

This is certify that the Ph.D. dissertation titled

"Structure-function analysis of pancreatic ATP-sensitive potassium channels"

by

Yu-Wen Lin

has been approved

[redacted]

Mentor / Advisor

[redacted]

Member

[redacted]

Member

[redacted]

Member

[redacted]

Member

TABLE of CONTENTS

Acknowledgments

I am very grateful to several people for helping me in completing my PhD. This is not an easy task, especially for me as a foreigner. Without my advisor Show-Ling, I could not have done this. As a graduate student in her lab, I learned a lot about writing papers and presentation skills, in addition to experimental design. Of course, I am still in the process of learning and that is a life long process of adventure. I also want to acknowledge all of the people that have worked in her lab: Annie, Taiping, Adam, Grit, Shu, Satoko, Beth, Chia-Wei, Etienne, Feifei, Jill, Malini, Emily and Jessie. They have been such wonderful labmates and have made my days at OHSU quite happy. In addition, I want to acknowledge my IBMS classmates: Brenda, Teresa, Catherine, Daisy and Jeff. We went through the required courses and qualifying exams together and they have been really great/supportive classmates. Now in 2006 we all have our thesis defenses within a few months of each other. Of course I could never leave out my family - my parents, my sister and brother for their strong support. Lastly, I want to acknowledge my church friends and my spiritual mentor, Pastor Joshua for all that they have taught me, as well as their company, which has helped me grow immensely.

ABSTRACT

The goal of this dissertation is to link the function of ATP sensitive potassium (K_{ATP}) channels to its structure. When mutated, these proteins alter normal channel function by causing gating and/or trafficking defects. Through investigating the molecular mechanisms of these mutations, we improve our understanding of the structure- function relationship of pancreatic K_{ATP} channels and such knowledge will aid the development of drugs that effectively target these channels to manage islet dysfunction.

Chapter one is an introduction that provides the background of this dissertation about K_{ATP} channels in terms of their physiological function, pharmacology, molecular structure, trafficking regulation, gating regulation and diseases caused by channel dysfunction.

Chapter two contains work that identifies an ion pair in the intracellular C-terminus of the inwardly rectifying potassium channel (Kir6.2) that is important for gating. Mutation of either residue of this ion pair (E229 and R314) to alanine induces fast current decay due to the disruption of the salt bridge. We demonstrate that this ion pair forms by residues from two adjacent Kir6.2 subunits. We propose a model in which the E229/R314 intersubunit ion pairs contribute to a structural framework that facilitates the ability of other positively charged residues to interact with membrane phospholipids and thus are required for normal channel gating.

In chapter three, we report the identification of a novel *KCNJ11* mutation associated with the disease congenital hyperinsulinism that renders a missense mutation, F55L, in the Kir6.2 protein. Mutant channels reconstituted in COS cells

exhibited wild-type like surface expression level and normal sensitivity to ATP, MgADP, and diazoxide. However, the intrinsic open probability of the mutant channel was greatly reduced, by ~10-fold. This low open probability defect could be reversed by application of phosphatidylinositol 4,5-bisphosphates or oleoyl CoA to the cytoplasmic face of the channel, indicating that reduced channel response to membrane phospholipids and/or long chain acyl CoAs underlies the low intrinsic open probability in the mutant. Our findings reveal a novel molecular mechanism for loss of K_{ATP} channel function and congenital hyperinsulinism, and support the importance of phospholipids and/or long chain acyl CoAs in setting the physiological activity of β-cell K_{ATP} channels.

Chapter four presents our findings that some permanent neonatal diabetes mellitus (PNDM) mutations not only reduce channel ATP sensitivity but also impair channel expression at the cell surface to varying degrees. Comparison of the various PNDM mutations in their effects on channel ATP sensitivity, expression, as well as disease phenotype suggests that both channel gating defect and expression level may play a role in determining disease severity. Interestingly, sulfonylureas significantly increase surface expression of a number of PNDM mutant channels, raising new questions about the use of these drugs in treatment of PNDM caused by Kir6.2 mutations.

In chapter five, unpublished data investigating the molecular consequences of novel Kir6.2 mutations identified in Congenital Hyperinsulinism are presented. Finally, I will discuss future experiments that will address the questions raised by research

presented in this dissertation to further advance our understanding of the structure-function relationship of K_{ATP} channels.

Chapter 1

Introduction

The physiological roles of K_{ATP} channels

ATP sensitive potassium (K_{ATP}) channels are widely distributed in various tissues and cell types where they couple cell metabolism to cell excitability and thus play important physiological roles. For example, in pancreatic beta cells, K_{ATP} channels sense changes in blood glucose concentration and regulate insulin secretion (Ashcroft et al., 1984, 1988). When the blood glucose concentration is high, the ATP to ADP ratio rises (Figure 1). ATP inhibits channel activity but MgADP stimulates it; therefore, the high ATP/ADP ratio closes K_{ATP} channels and subsequently depolarizes the membrane potential. This depolarization opens the voltage dependent calcium channels and results in the influx of calcium ions. When calcium ions enter pancreatic beta cells, insulin is secreted. In contrast, when the blood glucose concentration is low, the K_{ATP} channel remains open and insulin is not secreted.

In addition, K_{ATP} channels are important for cytoprotection in the cardiovascular system. Opening of cardiac K_{ATP} channels in response to ischemic insult results in shortened duration of the action potential by hyperpolarizing the cell membrane, thus preconditioning the tissue against subsequent ischemic injuries (Barbenko AP., 1992, Kantor et al., 1990, Faivre JF., 1990). Similarly, in arterial smooth muscle and cerebral arteries, K_{ATP} channels regulate vessel tones. Opening of K_{ATP} channels contributes to hypoxia-induced vasodilation during ischemic or hypoxic conditions (Daut J., 1990). In fact K_{ATP} channels are major targets for endogenous and pharmacological vasodilators to regulate vessel tones in smooth muscle.

Another example illustrating the importance of K_{ATP} channels is the neuroprotective role it plays. Because the brain requires continuous oxygen and glucose

supply to maintain its function, deprivation of energy source under stroke, ischemia or respiratory failure leads to cessation of cerebral activity and loss of consciousness and ultimately to generalized seizure. It has bee shown that K_{ATP} channels in substantia nigra pars reticulata (SNr) play a protective role in brain hypoxia by suppressing seizure propagation (Yamada K. et al, 2001; Yamada K. et al, 2005). Yamada et al shows that mutant mice lacking Kir6.2 subunit (Kir6.2 knockout mice) are more susceptible to generalized seizures after brief hypoxia compared to normal mice. Their data suggest the presence of K_{ATP} channels in SNr neurons might exert a depressant effect on the neuronal activity during hypoxia and maybe be involved in the protection mechanism against generalized seizures. Additionally, Miki et al demonstrated that K_{ATP} channels in ventromedial hypothalamus (VMH) are essential for the maintenance of glucose homeostasis by studying the Kir6.2 knockout mice. In their study, Kir6.2 knockout mice exhibited a severe defect in glucagon secretion in response to systematic hypoglycemia suggesting that K_{ATP} channels play a key role in glucose sensing in VMH glucose response neurons (Miki T. et al, 2001).

The subunits and the isoforms of K_{ATP} channels

K_{ATP} channels are octameric complexes, each assembled from four inwardly rectifying potassium channel (Kir6.x) subunits and four sulfonylurea receptor (SUR.x) subunits (Aguilar-Bryan L. and Bryan J., 1999, Ashcroft FM. and Gribble FM., 1998, Barbenko AP. et al, 1998a; Loussouarn G. et al., 2002). Kir6 serves as the pore-forming subunit while SUR plays a key role in regulating both channel trafficking and gating. Both SUR and Kir6 subunits are required for proper channel function (Zerangue, N.,

1998). There are several isoforms of SUR, the major ones being SUR1, SUR2A and SUR2B, and two isoforms of Kir6, Kir6.1 and 6.2 (Ashcroft FM., 1988, Aguilar-Bryan L. et al., 1998, Aguilar-Bryan L. and Bryan J. 1999; Babenko AP. et al., 1998a; Chutkow WA. et al., 1996; Inagaki N. and Seino S., 1998; Quayle JM. et al., 1997). The different isoforms of SUR and Kir6 proteins combine to generate subtypes of K_{ATP} channels with unique properties. The SUR2A and Kir6.2 form the cardiac sarcolemmal K_{ATP} channel, SUR2B and Kir6.1 form the vascular smooth muscle (VSM) channel, and SUR1 together with Kir6.2 form the pancreatic/neuronal channel. (See Table I)

Table I

Tissue	**Kir isoform**	**SUR isoform**
Pancreas	Kir6.2	SUR1
Cardiomyocytes	Kir6.2	SUR2A
Smooth muscle	Kir6.1	SUR2B
Brain	Kir6.2	SUR1

So far two SUR genes have been identified in rodents and humans: SUR1 (ABCC8) and SUR2 (ABCC9) showing 70% sequence identity. SUR1 has 1582 amino acids and higher affinity for the sulfonylureas. SUR2 gives rise to two major splice variants, SUR2A and SUR2B, which have lower affinity to sulfonylureas (Aguliar

Bryan L. et al., 1995, Inagaki N., et al, 1996). SUR2A and SUR2B differ only in their last forty-two amino acids.

SURs belong to the ATP binding cassette (ABC) transporter superfamily and mutations in various members of this superfamily have been associated with human genetic disorders including cystic fibrosis, and congenital hyperinsulinism etc. Among the ABC transporter superfamily, SURs have the greatest similarity to multidrug resistance related proteins (MRP) in that N-terminal transmembrane domain called TMD0 precedes the core ABC transporter structure consisting of two transmembrane domains (TMD1 and TMD2) and two cytoplasmic nucleotide-binding domains (NBF1 and NBF2).

SUR has 17 transmembrane segments (TM) distributed into three transmembrane domains (TMDs) with TMD0, TMD1 and TMD2 containing five, six and six TMs respectively. The two nucleotide-binding folds (NBFs) are located in the cytoplasmic loop between TMD1 and TMD2 and the C-terminus, respectively. (Figure 2A and Figure 3). The NBF domains, just like other ABC transporters, contain the Walker A (-**GXXGXGKS/T**-, where X is any amino acid) and Walker B (-YYYYD-, where Y is a hydrophobic amino acid) consensus nucleotide binding motifs and a conserved -LSGGQ- sequence (Walker JE. et al., 1982).

Currently two Kir6 genes have been identified and they are designated as Kir6.1 and Kir6.2. The Kir6.1 cDNA was cloned originally by homology screening using a fragment of the G-protein activated inwardly rectifying potassium channel Kir3.4 (Kubo Y. et al., 1993; Inagaki N. et al., 1996). The human gene encoding Kir6.1 is designated as KCNJ8 and the encoded 424 amino acids protein shares 98% identity

with rat Kir6.1. KCNJ8 gene was mapped to chromosome 12p11.23, the same chromosome where the SUR2 gene ABCC9 is located (Inagaki N. et al., 1996). The Kir6.2 cDNA was cloned by homology screening with Kir6.1 and it contains a 390-amino acid protein (Inagaki N., et al., 1995). The human Kir6.2 gene is designated as KCNJ11 and was mapped to chromosome11 at 11p15.1, a region close to where SUR1 was mapped (Inagaki N. et al., 1995; Ayyagari R. et al., 1996).

The Kir6 belongs to the inwardly rectifying channels that pass potassium better in the inward direction than the outward direction. The mechanism of the inward rectification is due to blockade of the permeation pathway by polyamines and/or magnesium at positive voltages, as illustrated in Figure 4 (Doupnik CA. et al, 1995). However Kir6.1 and Kir6.2 are weakly rectifying members of this superfamily. The degree of rectification is dependent on the amino acids in the ion conductance region and a mutation (N160D) in the second transmembrane domain (TM2) converts the weakly rectifying Kir6.2 channel into a strong inwardly rectifier. The mutant channel tagged with this N160D mutation have been used to study the heterozygous expression level and the stoichiometry of ATP gating of the channel, which will be further discussed in chapter 4.

The membrane topology of Kir6 reveals two transmembrane domains connected with a pore loop flip into the plasma membrane (Chutkow WA. et al., 1996, Barbenko AP., 1998). Recently, two homologous structures, G protein activated inwardly rectifying potassium channel (GIRK1) and a bacterial inwardly rectifying potassium channel (KirBac1.1), have been resolved; these structures provide a model template for

Kir6 (Nishida M. and Mackinnon R., 2002; Kuo A. et al., 2003) (Figure 5 and Figure 6). The features of these Kir structures will be shown in detail later.

Trafficking regulation of K_{ATP} channels

Unlike other members in the Kir family, Kir6 subfamily requires SUR subunit to form a functional channel (Inagaki N. et al., 1995) Zerangue N. et al. showed that full assembly of Kir6.2 subunit and SUR1 as octomer is essential for K_{ATP} channel surface expression (Zerangue N. et al., 1999). Both Kir6.2 and SUR1 contain an endoplasmic reticulum (ER) retention/retrieval sequence (RKR). This RKR sequence is required for preventing surface expression. Expression of Kir6.2 alone without SUR1 does not generate channel activity, for the RKR sequence is exposed and the protein is retained in the ER. However, expression of Kir6.2 lacking RKR sequence (for example, a C-terminal deletion mutant KirΔC35) results in basal potassium current. It has been proposed that the fully coassembled octomer masks the RKR sequence in both SUR1 and Kir6.2 and is therefore able to exit the ER and traffic to cell surface (see Figure 2B). Their studies explain how assembly of an ion channel complex is coupled to intracellular trafficking and thus demonstrate the role of SUR1 in regulating the surface expression of Kir6.2 subunits.

Physiological gating of K_{ATP} channels: the role of Kir6.2

The activity of K_{ATP} channels is governed by a diverse group of physiological molecules, including the intracellular nucleotides ATP and ADP, membrane

phosphoinositides such as phosphatidylinositol-4,5-bisphosphate PIP_2 and the lipid metabolite, long chain acyl CoA. (Hilgemann DW. and Ball R., 1996; Fan Z. and Makielski JC., 1997; Baukrowitz T. et al., 1998; Branstrom, R. et al., 1998; 2004; Gribble FM. et al, 1998; Shyng SL. and Nichols CG, 1998 ; Enkvetchakul, D et al., 2000; Schulze D. et al., 2003). The defining feature of K_{ATP} channels is their inhibition by intracellular ATP. It is now clear that this inhibition occurs as a result of ATP binding to the pore-forming Kir6.2 subunit, as channels formed by Kir6.2ΔC35 in the absence of SUR1 are still sensitive to ATP inhibition. Much mutagenesis work has been done to identify Kir6.2 residues that are involved in controlling ATP sensitivity (Shyng SL.et al., 1997, 2000; Tucker SJ. et al., 1997, 1998; Shyng SL. and Nichols CG., 1998; Trapp S. et al., 1998; Koster JC. et al., 1999; Proks P.et al., 1999; Tanabe K. et al., 1999; Enkvetchakul D. et al., 2000; Cukras CA. et al., 2002a,b). Mutations of most of these residues resulted in altered apparent channel ATP sensitivity indirectly by affecting the intrinsic open probability of the channel. However, a few residues including R50 located in the N-terminus and I182, K185, R201and G334 in the C-terminus are likely involved in ATP binding, as mutations in these residues alter channel ATP sensitivity without changing the intrinsic channel open probability (Cukras CA. et al., 2002a, 2002b; Drain P. et al., 1998; Koster JC. et al., 1999; Li DP. et al., 2000; Proks P. et al., 1999; Tucker SJ. et al., 1997; 1998).

Mapping the corresponding residues of ATP binding sites to the GIRK-NC structure (Nishida M. and MacKinnon R, 2002) reveals that these residues are all located in a single patch on the external surface of each subunit (Figure 7) (Enkvetchakul D. and Nichols CG., 2003). Using homology modeling and ligand-

docking, Antcliff JF. et al. constructed a model of the ATP binding pockets in the Kir6.2 tetramer and found this model to be consistent with the functional data obtained from mutagenesis studies (See Figure 8). Interestingly, the ATP binding site appears to lie in between two adjacent Kir6.2 subunits (Antcliff JF. et al., 2005).

In addition to ATP regulation, K_{ATP} channels are stimulated by negatively charged phospholipids such as PIP_2, which also activate other Kir channels (Hilgemann DW. and Ball R., 1996; Fan Z. and Makielski JC., 1997; Liou HH. et al., 1999; Zhang H. et al., 1999; Lopes CM. et al., 2002). Evidence suggests that PIP_2 stimulates channel activity by binding to Kir6.2. Many studies have sought to localize the PIP_2 binding site on Kir6.2 and several PIP_2-interacting residues such as R54, R176, R177 and R206 have been proposed (Baukrowitz T. et al., 1998; Shyng SL. and Nichols CG, 1998; Shyng SL. et al., 2000; Cukras CA. et al., 2002a,b; Schulze D. et al., 2003). When mapped onto the GIRK structure, these PIP_2 binding sites (residues in red in Figure 7) are close to the membrane, directly opposing lipid headgroups. Importantly, PIP_2 has also been shown to antagonize the inhibitory effect of ATP on Kir6.2 channels (Baukrowitz T. et al., 1998; Shyng SL. and Nichols CG., 1998; Xie Yet al., 1999a, 1999b). It has been proposed that modulation of K_{ATP} channels by PIP_2 serves as an important mechanism to bring the ATP sensitivity of the channel into the physiological concentration range of ATP (Ashcroft FM, 1998; Shyng SL. and Nichols CG., 1998).

Moreover, long chain acyl CoA (LC CoA) has been proposed to activate pancreatic and cardiac K_{ATP} channels via similar mechanisms as PIP_2. Studies have shown that the mutations (R54E/Q, R176A) of Kir6.2 that greatly reduce PIP2 modulation of ATP sensitivity likewise reduce the modulation by long chain acyl CoA

(Schulze D et al., 2003). The fact that PIP_2 and LC CoA appear to share the same binding residues is not surprising because LC CoA and PIP_2 do have similar structures (Figure 9). Though both LC CoA and PIP_2 activate K_{ATP} channels and reduce the ATP sensitivity, the potency and reversibility of the effect is somehow quite different. By comparing the effect of the same concentration of exogenous oleoyl CoA(C18:1) and PIP_2 on the same patch of mutant channel, we found oleoyl CoA has greater potency to activate the mutant channels but it is washed off more easily compared to PIP_2 (See Figure 25C in chapter 3). Our data suggest that PIP_2 might have a long-term effect on K_{ATP} channel regulation while long chain acyl CoA has a short-term or rapid effect on channel activity.

As acyl CoA level is elevated in obese and type II diabetic individuals, it has been proposed that this elevation may contribute to reduced beta cell excitability by activating the pancreatic K_{ATP} channels, thereby impairing glucose-stimulated insulin secretion (Salmeron J. et al., 2001). Riedel et al have shown that saturated and trans fatty acids with longer chains exert a larger stimulatory effect on K_{ATP} channels and suggested that dietary fat composition may determine the severity of impaired glucose-stimulated insulin secretion via differential activation of beta-cell K_{ATP} channels. (Riedel MJ. and Light PE., 2005)

Physiological gating of K_{ATP} channels: the role of SUR1

SUR1 not only regulates the trafficking of Kir6.2 subunit, it also controls the gating of Kir6.2 subunit. As mentioned before, deletion of Kir6.2 RKR motif (KirΔC35 or KirΔC26) or mutation of this ER retention signal ($Kir6.2_{AAA}$) enables expression of

Kir6.2 tetramers alone at the cell surface. However, the gating kinetics of this channel is altered. The wild-type (WT) K_{ATP} channel activity occurs in bursts and interburst closures. Within the bursts there are brief openings and closings (flickering), which is referred as fast gating. These active burst episodes are separated by long-lived inactive interburst intervals and the transitions between a burst of activity and interburst closure is referred as slow gating (Alekseev AE. et al., 1997; Ashcroft FM. et al., 1984; Babenko AP. et al., 1999a, 1999b; Drain P. et al., 1998, 2000; Nichols CG et al., 1991; Trapp S. et al., 1998).(Figure 10A). In contrast, the KirΔC26 or $Kir6.2_{AAA}$ channels display a non-bursting gating kinetics in which the long-lived inactive interburst intervals are gone and only brief closing/opening events remain (Figure 10B). The open probability of KirΔC35 or $Kir6.2_{AAA}$ channels is only 1/10 that of the WT Kir6.2 coexpressed with SUR1 subunit. These findings indicate that the SUR1 subunit facilitates the opening of the channel. In addition, the SUR subunit hypersensitizes the channel to the ATP inhibition. The ATP sensitivity of the KirΔC35 channel is about 10 to 30 folds lower that that of KirΔC35 +SUR1 channels and WT channels

Furthermore, SUR modulates channel activity via its ATPase activity. SUR contains two cytoplasmic nucleotide binding domains and functions as an ATPase; the enzymatic activity of SUR is coupled to opening and closing of the channel. In a prehydrolytic conformation when MgATP is bound, the channel tends to be closed, whereas in a posthydrolytic conformation when MgADP is bound, the channel tends to be open (Zingman LV. et al., 2001). Together with the inhibitory effect of ATP on Kir6 subunit, the stimulatory effect of MgADP via the SUR subunit determine channel activity in response to altered ATP and ADP concentrations: an increase in the

intracellular ATP/ADP ratio has a net effect of reducing channel activity while a decrease in the ATP/ADP ratio has a net effect of stimulating channel activity.

Pharmacology of K_{ATP} channels

K_{ATP} channels are the targets of a number of pharmacological reagents, which modulate channel activity primarily through interactions with the SUR subunit. These pharmacological agents have been widely used in the treatment of insulin secretion disorders.

Sulfonylureas drugs, such as glibenclamide and tolbutamide, inhibit channel activity, whereas potassium channel openers, a chemically diverse group of molecules including cromakalim, pinacidil, nicorandil and diazoxide, stimulate channel activity. The sensitivities and specificities of K_{ATP} channels towards these reagents are dictated by the SUR isoform that constitutes the channel. Thus, the pancreatic channel containing the SUR1 isoform is blocked with high affinity by sulfonylureas (Gribble FM. and Reimann F., 2002) and opened by only one potassium channel opener, diazoxide (D'Hahan N. et al., 1999). In comparison, the cardiac and vascular smooth muscle channels containing the SUR2A and SUR2B isoforms, respectively, are less sensitive to sulfonylurea inhibition and can be stimulated by a full range of potassium channel openers (Babenko AP. et al., 1998b; D'Hahan N. et al., 1999; Inagaki N. et al., 1995; Inagaki N. et al., 1996; Isomoto S. et al., 1996; Quayle JM. et al., 1997). These pharmacological reagents are useful for distinguishing the subtypes of K_{ATP} channels in native tissues; for example, both the SUR1and SUR2B containing K_{ATP} channels could be activated by diazoxide whereas the SUR2A containing channels could not. They

also have clinical application; for example, sulfonylurea drugs are commonly used to treat type II Diabetes patients to stimulate their insulin secretion. Although potassium channel openers such as diazoxide is effective for treating conditions such as hypertension, ischemia and certain cases of hyperinsulinism as they can down regulate cell excitability, clinical use of these drugs has been limited by insufficient tissue specificity and somewhat low affinity, a situation that can only be improved with a better understanding of the structural mechanisms by which these drugs interact with, and open, the channel. Further study of the channel structure, pharmacological regulation and tissue specific distribution of the K_{ATP} channels will help to solve these problems (Lawson K., 2000).

The molecular structure of K_{ATP} channels

So far the crystal structure of Kir6 has not been determined. However, several crystallized potassium channels including **KcsA** (Doyle DA. et al, 1998), **MthK** (Jiang Y. et al., 2002), **mGIRK1** (Nishida M. and Mackinnon R., 2002), **KirBac1.1**. (Kuo A. et al., 2003), **Kir2.1$_L$ and Kir3.1$_S$** (Pegan S. et al., 2005) provide knowledge basis for our understanding of two-transmembrane segment potassium channels. KcsA is the first crystallized channel and it can be divided into five regions, outer helix (TM1), turret, pore helix, selectivity filter and inner helix (TM2). These regions are conserved among all of the potassium channel family. As mentioned earlier, GIRK1 and KirBac1.1 are the two homologous Kir structures that had been resolved and these structures provide a model toward understanding the configuration and function of Kir6 subunits (Figure 5 and Figure 6). The GIRK structure is the first revealed mammalian potassium channel

and it contains only cytoplasmic domain with linked N- and C termini from mGIRK1 but lacks its tramsmembrane domain. The crystal structure in a single subunit shows that the C-terminal segments (Figure 5A green part) form a globular, mainly β sheet protein (βA through βN) with a protruding α helix (αA). The N terminus (Figure 5A red part) interacts with the C terminus through a short parallel β sheet formed between βA and βM. This structure forms a tetramer of identical subunits with cyclic 4-fold symmetry with large interface between adjacent subunits (Figure 5B and 5C). Additionally, the N terminus forms part of this interface by running in a groove located between adjacent C-terminal domains. Though mGIRK1 is missing its transmembrane domain as an intact channel protein, this structure provides a molecular basis for the inwardly rectifying potassium channel family and improves our understanding of the specified cytoplasmic domain of the Kir channels.

A year later, Doyle's group crystallized a full-length prokaryotic Kir channel, KirBac1.1. (Kuo A. et al., 2003) This structure is divided into five regions. On the extracellular side is the selectivity filter followed by a cavity, gate, flexible linkers and cytoplasmic vestibule (Illustrated in Figure 6A). Interestingly, the transmembrane section displays four-fold symmetry and the intracellular domains are in a two-fold arrangement. This structure also reveals a unique structure, slide helix, between N terminus and the first transmembrane domain (TM1). This amphipathic slide helix runs parallel with the membrane/cytoplasmic interface and is hypothesized to play a central role to couple ligand binding to channel gating (Figure 6B). It is proposed that the slide helix moves laterally, resulting in displacement of the M1 helix, which in turn allows room for the M2 helix to bend and the pore to open during channel gating (Xiao J. et al,

2003). Interestingly, the N-terminal slide helix from one subunit is connected to the C-terminal domain of an adjacent subunit through an intersubunit N- and C-terminal domain interaction mediated by two short beta strands each from the two neighboring subunits (see Figure 6B). These structural connections raise the possibility that subunit-subunit interactions may be key components that coordinate the different moving parts of the channel during gating. Regardless of the differences, these structures are invaluable in guiding future structure-functional studies to understand the details of how gating occurs in the different Kir channels.

Similarly, the molecular structure of SUR is not available yet but the NBD structures of several prokaryotic ABC proteins have been solved (Diederichs K. et al., 2000; Gauder R. & Wileyn DC., 2001; Hung LW. et al., 1998; Karpowich N. et al., 2001; Yuan YR. et al., 2001). Functional studies of both eukaryotic and bacterial ABC proteins have provided evidence that the two NBDs of ABC proteins interact and form a necleotide-sandwich dimer, with the signature sequence (linker) of one NBD monomer located close to the Walker A and Walker B motifs of the other NBD (Kerr, ID., 2002; Smith PC. et al., 2002).

In understanding the SUR1 structure in terms of the NBF domain, Campbell et al. constructed a homology-based model of the NBD dimer of SUR1 (see Figure 3)(Campbell JD. et al., 2003). It will be interesting to know whether the binding of MgATP/MgADP at the nucleotide-binding site induce a conformational change at this proposed NBD dimer and subsequently regulate the Kir6.2 gating. If so, does binding of MgADP/MgATP to the nucleotide-binding site promote or release the interaction of the NBD dimer to activate the K_{ATP} channels? This question is subject to further functional

studies. To investigate the above question, the relationship between channel activation and the interaction of the two NBDs could be tested by cross-linking two designated cysteine residues with various cross linkers or oxidizing reagents. Such approach will facilitate our comprehension of the SUR regulation by Mg-nucleotide and some pilot work towards this goal will be described in chapter 5.

To date most studies concerning K_{ATP} channel structure focus on understanding the molecular structure of Kir subunit and SUR NBD domain separately. However, the functional K_{ATP} channel is an octomeric complex containing both SUR and Kir subunits. Without fully illustrating the structures of both channel subunits, it is hard to completely understand the real channel conformation under physiological conditions. For example, the physical coupling between SUR and Kir subunits might play a key role in channel gating. Recently Mikhailov MV. et al. reported a K_{ATP} channel structure of a fusion protein consisting of SUR1 linked via its C-terminus to the N-terminus of Kir6.2 using electron microscopy (EM) in combination with molecular modeling (see Figure 11). This structure contains both channel subunits and provides an exciting picture for understanding the channel structure in an octomeric complex. Moreover, this simulated structure shows a narrow cleft located between adjacent SUR1 subunits and this cleft likely provides a potential route for ATP access, explaining how ATP transverses the SUR subunit to bind to the Kir6 subunit (Figure 12).

Gating mechanisms of K_{ATP} channels

The gating behavior of K_{ATP} channels is very complex. Even in the absence of ATP, single-channel analysis of the WT K_{ATP} channel reveals a bursting activity

separated by long-time interburst closures and intraburst events consisting of predominantly short openings and closings (see Figure 10A)(Alekseev AE. et al., 1998; Drain P. et al., 1998; Fan Z. and Makielski JC., 1999; Enkvetchakul D. et al., 2000, 2001). What is the structural basis responsible for this bursting behavior? Is the gate controlling the transitions between bursts and interburst closures (the slow gate) the same as the one modulating the flickering activity (fast gate)?

So far two locations for the gates have been proposed: the selectivity filter gate and the bundle-crossing gate. Proks et al have hypothesized a two-gate model for K_{ATP} channel gating: the upper gate, which is formed by the selectivity filter, governs the intraburst kinetics while the lower gate (bundle-crossing gate) regulates the long interburst closings. This model was based on the data that mutations near the bundle crossing affect long time closures without substantially affecting the flickering while mutations of residues near the selectivity filter disrupts the fast gating without affecting slow gating (Trapp S., et al., 1998; Tucker SJ. et al., 1998; Proks P. et al., 2001). Together, these results indicate the upper gate regulates fast gating and the lower gate is responsible for slow gating (See Figure 13). However, where is the ligand sensitive gate that is closed by inhibitory ATP and is opened by binding to PIP_2, upper gate or the lower gate? Because most K_{ATP} channel modulators like ATP, MgADP and sulfonylurea primarily affect slow gating by dramatically perturbing the burst duration but not the flickering kinetics, it was postulated that the ligand-sensitive gate is located in the bundle crossing. However, there are conflicting views to this question.

Phillips et al. proposed the lower gate as the ATP-sensing gate based on the data that the rate of modifying reagents interacting with engineered cysteines above the

bundle crossing is slower in the ATP closed state (Phillips LR. et al., 2003). In contrast, a study by Proks et al. later suggests that the ligand-sensitive gate (ATP-inhibition gate in this case) of the Kir6.2 is located within the selective filter by probing the blockade by internal barium ions (Proks P. et al., 2003). The conclusion is similar to that made for the ligand-sensitive gate of Cyclic Nucleotide Gated channel and PIP_2 activation gate of Kir2.1 (Flynn GE. and Zagotta WN., 2001; Xiao J. et al., 2003). These studies suggest that gating and permeation maybe closely coupled. Still the conflicting conclusions reached from different studies will need to be resolved with more experimental data.

Although these studies mentioned above did enhance our comprehension of the structural basis for channel gating by the physiological molecules such as PIP_2 and ATP, our knowledge toward the tertiary and quaternary structures that mediate channel gating upon ligand binding is limited. For example, the subunit-subunit interaction between Kir tetramers and SUR-Kir6 octomers in relation to channel gating remain to be elucidated. A previous study by Shyng et al. has shown that mutation of three positively charged arginine residues in the C-terminal cytoplasmic domain of Kir6.2 causes rapid decay of K_{ATP} currents, a phenomenon that has been termed "inactivation" (Shyng SL. et al., 2000). In addition, these mutants also display reduced sensitivities to ATP and PIP_2 (Lin et al., 2003). How do these mutations induce K_{ATP} channel inactivation and altered channel response to ATP and PIP_2 is the question I will address in the second chapter. By studying the molecular mechanisms of these inactivation mutations, we demonstrat that the intersubunit interactions underlie the framework of K_{ATP} channel structure and play a critical role in Kir channel gating.

K_{ATP} channels and insulin secretion disorders

The activity of pancreatic K_{ATP} channels regulates insulin secretion. Mutations in K_{ATP} channels usually lead to insulin secretion disorders. Mutations that cause loss of channel function lead to Congenital Hyperinsulinism (CHI). CHI is characterized by excessive release of insulin despite severe hypoglycemia. (Dunne MJ., et al., 2004). The hypoglycemia may cause irreversible brain damage if therapy is not applied in time. The disease usually presents at birth or within the first year of life. Among the general population, the incidence is estimated as 1 in 50,000 live births and this this can be even higher in particular groups. (e.g., 1 in 2,500 in the Arabian peninsula) (Dunne MJ. et al, 2004). Most cases of CHI are sporadic, but familial forms have been also described, and the disease may result from homozygous, compound heterozygous, or heterozygous mutations (Thomas, P.M. et al. 1995; Nestorowicz, A. et al. 1997; Huopio, H. et al. 2000; Magge, S.N. et al. 2004). In terms of clinical therapy, some mild cases of CHI can be managed with diazoxide treatment, but more severe forms require subtotal pancreatectomy, which results in pancreatic insufficiency and a high incidence of later onset of diabetes.

Mutations in several different genes (SUR1, Kir6.2, glucokinase and glutamate dehydrogenase) can cause CHI but 50% of the cases have been identified to have mutations in SUR1 genes (Dunne MJ. et al., 2004). Many CHI-associated SUR1 mutations have been described and the two major defects causing CHI are defective channel biosynthesis/trafficking and defective channel gating or both.

SUR1 mutations with defective channel biosynthesis/trafficking are characterized by the decrease or absence of K_{ATP} channels in the plasma membrane, which could result from impaired biosynthesis, abnormal protein maturation/folding, defective channel assembly, or defects in membrane trafficking (Dunne MJ. et al., 2004; Taschenberger, G. et al. 2002; Partridge, C.J., 2001; Yan F. et al, 2004). On the other hand, most of the SUR1 mutations with defective channel gating impair the ability of MgADP to stimulate channel activity and these mutations usually lie close to the nucleotide-binding domains of SUR1 (Huopio, H. et al. 2000; Nichols, C.G. et al. 1996).

As mentioned earlier, both sulfonylureas and K channel openers can bind to SUR subunit and have been reported to regulate K_{ATP} channel activity. However, these drugs can also act as chemical chaperones and correct surface trafficking defects associated with some SUR1 mutations (Partridge et al., 2001; Yan et al., 2004). As some of these mutant K_{ATP} channels have normal nucleotide sensitivity, drugs with similar chaperone activity but do not block channel activity could potentially be useful for treating CHI.

To date, most CHI mutations reported are in SUR1 and mutations in Kir6.2 are much more rare. Some of these Kir6.2 mutations introduce a premature stop codon and result in protein truncation and some mutations reduce Kir6.2 protein stability (Thomas, P. et al., 1996; Nestorowicz, A. et al., 1997; Crane A. and Aguilar-Bryan J., 2004; Henwood, M.J. et al., 2005). Recently we have obtained a set of novel Kir 6.2 mutations identified from CHI patients. Pursuing the molecular mechanisms of these disease mutations will not only help us understand the structure-function relationship of the

channel but also shed light on potential pharmacological approaches that can be applied to rescue the deficiency of these mutant channels. Studies addressing the molecular mechanisms of these novel mutants will be described in chapter 3 and chapter 5.

In contrast to the CHI, mutations in K_{ATP} channels that cause gain of channel function lead to Permanent Neonatal Diabetes Mellitus (PNDM). PNDM is characterized by hyperglycemia requiring insulin therapy. It is a rare disease affecting 1 in 400,000 live births (Shield, J.P. et al., 1996). Approximately half of PNDM cases result from mutations in Kir6.2. (Edghill, E.L. et al., 2004; Gloyn, AL. et al., 2004a, 2004b; Sagen, JV. et al., 2004; Vaxillaire, M. et al., 2004; Massa, O. et al., 2005)

The mutations reported causing PNDM were mapped onto the structural model of Kir6.2 shown in Figure 14. They form clusters in the putative ATP binding site and in cytosolic loops. The PNDM patients express a range of phenotypes, distinguished by increasing disease severity. The most common class of mutation produces PNDM alone, while another class of mutations causes severe phenotype referred to as DEND (Developmental delay, Epilepsy Neonatal Diabetes). Some patients exhibited intermediated disease phenotype between PNDM and DEND and they were classified as Intermediated DEND.. The PNDM patients were clinically characterized with low birth weight and diabetes while intermediate DEND patients have muscle weakness and developmental delay in addition to diabetes. The DEND patients have most severe disease phenotype including epilepsy, muscle weakness, dysmorphic features together with developmental delay and diabetes (Edghill, EL. et al., 2004; Gloyn, AL. et al., 2004a, 2004b; Sagen, JV. et al., 2004; Vaxillaire, M. et al., 2004; Massa, O. et al., 2005; Proks, P. et al., 2004, 2005; Ashcroft FM., 2005). Here some mutations and their

disease severity as well as disease phenotype of PNDM and DEND patients are shown in Table II.

TABLE II

Disease severity	**PNDM<**	**Intermediated DEND <**	**DEND**
Mutations	R201H, R201C	V59M	Q52R, V59G, I296L
Disease phenotype	Low birth weight, Diabetes	Muscle weakness, Developmental delay	Epilepsy, Dysmorphic features

All PNDM mutations studied to date are gain-of-channel function mutations that act by reducing the sensitivity of ATP. This effect appears to be greater in the presence of Mg^{2+} for several PNDM mutant channels, suggesting that MgATP activation via SUR1 may be enhanced (Gloyn, AL. et al., 2005; Proks P. et al., 2005). While in general, disease severity is well correlated with the extent to which mutations reduces channel sensitivity to MgATP, there are some exceptions. For example, mutations such as V59M results in channels much more sensitive to ATP than R201C or R201H, yet it is associated with more severe disease phenotype. This suggests that additional factors might contribute to the pathogenic potency of a mutation. A potential explanation for mismatch of disease severity and the MgATP sensitivity could be that the mutant is not

expressed as efficiently as the WT Kir6.2, a hypothesis that has not been tested. Although functional data reported to date has been largely obtained using the *Xenopus* oocyte expression system (Gloyn AL. et al., 2004; Proks P. et al., 2004), this system is less suitable for studying channel maturation and trafficking since many misfolded proteins which fail to mature in mammalian cells are tolerated in *Xenopus* oocytes (Drumm ML. et al., 1991; Yang K. 2005). We therefore examined channel expression in the mammalian cell line COSm6. Our data demonstrate defects in surface expression of PNDM mutants in addition to their gating defect, suggesting that the expression level of a mutation may play a role in determining disease severity, as described in chapter 4.

In this dissertation, my goal is to understand the structure-function relationship of K_{ATP} channels, with a focus on gating regulation. My overall hypothesis is that perturbation of structural components in the channel proteins that are important for gating will result in altered channel gating behavior and may lead to altered channel function and even disease.

Before any homologous Kir channel structure became available, my project involved probing the structure-function relationship of K_{ATP} channels using systematic scanning mutagenesis combined with electrophysiological measurement approach. In the study described in chapter two, we tested the hypothesis that an ion pair in the cytoplasmic domain of Kir6.2 is required for stabilizing channel activity and demonstrated that subunit-subunit interaction plays an important role during K_{ATP} channel gating.

Later taking advantage afforded by the structures of several homologous Kir channels, we tested new hypotheses regarding structure-function correlation by studying

the naturally occurring mutations identified from patients with insulin secretion disorders. In chapter three, we tested the hypothesis that a mutation in Kir6.2, F55L, identified from patient with congenital hyperinsulinism causes loss of channel function by altering the gating property of the channel. We found that the mutation results in channels with very low intrinsic open probability due to reduced sensitivity to membrane phospholipids and/or long chain acyl CoAs. As the F55L mutation is located in the slide helix of Kir6.2, a structural feature that has previously been proposed by others to play a role in channel gating, our results provide evidence that the slide helix is indeed critical for normal channel gating by membrane phospholipids and/or long chain acyl CoAs. In chapter four, we investigated the mechanism by which mutations in Kir6.2 causes permanent neonatal diabetes (PNDM). We provide evidence to support the hypothesis that in addition to causing gain of channel function gating defect as reported by others, these mutations also affect channel biogenesis and that disease severity is determined by the effect of a mutation on both channel gating and channel biogenesis. Finally I have extended my pursuit of channel structure-function relationship from the Kir6.2 subunit to SUR1 subunit, which plays an important role in modulating channel activity. While this project is still work in progress, I present preliminary data in chapter five that lay the foundation for future studies.

Collectively, the work presented in this dissertation allowed me to infer the importance of certain structural elements in gating based on functional phenotypes. The study improves our understanding of the structure-function relationship of K_{ATP} channels and has important implications in disease mechanisms and therapy.

Figure 1 Glucose induced insulin secretion through pancreatic K_{ATP} channels

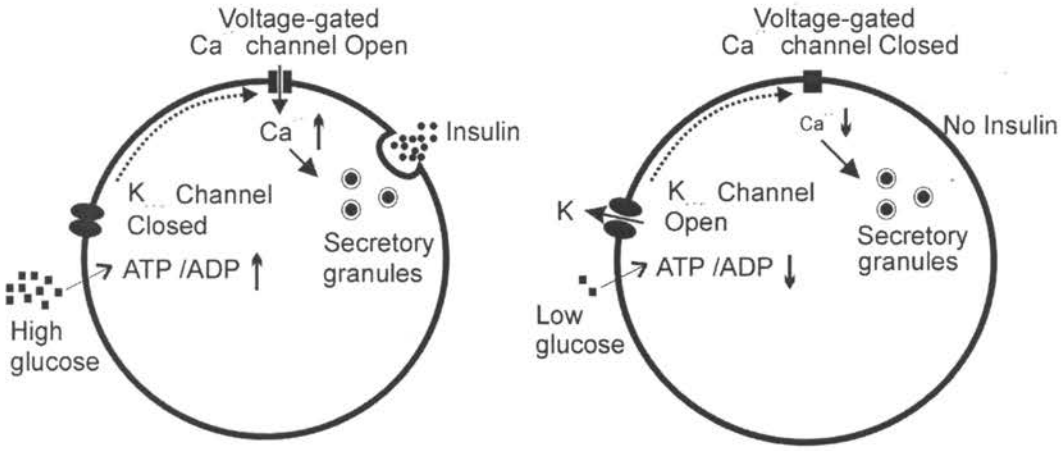

Figure 2 Regulation of K_{ATP} channel in trafficking

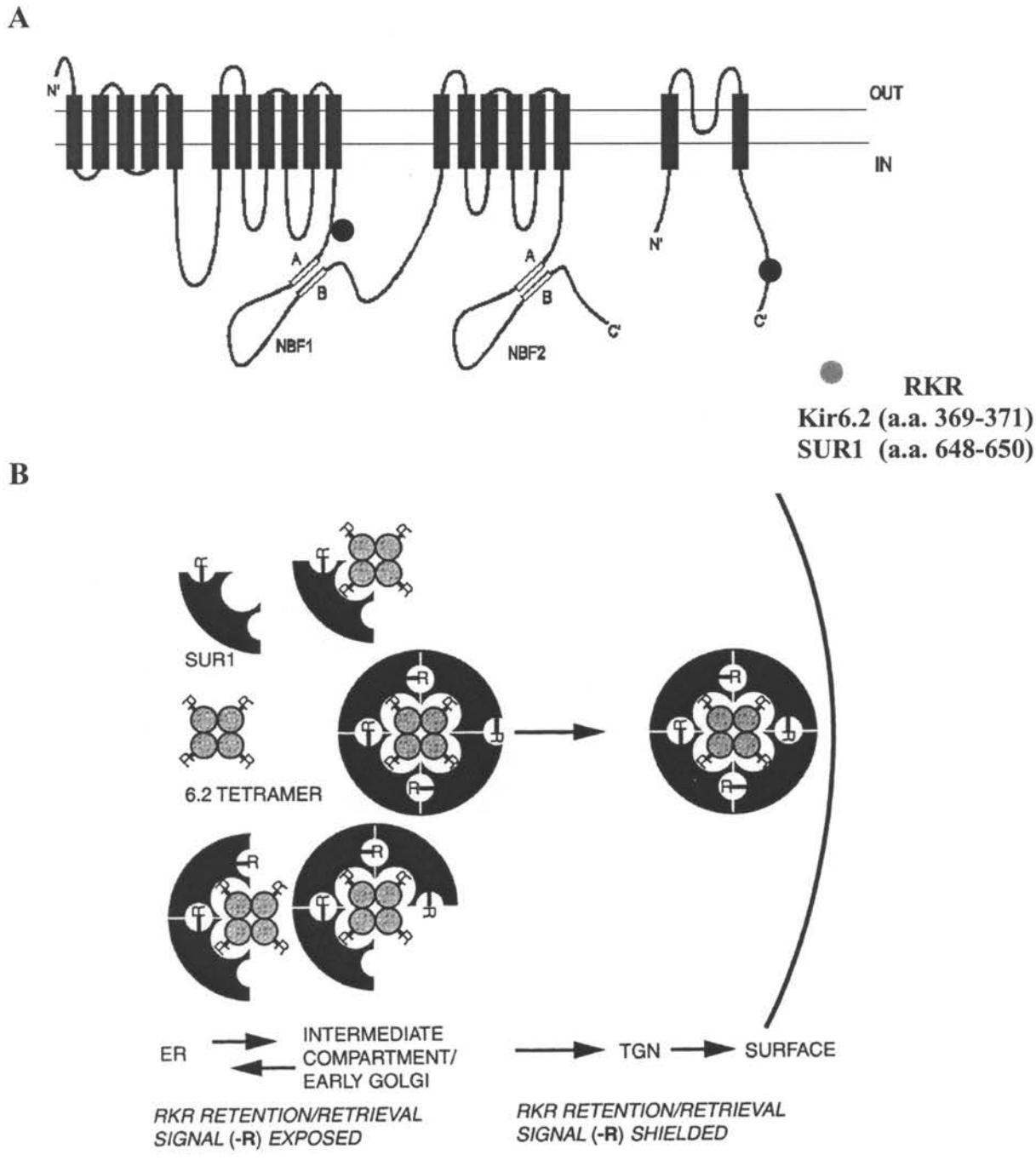

(A) Transmembrane topology of SUR1 and Kir6.2 subunits
(B) A model of quality control during K_{ATP} assembly

Zerangue N. et al., Neuron. 1999

Figure 3 The model of NBD dimer of SUR1

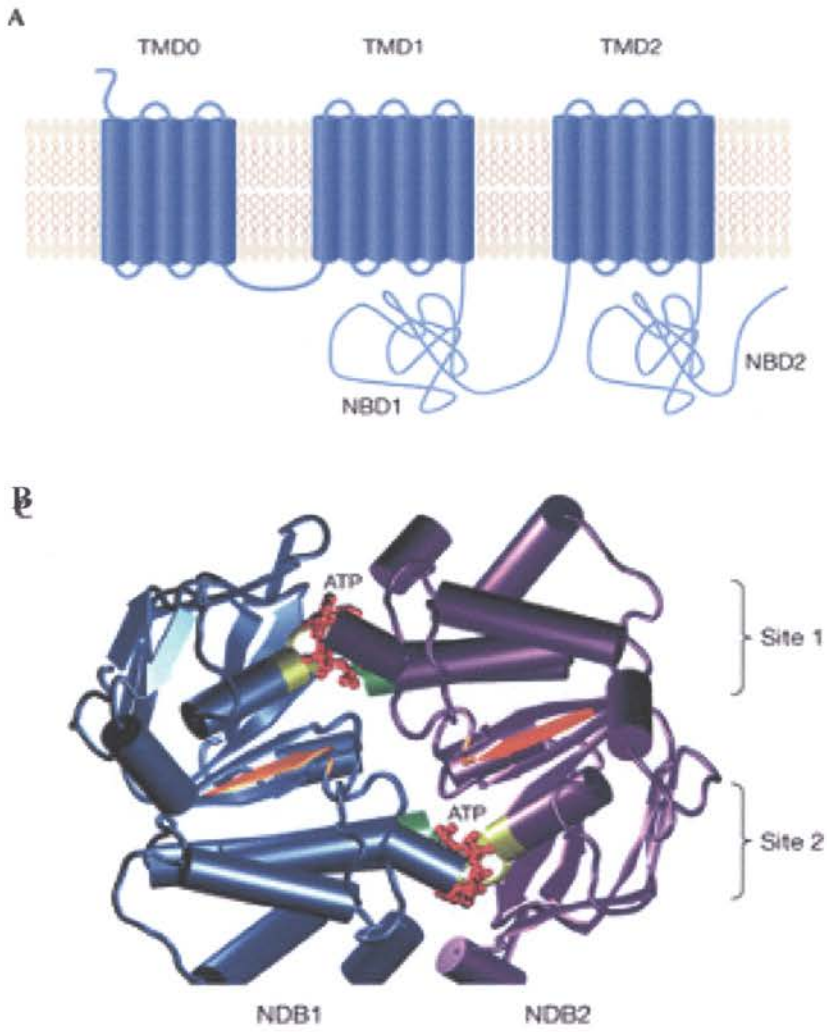

(A)The transmembrane topology of the sulphonylurea receptor SUR1, showing the transmembrane domains (TMDs) and the nucleotide-binding domains (NBDs).
(B)Model of the NBDs of SUR1, showing the nucleotide-sandwich dimer and the conserved motifs. The W_A, W_B motifs and signature sequence are yellow, orange and green, respectively. NBD1 is blue and NBD2 is purple. Site 1 and site 2 are indicated.

Campbell J., et al.: EMBO. 2003

Figure 4 The inward rectification of K_{ATP} channel

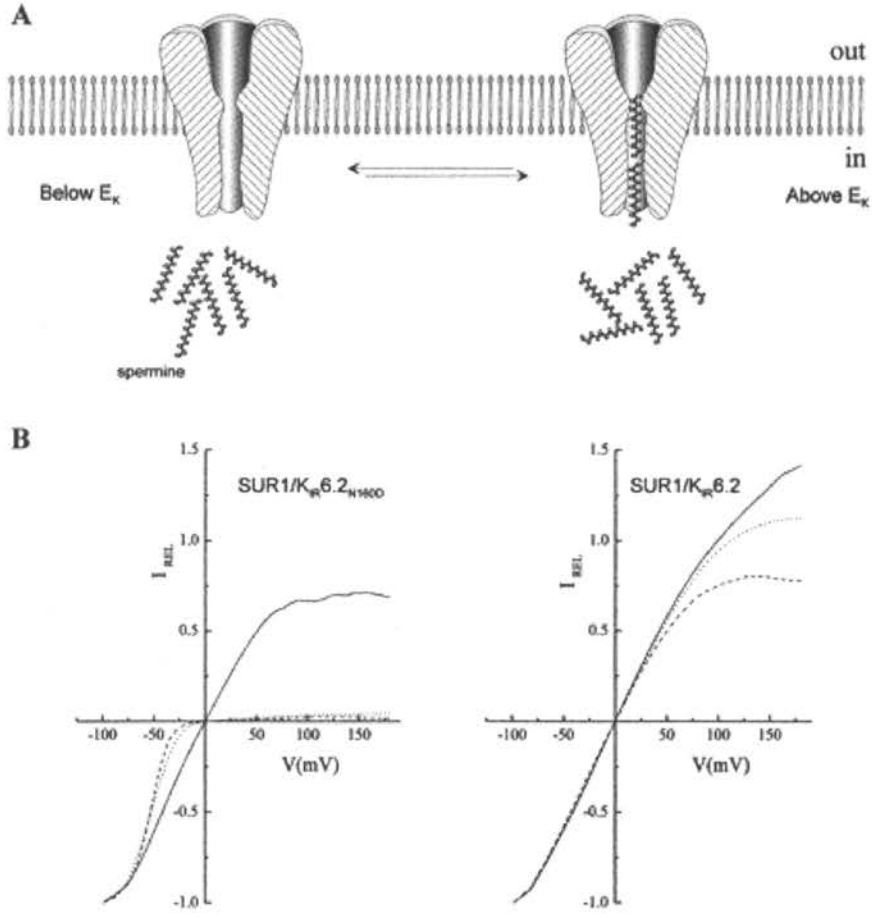

(A) A schematic representation of mechanism of inward rectification. Polyamines, like spermine, enter and bind in the pore, thus blocking flow of potassium ions. Affinity of polyamine binding depends on residues within pore. In Kir6.2, changing asparagines 160 to aspartic acid (N160D) increases affinity and alters rectification properties as indicated in B.

(B) Current (*I*)-voltage (*V*) relationships for WT and N160D K_{ATP} channels. *I-V* data were obtained from excised patches by ramping holding potential from 0 to +180 mV, holding for 400 ms to allow spermine to enter pore, then rapidly ramping to −100 mV. Current was sampled during ramp. Comparison of *I-V* curves WT versus N160D mutant channel shows N160D mutation greatly reduces outward current if spermine is present (solid line, no spermine; dotted line, 10 μM spermine; dashed line, 100 μM spermine).

Aguliar Bryan L. et al, 1998

Figure 5 Crystallized structure of GIRK1

A Structure of a Single Subunit of the mGIRK1. The transmembrane pore is on top and the central pore to the left. N- and C termini are colored red and green, respectively.

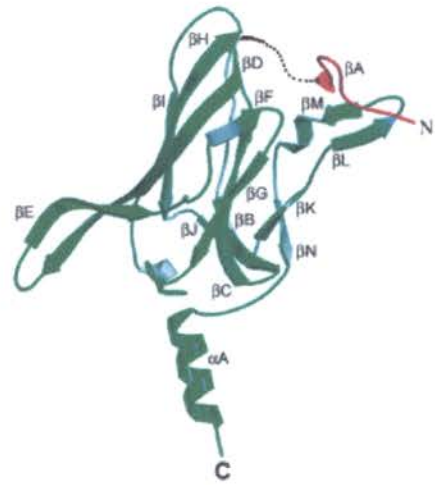

B. Stereo view of the Cα trace viewed along the 4-fold axis, peering from the membrane toward the cytoplasm. The N termini are red and the C termini blue or green. The dashed red line connects the N- to the C terminus, where the transmembrane pore has been excised.

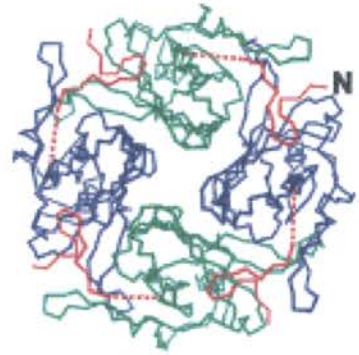

C. Stereo view of the Cα trace viewed from the side with the subunit nearest the viewer removed for clarity. The transmembrane pore is above and the cytoplasm below.

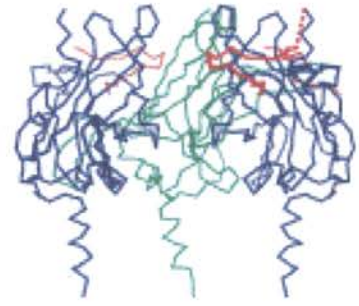

Nishida M. and Mackinnon R., Cell. 2002

Figure 6 Crystallized structure of KirBac1.1

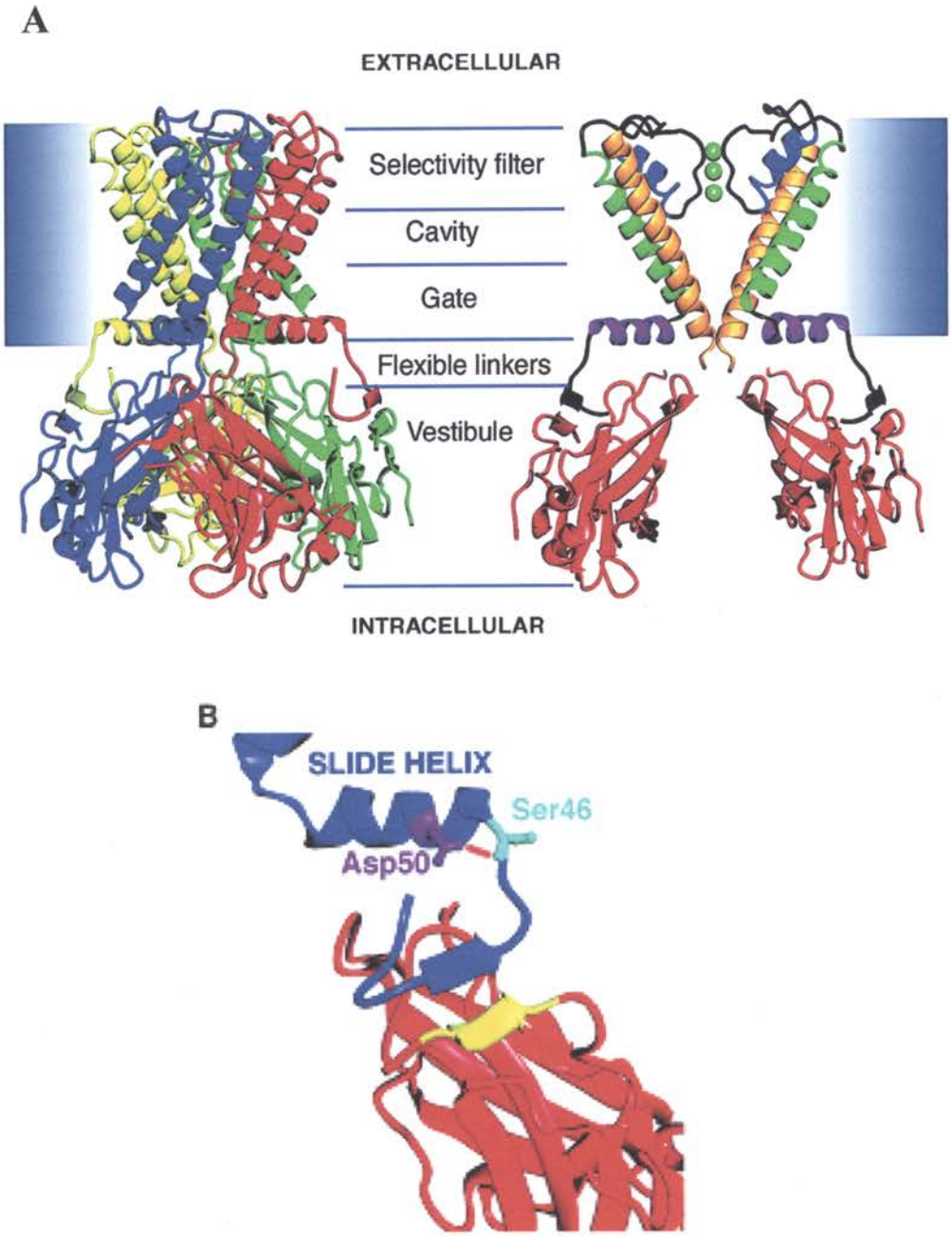

(A) Overview of the KirBac1.1 structure
(B) Close-up view of the parallel beta sheet interaction between red C-terminal domain (colored in yellow) with an adjacent blue N-terminus.

Kuo A. et al, Science. 2003

Figure 7 Structural basis of ATP and PIP_2 binding

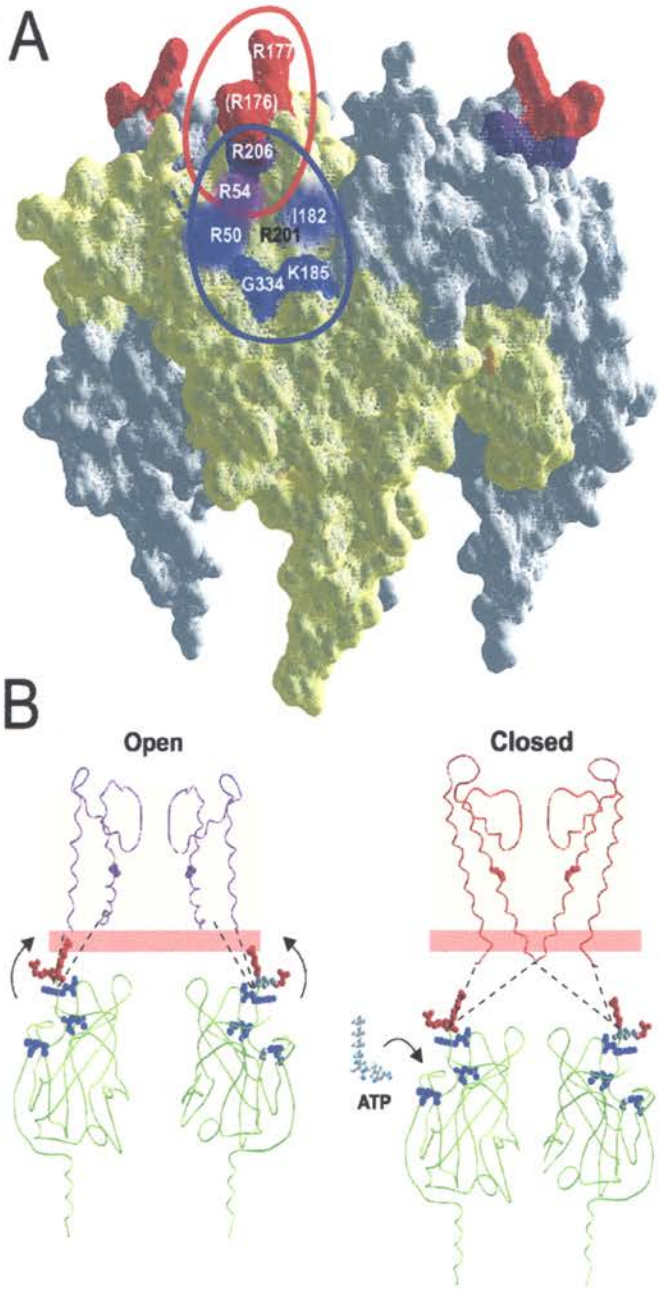

(A)The ATP binding residues are shown in blue and PIP_2 binding residues in red
(B)Model of PIP_2 and ATP regulation of channel gating

Modified from Enkvetchakul D., et al.; J. Gen. Physiol. 2003

Figure 8 Model of ATP binding pocket from two Kir6.2 Subunit

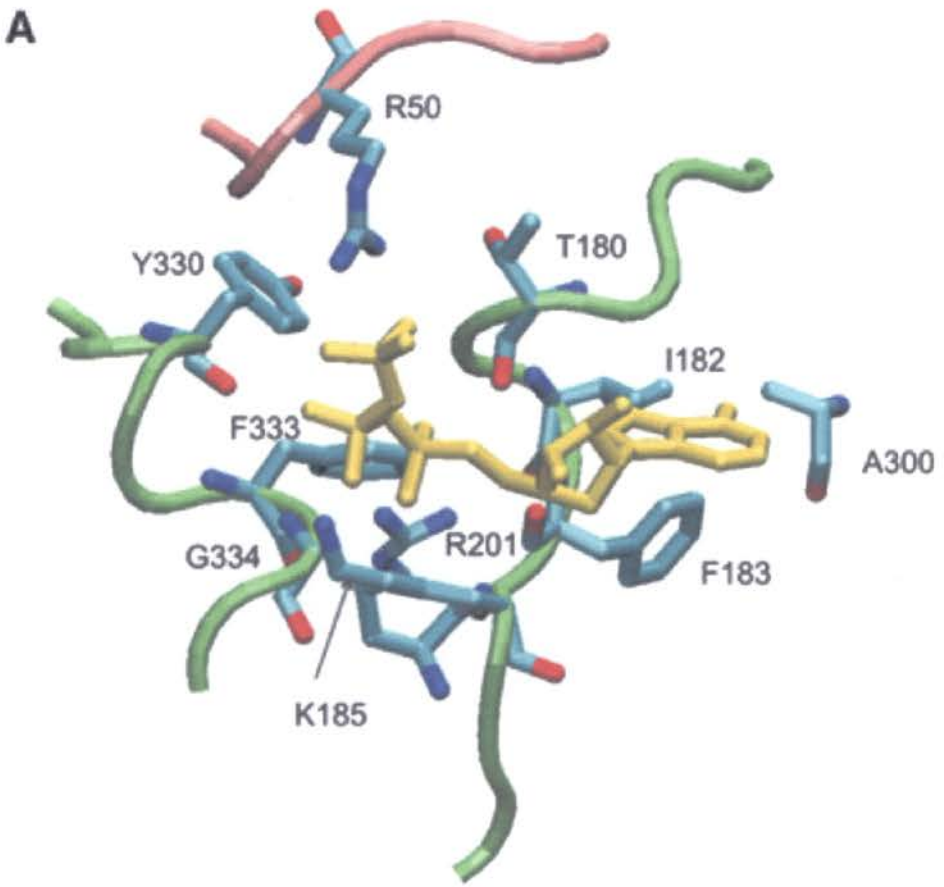

ATP (yellow) is docked into its binding site formed by adjacent subunits, in which N-terminus (pink) from one subunit and C-terminus (green) from another subunit.

Antcliff JF. et al., EMBO. 2005

Figure 9 The chemical structure of oleoyl CoA and PIP_2

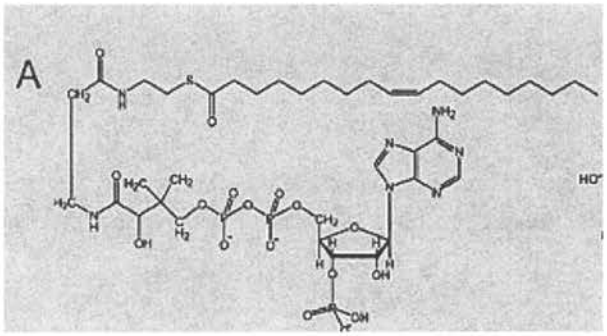

A. long chain acyl CoA (oleoyl CoA)

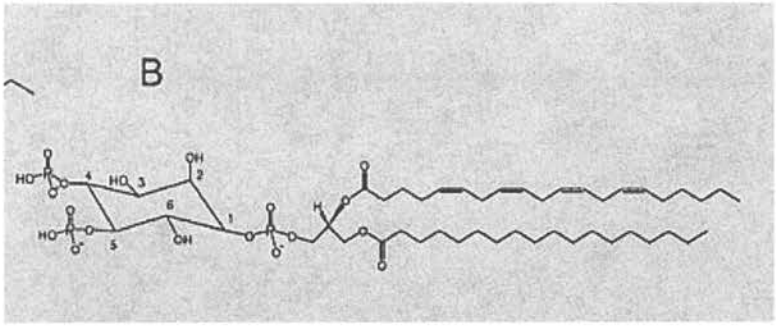

B. Phosphatidyl inositol 4, 5 biphosphate (PIP_2)

Figure 10. Single channel bursting of K_{ATP} channel

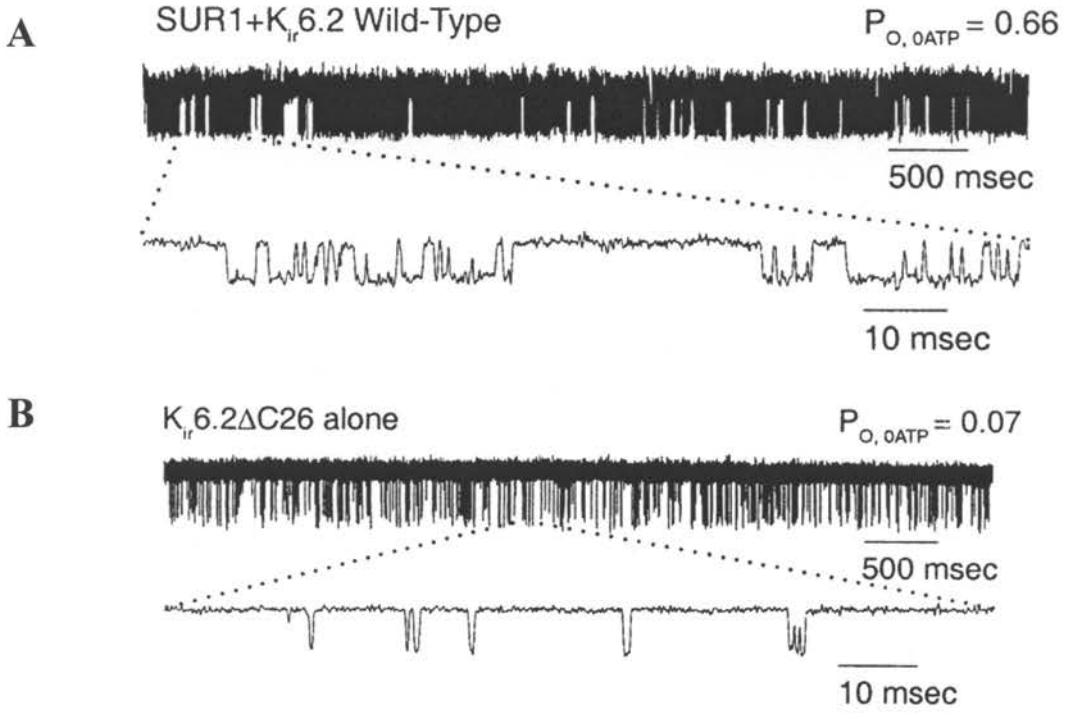

(A) Wild-type channel exhibits a relatively high open probability (P_O) in the absence of ATP, characterized by long bursts, comprising many brief openings, separated by long interburst intervals.
(B) Truncated ΔC26 channel without SUR1 exhibits a relatively low P_O in the absence of ATP, characterized by short bursts of one to a few openings, separated by long interburst intervals

Li L. et al., Biophysics. 2000

Figure 11 The 3D structure of K_{ATP} channel

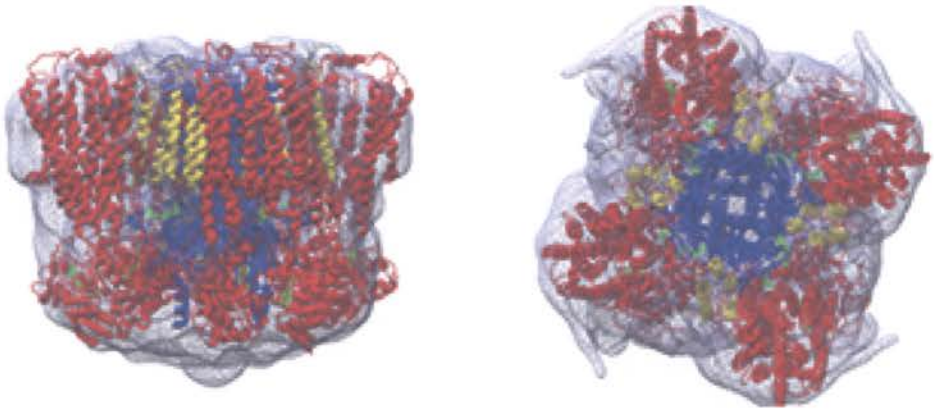

The side (left) and top (right) views of the EM density with models of Kir6.2 (blue), SUR1 minus TMD0 (red) and TMD0 (yellow). ATP molecules are shown in green. The surface (left) and transverse section (right) views of the EM density with models of Kir6.2 (blue), SUR1 minus TMD0 (red) and TMD0 (yellow). ATP molecules are shown in green. ATP could access its binding on Kir6.2.

Mikhailov M., et al, EMBO, 2005.

Figure 12 The 3D structure of K_{ATP} channel with the cleft

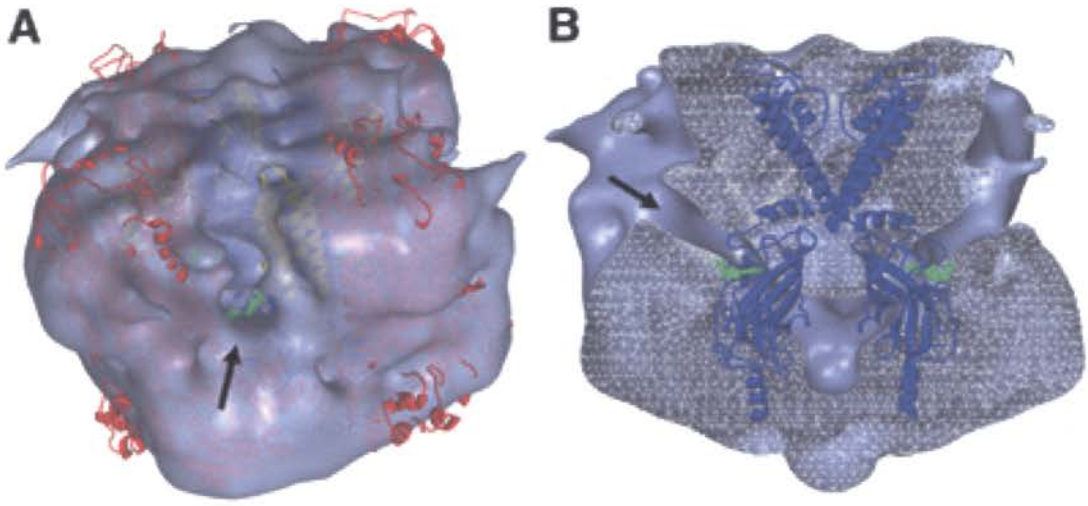

The surface (left) and transverse section (right) views of the EM density with models of Kir6.2 (blue), SUR1 minus TMD0 (red) and TMD0 (yellow). ATP molecules are shown in green. ATP could access its binding on Kir6.2.

Mikhailov M., et al, EMBO, 2005.

Figure 13 Two-gate model for K_{ATP} channel gating

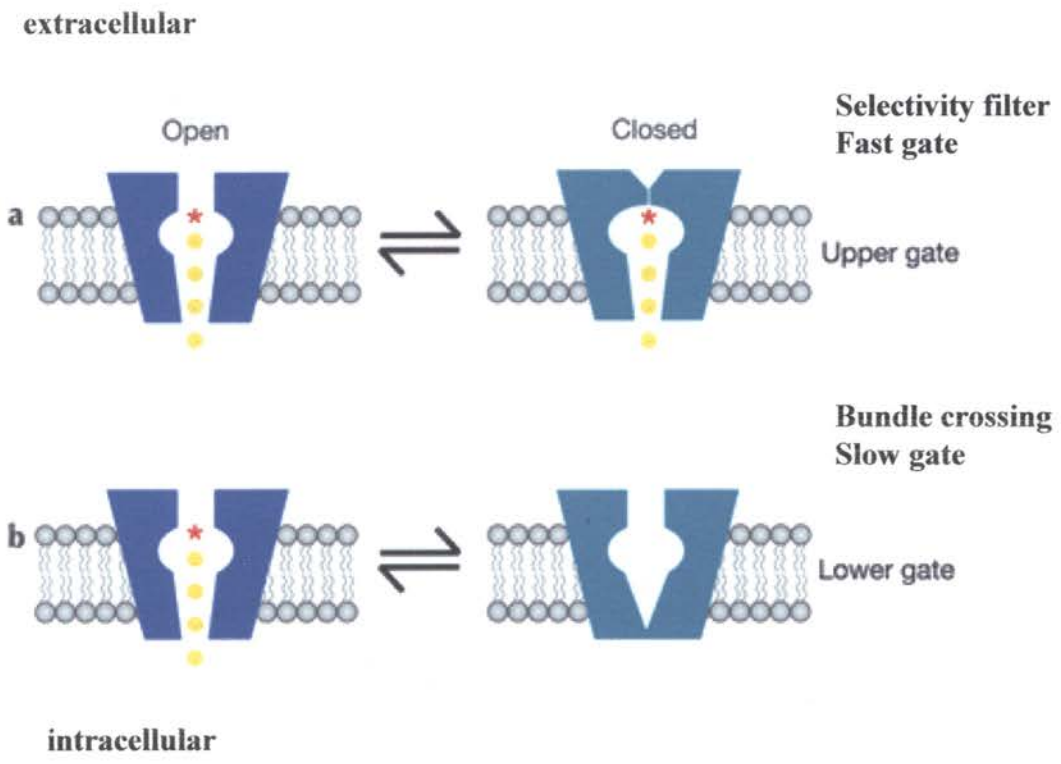

Proks P. et al., EMBO. 2003

Figure 14 Locolization of PNDM mutation

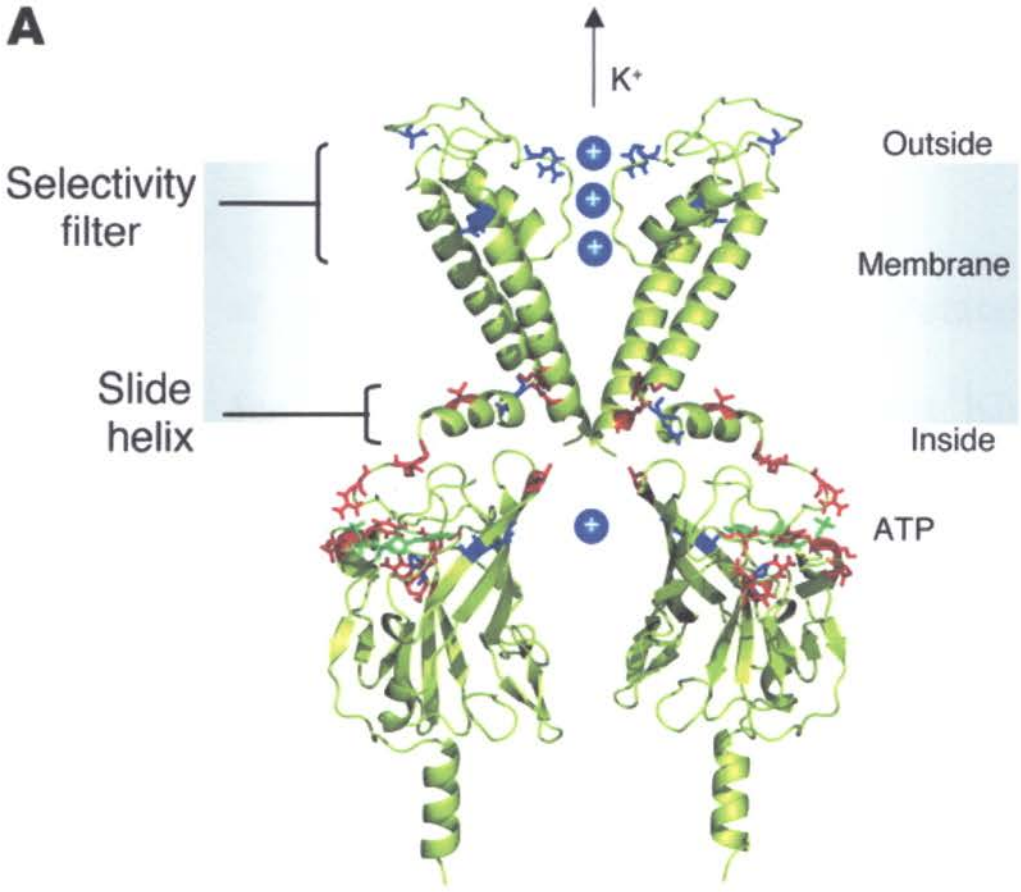

The residues causes PNDM is shown in red and those cause CHI in blue. ATP (green) is docked into its binding site.

Ashcroft FM., J Clin Invest. 2005

CHAPTER TWO

Stabilization of the Activity of ATP-sensitive Potassium Channels by Ion Pairs Formed between Adjacent Kir6.2 Subunits

Yu-Wen Lin, Taiping Jia, Anne M. Weinsoft, and S.-L. Shyng

Center for Research on Occupational and Environmental Toxicology, Oregon Health & Science University, Portland, Oregon 97239.

The work described in this chapter is published in the ***Journal of General Physiology*** (122), Aug 2003; p225-237. Taiping Jia did part of the screening work for the negatively charged mutations and Anne M. Weinsoft made most of the mutant constructs.

ABSTRACT

ATP-sensitive potassium (K_{ATP}) channels are formed by the coassembly of four Kir6.2 subunits and four sulfonylurea receptor subunits (SUR). The cytoplasmic domains of Kir6.2 mediate channel gating by ATP, which closes the channel, and membrane phosphoinositides, which stabilize the open channel. Little is known, however, about the tertiary or quaternary structures of the domains that are responsible for these interactions. Here, we report that an ion pair between glutamate 229 and arginine 314 in the intracellular C-terminus of Kir6.2 is critical for maintaining channel activity. Mutation of either residue to alanine induces inactivation, whereas charge reversal at positions 229 and 314 (E229R/R314E) abolishes inactivation and restores the wild-type channel phenotype. The close proximity of these two residues is demonstrated by disulfide bond formation between cysteine residues introduced at the two positions (E229C/R314C); disulfide bond formation abolishes inactivation and stabilizes the current. Using Kir6.2 tandem dimer constructs, we provide evidence that the ion pair likely forms by residues from two adjacent Kir6.2 subunits. We propose that the E229/R314 intersubunit ion pairs may contribute to a structural framework that facilitates the ability of other positively charged residues to interact with membrane phosphoinositides. Glutamate and arginine residues are found at homologous positions in many inward rectifier subunits, including the G-protein activated inwardly rectifying potassium channel (GIRK) whose cytoplasmic domain structure has recently been solved. In the GIRK structure, the E229- and R314-corresponding residues are oriented in opposite directions in a single subunit such that in the tetramer model, the E229 equivalent residue from one subunit is in close proximity of the R314 equivalent residue

from the adjacent subunit. The structure lends support to our findings in Kir6.2, and raises the possibility that a homologous ion pair may be involved in the gating of GIRKs.

Keywords: Inward rectifiers, salt bridge, K_{ATP}, PIP_2, gating

INTRODUCTION

Currents through inwardly rectifying potassium (Kir) channels are important determinants of the resting membrane potential in many cell types (Hille, 2001; Nichols and Lopatin, 1997). The Kir family has many members comprising seven subfamilies, and functional channels are tetrameric assemblies that may be homo- or heteromeric. All Kir subunits share the two transmembrane domain topology and distinct primary sequence homology, yet among the different subtypes, channel gating is controlled by a variety of stimuli (Hille, 2001; Nichols and Lopatin, 1997). Among them are ATP-sensitive potassium (K_{ATP}) channels that are gated by intracellular ATP and ADP, reflecting the energetic state of a cell (Aguilar-Bryan and Bryan, 1999; Ashcroft and Gribble, 1998; Bryan and Aguilar-Bryan, 1997). K_{ATP} channels underlie numerous important physiological processes, including regulation of insulin secretion, control of vascular tone, and electrophysiological changes during ischemia in cardiac and neuronal cells (Aguilar-Bryan and Bryan, 1999).

K_{ATP} channels are assembled from four Kir6.2 subunits and in addition require four sulfonylurea receptor subunits (SUR) (Clement et al., 1997; Inagaki et al., 1995;

Inagaki et al., 1997; Shyng and Nichols, 1997). The activity of K_{ATP} channels is determined by orchestrated interactions between the channel subunits and intracellular ATP and ADP. ATP inhibits channel opening by binding to the pore-forming Kir6.2 subunits, an effect that does not involve ATP hydrolysis (Drain et al., 1998; Tanabe et al., 1999; Tucker et al., 1998; Tucker et al., 1997). On the other hand, ATP stimulates channel opening by interacting with SUR1, an effect that requires Mg^{2+} and ATP hydrolysis at the second nucleotide binding fold, or NBF2 (Ashcroft and Gribble, 1998; Gribble et al., 1998b; Shyng et al., 1997b). ADP, accompanied by Mg^{2+}, also interacts with NBF2 of SUR1 and stabilizes the protein in a post-nucleotide hydrolysis state to stimulate channel activity (Gribble et al., 1997; Nichols et al., 1996; Shyng et al., 1997b; Zingman et al., 2001). In addition to intracellular nucleotides, membrane phosphoinositides (PIPs), such as phosphatidylinositol bisphosphate (PIP_2), and phosphatidylinositol trisphosphate (PIP_3) have a profound effect on channel activity (Baukrowitz et al., 1998; Fan and Makielski, 1997; Shyng and Nichols, 1998). PIP_2 and PIP_3 increase the open probability of the channel and antagonize the inhibitory effect of ATP. Although many reports support a model in which ATP and phosphoinositides bind directly to the cytoplasmic domains of Kir6.2 to promote channel closure and opening, respectively (Baukrowitz et al., 1998; MacGregor et al., 2002; Shyng and Nichols, 1998; Tanabe et al., 1999; Tucker et al., 1998; Wang et al., 2002), little is known about the tertiary or quaternary structural elements in these domains that are involved in ligand binding and channel gating (Cukras et al., 2002a; Cukras et al., 2002b; MacGregor et al., 2002).

In an earlier study, we have systematically mutated each positively charged amino acid in the cytoplasmic domain of Kir6.2 to alanine, to identify residues that are involved in interactions between the K_{ATP} channel and the negatively charged phosphate groups in PIPs (Shyng et al., 2000b). Three of the arginine-to-alanine mutations (R192A, R301A, and R314A) that exhibited reduced response to exogenously applied PIP_2 also displayed rapid spontaneous decay of currents after membrane excision into ATP-free solutions, a behavior which we have termed "inactivation" (Shyng et al., 2000b). Channel inactivation appears different from the "rundown" phenomenon frequently observed with wild-type (WT) channels in that it is faster and can be recovered by exposure and then washout of ATP even in the absence of Mg^{2+} (Ribalet et al., 2000; Shyng et al., 2000b).

In this study, the mechanisms underlying K_{ATP} channel inactivation were investigated. Although it is possible that the three arginine residues (192, 301, and 314) are directly responsible for binding to the negatively charged phosphate groups in PIP_2, an alternative hypothesis is that the arginine residues are involved in maintaining structural conformations necessary for channel activity. Specifically, we tested whether the R192A, R301A, and R314A mutations cause channel inactivation by disrupting electrostatic interactions within the channel complex. Through systematic mutation of each of the negatively charged residues in the cytoplasmic regions of Kir6.2 to alanine, we found that mutation E229A also induces fast channel inactivation similar to that seen in the R192A, R301A, and R314A mutants. Double charge reversal at positions 229 and 314 (E229R/R314E) abolished inactivation and restored the WT channel phenotype,

indicating that these residues form an ion pair. The close proximity of these two residues was supported by disulfide bond formation between cysteine residues introduced at the two positions (E229C/R314C); disulfide bond formation abolished inactivation and stabilized the current. Experiments using a series of Kir6.2 tandem dimer constructs containing mutations at position 229 and/or 314 in one or both subunits showed that the E229/R314 ion pair is likely formed between two adjacent Kir6.2 subunits.

MATERIALS AND METHODS

Molecular biology

Mouse Kir6.2 cDNA in the pCMV6b vector was used as a template for introducing point mutations in Kir6.2. Site-directed mutagenesis was carried out by overlap extension at the junctions of the relevant residues by sequential polymerase chain reaction (PCR) or by the QuickChange site-directed mutagenesis kit (Stratagene). All constructs were sequenced to verify the correct mutations. Mutant clones from multiple PCR reactions were analyzed to avoid false results caused by undesired mutations introduced by PCR.

The Kir6.2 tandem dimer was constructed as follows. Two Kir6.2 PCR fragments with unique restriction sites and linkers were generated. The first fragment has a ClaI site at the 5' end and a five glutamine linker with an NheI site replacing the stop codon at the 3' end. The second fragment has an NheI site followed by a five glutamine linker at the 5' end and an EcoRI site at the 3' end. The two fragments were

ligated into the pCMV6b vector. The resulting construct has a –QQQQQASQQQQQ- linker between the two Kir6.2 subunits.

Inside-out Patch-clamp Recordings

COSm6 cells were tranfected using Fugene 6 (Roche) and plated onto coverslips. The cDNA for the green fluorescent protein (GFP) was co-transfected with SUR1 and Kir6.2 to facilitate identification of positively transfected cells. Patch-clamp recordings were performed 36-72 hours post-transfection at room temperature, in a chamber which allowed rapid exchange of bathing solution. Micropipettes were pulled from non-heparinized Kimble glass (Fisher Scientific) on a horizontal puller (Sutter Instrument, Co., Novato, CA, USA). Electrode resistance was typically 0.5-1 MΩ when filled with K-INT (below). Inside-out patches were voltage-clamped with an Axopatch 1B amplifier (Axon Inc., Foster City, CA). The standard bath (intracellular) and pipette (extracellular) solution (K-INT) had the following composition: 140 mM KCl, 10 mM K-HEPES, 1 mM K-EGTA, pH 7.3. ATP and AMP-PNP (Sigma) were added as the potassium salt. In the majority of the experiments, 1 mM EDTA was included in the K-INT solution to chelate residual Mg^{2+}. PIP_2 (Roche) was prepared as described previously (Shyng and Nichols, 1998). Dithiothreotol (DTT) at 1 mM was used to reduce disulfide bonds. All currents were measured at a membrane potential of -50 mV (pipette voltage = +50 mV) and inward currents were shown as upward deflections. Data were filtered at 2 kHz and analyzed using pCLAMP software. All data are expressed as means ± standard error of the means (s.e.m.).

Immunofluorescent Staining

For cell surface staining of FLAG-tagged SUR1, living COSm6 cells transiently expressing FLAG-tagged SUR1 and various Kir6.2 mutants were incubated with 10 μg/ml anti-FLAG M2 monoclonal antibody (in 0.1 mg BSA /ml OptiMEM) for one hour at 4°C. They were washed with ice-cold PBS and incubated with Cy-3 conjugated donkey anti-mouse secondary antibodies (diluted in 0.1 mg BSA /ml OptiMEM) for 30 min at 4°C. After extensive wash in ice cold PBS, cells were fixed with 4% paraformaldehyde and viewed using a Leica fluorescent microscope.

RESULTS

Mutation of Glutamate 229 in Kir6.2 to Alanine Induces K_{ATP} Channel Inactivation

K_{ATP} currents generated by co-expression of SUR1 and Kir6.2 mutants R192A, R301A, or R314A have previously been shown to inactivate after inside-out patch excision into ATP-free solutions (Shyng et al., 2000b). We hypothesized that the three arginines may form ion pairs with negatively charged residues in Kir6.2 and that these ion pairs are important for maintaining channel activities; if true, neutralization of the negatively charged residues should induce similar channel inactivation. There are 30 negatively charged residues in the cytoplasmic regions of Kir6.2, each of which was individually replaced with an alanine and screened for inactivation. Mutation of glutamate 229 to alanine (E229A) resulted in robust current inactivation (Fig.15B, 16A, and 16B), with characteristics similar to those seen with the R192A, R301A, and

R314A channels (Shyng et al., 2000b).

Quantitation of Channel Inactivation: Comparison with Channel Rundown

K_{ATP} currents run down after patch excision into K-INT solution (140 mM KCl, 10 mM HEPES, 1 mM EGTA, pH 7.3; Fig.15A, *left*). The rate of rundown varies and can be rapid in some patches, making it difficult to distinguish from inactivation. Ribalet *et al.* have previously reported that channel rundown involves multiple factors including loss of MgADP stimulation, loss of membrane PIP_2, and protein dephosphorylation (Ribalet et al., 2000). We reasoned that since many protein phosphatases, as well as phospholipases and lipid phosphatases that break down membrane PIPs require Mg^{2+} or Ca^{2+} (Cohen, 1989; Hilgemann and Ball, 1996; Matzaris et al., 1994; Palmer et al., 1994; Singer et al., 1997), removal of residual Mg^{2+} and other metal ions in the bath solution might prevent rundown. We found that addition of 1 mM EDTA to the K-INT solution (K-INT/EDTA) dramatically reduced channel rundown (Fig.15A, *right*). Using K-INT/EDTA bath solution, the WT current decayed only by 10.72 ± 3.66 % over a 20-seconds period following patch excision (n=10; Table III), in contrast to 57.06 ± 3.37% in K-INT solution without EDTA (n=38). The significant reduction of channel rundown made it possible to quantitatively compare the current stability of WT to that of inactivation mutants (Fig.15B). In K-INT/EDTA solution, the current from the E229A mutant still inactivated rapidly; the current decay was 81.19 ± 5.39 % at 20 seconds following patch excision (n=7; Fig.15B, Table III). The time course of inactivation of E229A channels was fit by a single exponential, yielding a time constant (τ_i) of 6.64 ± 1.80 seconds. Under the same recording

condition, the inactivation time constants were 4.79 ± 1.34 , 0.32 ± 0.03, and 3.08 ± 0.43 seconds for R192A, R301A, and R314A channels, respectively (n =7-9 patches in each case as shown in Table III; the slow current decay in WT could not be fit by a single exponential, therefore no value was given).

The fast phase of channel rundown has been largely attributed to loss of MgADP-dependent functional coupling between SUR1 and Kir6.2 (Ribalet et al., 2000). We asked whether the current decay seen in the inactivation mutants could be due to uncoupling between SUR1 and Kir6.2. Kir6.2, when its distal C-terminal 25 or 35 amino acids are deleted, can form functional channels in the absence of SUR1 (Tucker et al., 1997). We constructed Kir6.2ΔC25 containing either the E229A or the R314A mutation and tested whether the resulting channels also exhibited rapid current decay. Figure 15C shows that, in contrast to WT-Kir6.2ΔC25 channels whose activities were stable over the course of the recording, the E229A- and R314A-Kir6.2ΔC25 channels inactivated similar to E229A- and R314A channels formed in the presence of SUR1. The extent of current decay measured at 20 seconds following patch excision and the estimated inactivation time constant are 100 ± 0 % (n=3) and 2.5 seconds (n=2) for E229A-Kir6.2ΔC25, and 90.3 ± 11.2 % (n=4) and 5.2 seconds (n=2) for R314A-Kir6.2ΔC25. The fact that inactivation occurs even in the absence of SUR1 indicates that a structural change in the Kir6.2 tetramer itself is a major mechanism underlying inactivation.

Channel Inactivation Caused by the E229A Mutation Can Be Recovered by Exposure to ATP and Subsequent Washout of ATP, and Is Reversed by PIP_2

A defining feature of channel inactivation is that after exposure to ATP and subsequent washout of ATP, the inactivated channels become reactivated (Shyng et al., 2000b); this is also seen in the E229A mutant channels (Fig. 16A). The "reactivation" effect by ATP is dose- and time-dependent: the higher the concentration and the longer the exposure time, the more complete the reactivation effect. A non-hydrolysable ATP analog, AMP-PNP, mimics the effect of ATP in reactivating the E229A and R314A mutant channels (Fig.16B). Therefore, the reactivation effect of ATP is not mediated by nucleotide hydrolysis at the NBF2 of SUR1 (Zingman et al., 2001), or by phosphorylation of the channel proteins (Beguin et al., 1999; Light et al., 2000; Lin et al., 2000). Interestingly, in channels formed by E229A-Kir6.2ΔC25 alone, current decay could not be recovered by ATP exposure and its subsequent removal (Fig.16C, *left*). However, when coexpressed with SUR1, inactivated E229A-Kir6.2ΔC25 channels could be reactivated by ATP and subsequent washout of ATP (Fig.16C, *right*). Similar observations were made with the R314A mutation (not shown). These results suggest that SUR1 plays a role in mediating the reactivation effect of ATP.

Aside from exposure to ATP and subsequent removal of ATP, PIP_2 can also reverse channel inactivation caused by the E229A mutation, similar to that found in the R192A, R301A, or R314A mutant channels (Shyng et al., 2000b). Following inactivation of E229A channels, PIP_2 gradually increased the current to a stable maximum that exceeded the amplitude observed at the time of patch excision; PIP_2 also

rendered the channel less sensitive to ATP inhibition (Fig. 17).

The Double Mutation E229R/R314E Rescues Channel Inactivation Induced by E229R or R314E

The similar inactivation behavior caused by charge neutralization of E229 and one of the R192, R301, and R314 residues prompted us to examine the possibility that E229 may form a salt bridge with one of the three arginine residues to maintain channel activities. If true, disruption of the ion pair should cause inactivation, whereas exchanging the residues at the two positions should preserve the electrostatic interaction and retain WT channel behavior. Currents from patches containing channels harboring the individual charge reversal mutations E229R, R192E, or R314E all inactivated like the charge neutralization mutants at those positions, with similar kinetics (Fig.18A, Table III), while no macroscopic currents were detected in patches from cells transfected with the R301E Kir6.2 mutant. Immunostaining and Western blot experiments detected only very low levels of the R301E Kir6.2 mutant protein (not shown), suggesting that the R301E mutation may have adversely affected the stability of the protein.

Next, the three double mutants, E229R/R192E, E229R/R301E, and E229R/R314E, were constructed in which the residues at the two positions in each potential ion pair were exchanged. E229R/R301E failed to generate measurable currents (Fig.18B) while E229R/R192E displayed inactivation similar to the E229R and the R192E single mutations (66.06 ± 3.98 % current decay over 20 seconds in K-INT/EDTA, with τ_i = 7.70 ± 0.06 seconds; Table III). In contrast, the E229R/R314E double mutant exhibited WT-like behavior, lacking the rapid current decay induced by

either the E229R or the R314E single charge reversal mutations (Fig.18B). For E229R/R314E channels, the extent of current decay measured at 20 seconds following patch excision into K-INT/EDTA is only 6.95 ± 3.27 % (n=5), comparable to that of WT channels (10.72 ± 3.66 % ; see Table III). These results are consistent with the idea that an ion pair formed between E229 and R314 stabilizes K_{ATP} channel activity.

E229 and R314 of Kir6.2 Form an Ion Pair that Increases K_{ATP} Channel Activity

Although the data presented above suggest electrostatic interactions between E229 and R314, they do not demonstrate definitively that the two residues interact directly with each other. One approach to assess the proximity of protein domains is to exploit the ability of cysteine residues to form disulfide bonds. This approach has been successfully used to study the structure-function relationships for a number of ion channels, including *shaker* potassium channels, cyclic nucleotide-gated (CNG) channels, and $GABA_A$ receptors (Gordon et al., 1997; Gordon and Zagotta, 1995; Horenstein et al., 2001; Larsson and Elinder, 2000; Papazian et al., 1995). Accordingly, we further probed the interaction between E229 and R314 by substituting them with two cysteine residues. If the two residues are in close proximity, it should be possible to form a disulfide bond, and this covalent bonding should stabilize channel opening.

In channels carrying a single cysteine mutation at position 229 of Kir6.2, rapid inactivation was observed, similar to that of E229A or E229R mutant channels (Fig. 19A, Table III). However, mutation of R314 to cysteine resulted in channels that did not give rise to detectable currents, although Western blots confirmed expression of the

mutant protein (not shown). To see whether the R314C mutant Kir6.2 was indeed incorporated into the channel complex, we performed surface immunostaining for the FLAG-epitope in cells co-transfected with R314C Kir6.2 and FLAG-tagged SUR1 (Cartier et al., 2001). Surface expression of FLAG-SUR1 requires that the protein co-assemble with Kir6.2 to form an octameric channel complex, which shields the –RKR-tripeptide ER retention/retrieval signals in the individual subunits (Zerangue et al., 1999). Figure 19B shows that the surface FLAG staining in cells co-expressing FLAG-SUR1 and R314C Kir6.2 is equivalent to cells co-expressing FLAG-SUR1 and WT Kir6.2, indicating that the R314C Kir6.2 does form octameric channel complexes with SUR1 (Zerangue et al., 1999), but that the open probability of the resulting channels may be too low to be detected. These results are consistent with those of John *et al.* obtained with R314C-Kir6.2 linked to GFP (John et al., 2001).

The E229C/R314C double cysteine mutant channels opened, upon patch isolation into ATP-free K-INT /EDTA solution. The initial current amplitude after patch excision was low, and the rate of current decay was faster than WT channels, but slower than the E229A and the R314A channels (the percentage of current decay in 20 seconds is 46.98 ± 5.96, compared with 10.72 ± 3.66, 81.19 ± 5.39, and 94.98 ± 1.89 for WT, E229A, and E314A channels, respectively; see Table III). We found that given enough time, nearly all patches (21 out of a total of 23 patches) exhibited gradual increases and stabilization of the currents, after repeated exposure to 5 mM ATP (fold increase = 6.02 ± 1.01, n=21; two examples shown in Fig. 20). The rate at which this current increase occurred varied. In general, the more frequent and longer the patch was exposed to

ATP, the faster the current increase was observed upon subsequent washout of ATP. Since the cytoplasmic environment is reducing and does not favor disulfide-bond formation, it is likely that immediately after patch excision most channels are already in the "inactivated" state, explaining the low initial current amplitude. After patch excision and exposure to ATP to close the channels, subsequent washout of ATP permits the channels to become "reactivated" (see Discussion). The patch now is exposed to an oxidizing environment and spontaneous disulfide bond formation between 229C and 314C stabilizes the reactivated channels and increases current amplitudes. Consistent with this interpretation, subsequent exposure of these patches to the reducing reagent DTT (1 mM) caused rapid inactivation of the reactivated channels in a reversible manner (Fig. 20, *top trace*). Interestingly, the open probability of the E229C/R314C channel after its current has reached a maximum is ~0.5, comparable to that observed in WT channels under normal conditions [estimated by noise analysis; (Shyng et al., 1997a)]. Application of 5 μM PIP_2 further stimulated the current by ~2-fold (Fig. 20, *bottom trace*).

It is conceivable that disulfide bond formation is mediated by other endogenous cysteine residues in the channel, or by single engineered cysteine from two different Kir6.2 subunits. However, neither WT channels nor the single cysteine mutant channels, E229C and R314C, exhibited the time-dependent current increase as that seen in the E229C/R314C double cysteine mutant channels (Fig. 21, n = 4-5 in each case; no recording for R314C is shown since there were no measurable currents). Further, DTT had little effects on the kinetics of either WT or E229C channels (Fig.21). Taken

together, these results strongly support disulfide bond formation between C229 and C314, and that the disulfide bond increases the stability of channel activities.

The E229-R314 Ion Pair Is Formed between Two Kir6.2 Subunits

To determine whether the ionic interaction between E229 and R314 occurs between two Kir6.2 subunits, or within a single Kir6.2 subunit, we conducted experiments using Kir6.2 tandem dimers. Tandem dimers were constructed such that the C-terminus of subunit one is joined to the N-terminus of subunit two by a linker of twelve amino acids (see Materials and Methods). Work on other potassium and CNG channels has suggested that assembly of such dimers likely follow the head-to-tail direction, such that the leading subunits of the two dimers are positioned diagonally to each other (Gordon and Zagotta, 1995; He et al., 2000; Isacoff et al., 1990; Liu et al., 1998; Pascual et al., 1995; Shapiro and Zagotta, 2000). Such head-to-tail cyclic symmetry was also observed in the crystal structure of GIRK1 (Nishida and MacKinnon, 2002). In principle, with tandem dimers, one can constrain the ability of the channel to form intra- or inter-subunit ion pairing, by introducing mutations at the E229 and R314 positions in designated subunits. For example, only intersubunit ion pairing is possible, but no intrasubunit ion pairing is possible, in a construct that has R314 mutated to E in the first subunit, and E229 mutated to R in the second subunit (we name this the EE-RR dimer, where the amino acids at position 229 and 314 shown in single letter codes in the first subunit are joined by a hyphen with the amino acids at position 229 and 314 of the second subunit; Fig.22B). On the other hand, only intrasubunit ion pairing is possible, but no intersubunit ion pairing is possible, in a

construct in which the first subunit carries the E229R/R314E double charge reversal mutations and the second subunit is WT (the RE-ER dimer; Fig.22D).

When coexpressed with SUR1, the WT-WT Kir6.2 tandem dimer (or the ER-ER dimer) gave rise to channels with stable currents that were inhibited by ATP (Fig.22A). Mutation of E229 to alanine in both subunits (the AR-AR dimer) induced marked current inactivation, as expected (Fig. 22C). The time course and the extent of current decay seen from AR-AR dimer channels were not as pronounced as those seen from the E229A monomer channels. A potential explanation for this difference is that the dimer channels exhibit a slightly higher open probability (Po=0.88 ± 0.02; n=6) than channels formed by Kir6.2 monomers (Po=0.67 ± 0.05; n=8); this higher Po likely exerts an antagonizing effect on channel inactivation induced by the E229A mutation. Because of the slower inactivation rate seen in the dimer mutant channels, we measured the extent of current decay at 40 seconds following patch excision into K-INT/EDTA, as shown in Table IV. Currents from the WT-WT and the AR-AR dimer channels decayed by 6.08 ± 2.19 % and 48.35 ± 6.54 %, respectively, at 40 seconds following patch excision. The EE-RR dimer, in which intrasubunit ion pair formation is prohibited but intersubunit ion pair formation is allowed, generated channels that had relatively stable currents in ATP-free solution, resembling WT and WT-WT dimer channels (Fig.22B). The percentage of current decay is 14.94 ± 6.73 % at 40 seconds after patch excision into K-INT/EDTA solution (Table IV). By contrast, the ER-RE dimer, in which only intrasubunit ion pair formation is allowed, generated currents that decayed much faster than the WT-WT and the EE-RR dimers (Fig.22D). The percentage of current decay is 38.05 ± 6.07 % at 40

seconds following patch excision (Table IV). Collectively, these results are consistent with the E229/R314 ion pair being formed between two Kir6.2 subunits.

DISCUSSION

Electrostatic and hydrogen bonding interactions between two oppositely charged amino acids are important determinants of ion channels structures and their disruption can often lead to altered or lost functions (Doyle et al., 1998; Papazian et al., 1995; Yang et al., 1997). The data presented here demonstrate that electrostatic interactions between glutamate 229 and arginine 314 in Kir6.2 are critical for maintaining K_{ATP} channel activity. First, mutation of either charged residue to a neutral alanine, or to an oppositely charged amino acid, induces rapid inactivation of K_{ATP} currents. Second, exchanging the amino acids at positions 229 and 314 restores current stability comparable to the WT channel. Third, currents are stabilized by disulfide bond formation between two engineered cysteine residues at positions 229 and 314 in Kir6.2. Disulfide bond formation between the two cysteine residues indicates that the distance between the α-carbons of the two cysteines is ~5.6 Å (Careaga and Falke, 1992; Krovetz et al., 1997).

Relationship between channel inactivation and channel rundown: the role of SUR1 and Kir6.2

Channel inactivation and the fast-phase of channel rundown both result in rapid current decay. What is the relationship between these two phenomena? One major mechanism accounting for the fast-phase rundown in WT channels is uncoupling

between Kir6.2 and SUR1 due to loss of MgADP at NBF2; channels formed by Kir6.2 alone do not show fast-phase rundown (Ribalet et al., 2000). Our result that channels formed by E229A- or R314A-Kir6.2ΔC25 still inactivate at rates comparable to channels formed by SUR1 and E229A- or R314A-Kir6.2, demonstrates that the rapid current decay induced by the E229A or R314A mutation is due, to a large extent, to an effect on the Kir6.2 tetramer structure itself. However, one cannot exclude the possibility that disrupting the ion pair may also affect Kir6.2-SUR1 interactions, which may in turn contribute to channel inactivation.

Mechanisms of inactivation

Channels in which the ion pair between complementary charges at positions 229 and 314 has been disrupted open upon exposure to ATP-free internal solution, but the current decays rapidly. This current decay can be recovered by three manipulations: 1) reestablishment of the physical interaction between residue 229 and 314 through disulfide bonds; 2) application of PIP_2; or 3) reapplication of ATP, and subsequent washout of ATP. What is the molecular mechanism of inactivation and recovery from inactivation in K_{ATP} channels, and how do ATP and PIP_2 affect these processes?

Membrane phospholipids such as PIP_2 and PIP_3 stimulate K_{ATP} channel activity by increasing the open probability of the channel (Baukrowitz and Fakler, 2000; Baukrowitz et al., 1998; Shyng and Nichols, 1998). Depleting membrane phospholipids or interfering with the interactions between the channels and membrane phospholipids leads to loss of channel activity (Baukrowitz et al., 1998; Gribble et al., 1998a; Liu et al., 2001;

Shyng et al., 2000a; Shyng et al., 2000b; Shyng and Nichols, 1998; Xie et al., 1999). Structure-functional studies suggest that the effect of PIP_2 is mediated largely by direct electrostatic interactions between the cytoplasmic domain of Kir6.2 and phospholipids in the membrane (Baukrowitz et al., 1998; Enkvetchakul et al., 2000; Shyng and Nichols, 1998). Recent biochemical studies which demonstrate binding of phospholipids to recombinant proteins containing the C-terminus of Kir6.2 lend further support to this hypothesis (MacGregor et al., 2002; Wang et al., 2002). However, a role of SUR in channel response to PIP_2 is also evident (Baukrowitz et al., 1998; John et al., 2001; Shyng and Nichols, 1998; Song and Ashcroft, 2001). Channels formed by SUR and Kir6.2 have a much higher open probability and respond to PIP_2 better than channels formed by Kir6.2 alone, suggesting that physical association between SUR and Kir6.2 may facilitate channel interaction with membrane PIP_2. One model consistent with our data is that, in the wild-type SUR1-Kir6.2 channel complex, E229 and R314 are in close proximity and form an ion pair. This ion pair provides structural stability to a channel conformation that facilitates interactions between membrane PIP_2 and channel protein residues that are directly involved in PIP_2 binding (Baukrowitz et al., 1998; Huang et al., 1998; Shyng et al., 2000b; Shyng and Nichols, 1998). Mutations which disrupt the E229/R314 ion pair destabilize channel interaction with PIP_2, effectively lowering the apparent affinity of the channel for PIP_2, which in turn results in channel inactivation and decreased channel activity (Fig.23A). Application of exogenous PIP_2 overcomes the reduced affinity between inactivated channels and PIP_2, and reverses channel inactivation. In the E229C/R314C mutant, by covalently linking the two residues through a disulfide bond, channel interaction with PIP_2 is restabilized and channel

inactivation reversed. It is worth noting that disulfide bond formation between 229C and 314C in the E229C/R314C mutant does not increase channel activity beyond that observed for WT channels under normal conditions (see Fig.20, *bottom trace*). This suggests that although close interactions between the 229 and 314 residues are necessary to stabilize the active states of the channel, other factors, including the concentration of phospholipids in the membrane and the intrinsic affinity of the channel to phospholipids, determine the overall activity of the channel (Baukrowitz et al., 1998; Huang et al., 1998; Shyng et al., 2000a; Shyng and Nichols, 1998; Xie et al., 1999; Zhang et al., 1999).

Exposure to ATP and subsequent removal of ATP reopen inactivated channels, which undergo another round of inactivation (Fig.16A). The ATP recovery effect is unlikely to involve nucleotide hydrolysis at SUR1, protein phosphorylation, or replenishment of membrane PIPs since the effect can be mimicked by the nonhydrolyzable ATP analog, AMP-PNP (Fig.16B). Though speculative, ATP binding to the inactivated channel may induce a conformational change which brings 229 and 314 residues to close proximity resembling that seen in the WT channel, such that channels can again open upon subsequent removal of ATP (Fig.23A). Consistent with this idea, in the E229C/R314C channels, covalent bonding between 229 and 314 does not prevent the channel from entering the ATP-bound closed state or from retransitioning back to the open state (Fig.20), implying that in WT channels the salt bridge is maintained in the ATP-bound closed state. Further, simultaneous application of DTT (1 mM) and ATP (5 mM) to the E229C/R314C channels abolishes the ability of

ATP to recover channels from inactivation (not shown), implicating that the two residues form a disulfide bond in the ATP-bound state. Of note, the recovery effect of ATP appears to require SUR1; inactivation of channels formed by E229A- or R314A-Kir6.2ΔC25 alone can not be recovered by exposure to ATP and subsequent removal of ATP (Fig.16C, *left*). Future studies will determine the mechanism by which SUR1 mediates the reactivation effect of ATP.

Structural implications

The K_{ATP} channel pore is formed by assembly of four Kir6.2 subunits. The electrostatic interaction between E229 and R314 could occur within a single Kir6.2 subunit or between two subunits. The results from experiments using Kir6.2 tandem dimers with mutations introduced into specific positions indicate that the E229-R314 ion pair is formed between two adjacent Kir6.2 subunits rather than within a single subunit. In the EE-RR dimer channels, in which intrasubunit ion pair formation is prohibited but intersubunit ion pair formation is allowed, K^+ currents remain relatively stable in ATP-free solutions. On the other hand, the RE-ER dimer, which prohibits intersubunit ion pair formation but allows intrasubunit ion pair formation, forms channels that display current decay similar to inactivation. The conclusion that the E229/R314 ion pair is formed between two adjacent Kir6.2 subunits is consistent with the recently published cytoplasmic domain structure of GIRK1 (Nishida and MacKinnon, 2002), which shares significant sequence homology (~40%) with Kir6.2. In the structure of a single GIRK1 subunit, the E229 and R314 corresponding residues, E242 and R326, are located immediately before the βE strand and at the beginning of

the βK strand, respectively (Fig.23B, *left*). Such opposite orientations make it highly unlikely for the two residues to form an intrasubunit salt bridge. Rather, the two residues likely form an intersubunit ion pair, as one would predict from the GIRK1 tetramer model, in which E242 from one subunit lies in close proximity of R326 from the adjacent subunit (Fig.23B, *right*). In the AMPA-type glutamate receptor, alterations in the strength of subunit-subunit interfaces have been shown to underlie receptor desensitization (Sun et al., 2002). We speculate that the E229/R314 ion pair may be important in maintaining the quaternary structure of the Kir6.2 tetramer and/or its interaction with SUR1, and that disruption of this ion pair may cause inactivation of K_{ATP} channels by destabilizing subunit-subunit interactions. In this regard, it would be important to determine in the future whether R192 and R301 are also involved in subunit-subunit interactions by forming noncovalent chemical bonds, such as hydrogen bonds, with residues from adjacent Kir6.2 or SUR1 subunits.

In summary, our study demonstrates the critical role of an inter-subunit ion pair formed by two residues in the C-terminus of Kir6.2 in maintaining K_{ATP} channel activity. The study provides important insight into the structure of the C-terminal region of Kir6.2. The two residues at positions homologous to E229 and R314 of Kir6.2 are conserved in Kir1, 2, and 3. And like K_{ATP}, the activities of these channels are modulated by membrane PIPs (Huang et al., 1998; Lopes et al., 2002; Zhang et al., 1999). Future studies will determine whether an ion pair similar to the one we reported here plays a role in the gating of other Kir channels.

Acknowledgements We thank Dr. Anthony Auerbach for helpful suggestions on

the experiments. We are grateful to Drs. John Adelman, Peter H. Larsson, and Colin Nichols for comments on the manuscript, and to Drs. Joe Bryan and S. Seino for providing the hamster SUR1 and mouse Kir6.2 cDNA . This work was supported by National Institutes of Health Grant DK57699 (to S.-L. S.), a research grant from the March of Dimes Birth Defects Foundation (to S.-L. S.), and a research grant from the Juvenile Diabetes Foundation (to S.-L. S.).

Table III. Current stability of channels formed by SUR1 and Kir6.2 monomers

Mutation	% Current decay in 20 seconds	Inactivation time constant[1] τ_i (seconds)	Number of patches (n)
WT	10.72 ± 3.66	N/A	10
E229A	81.19 ± 5.39	6.64 ± 1.80	7
R192A	78.24 ± 5.92	4.79 ± 1.34	9
R301A	>99.00	0.32 ± 0.03	8
R314A	94.98 ± 1.89	3.08 ± 0.43	8
E229R	92.94 ± 2.22	3.02 ± 0.31	3
R192E	84.83 ± 1.10	5.19 ± 0.67	9
R301E	No currents	N/A	16
R314E	78.15 ± 3.44	1.28 ± 0.13	3
E229R/R192E	66.06 ± 3.98	7.70 ± 0.06	11
E229R/R301E	No currents	N/A	9
E229R/R314E	6.95 ± 3.27	N/A	5
E229C	75.14 ± 7.65	4.83 ± 0.96	7
R314C	No currents	N/A	20
E229C/R314C	46.98 ± 5.96	N/A	6

[1]Values were given only for those mutants whose time course of inactivation could be fit well by a single exponential.

Table IV. Current stability of channels formed by SUR1 and Kir6.2 tandem dimers

Mutation	% Current decay in 40 seconds	Number of patches (n)
WT-WT (ER-ER) dimer	6.08 ± 2.19	17
AR-AR dimer	48.35 ± 6.54	15
EE-RR dimer	14.94 ± 6.73	8
ER-RE dimer	38.05 ± 6.07	14

Figure 15

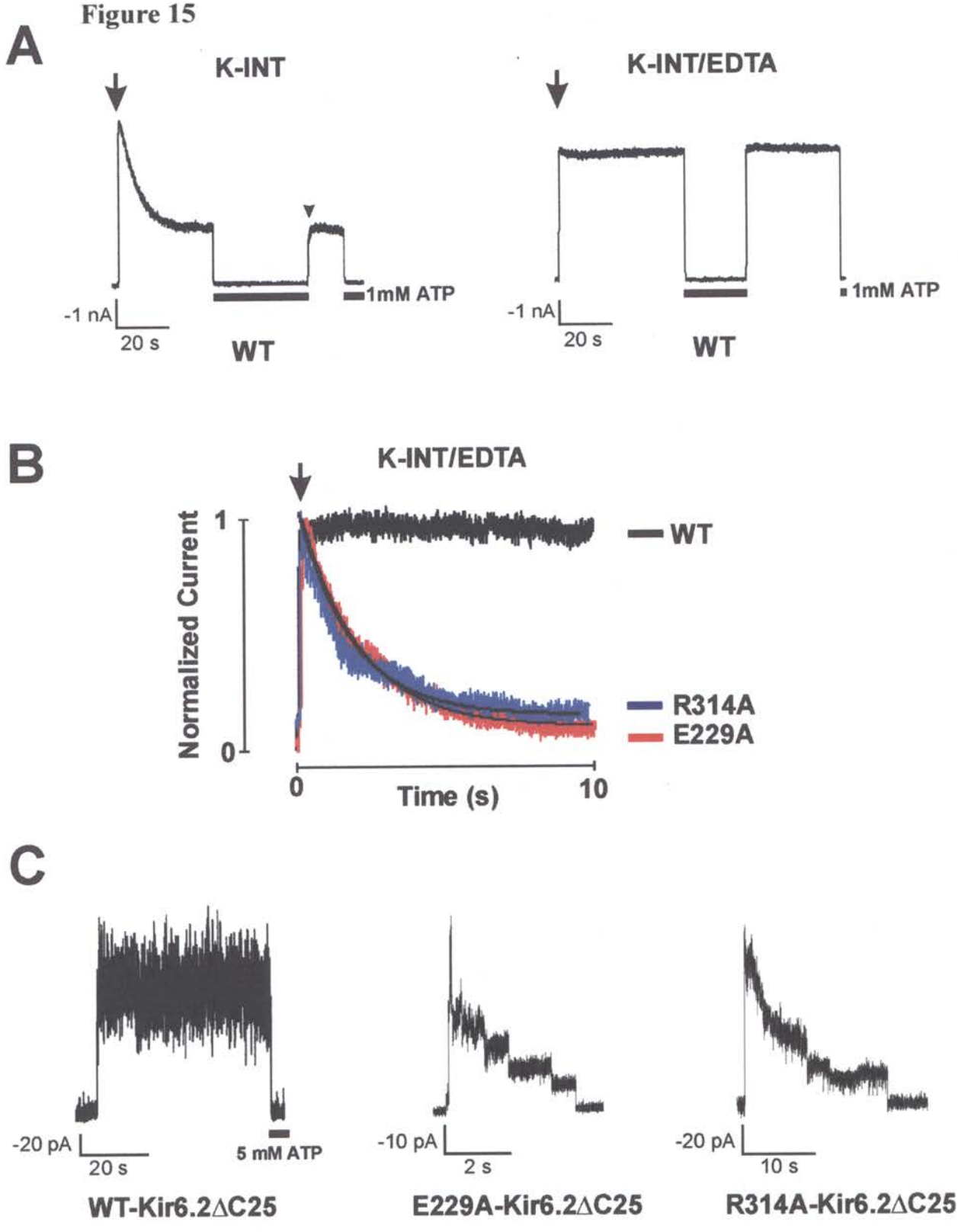

Lin et al. Figure1

Figure 15. Identification of E229A as an inactivation mutant. (A) WT channel activities recorded in inside-out membrane patches using K-INT (*left*) or K-INT + 1mM EDTA (*right*) bath solution. Arrows indicate patch excision. Channel rundown is dramatically reduced by the addition of 1 mM EDTA to the bath solution. (B) Using K-INT/EDTA solution, inactivation is observed in the E229A mutant channels. Representative currents recorded from inside-out membrane patches containing wild-type, the E229A, or the R314A mutant channels are superimposed for comparison. The arrow indicates patch excision into K-INT/EDTA. The kinetics of inactivation of the E229A channels are similar to the R314A channels. The inactivation time course of both E229A and R314A channels was fitted by a single exponential (indicated by the black curves). (C) Channels formed by WT-Kir6.2ΔC25 in the absence of SUR1 exhibited stable activities after patch excision into K-INT/EDTA (*left*). In contrast, channels formed by E229A-Kir6.2ΔC25 (*middle*) or R314A-Kir6.2ΔC25 (*right*) in the absence of SUR1 showed rapid current decay. Currents in this and subsequent figures were recorded at -50 mV membrane potential. Inward currents are shown as upward deflections.

Figure 16

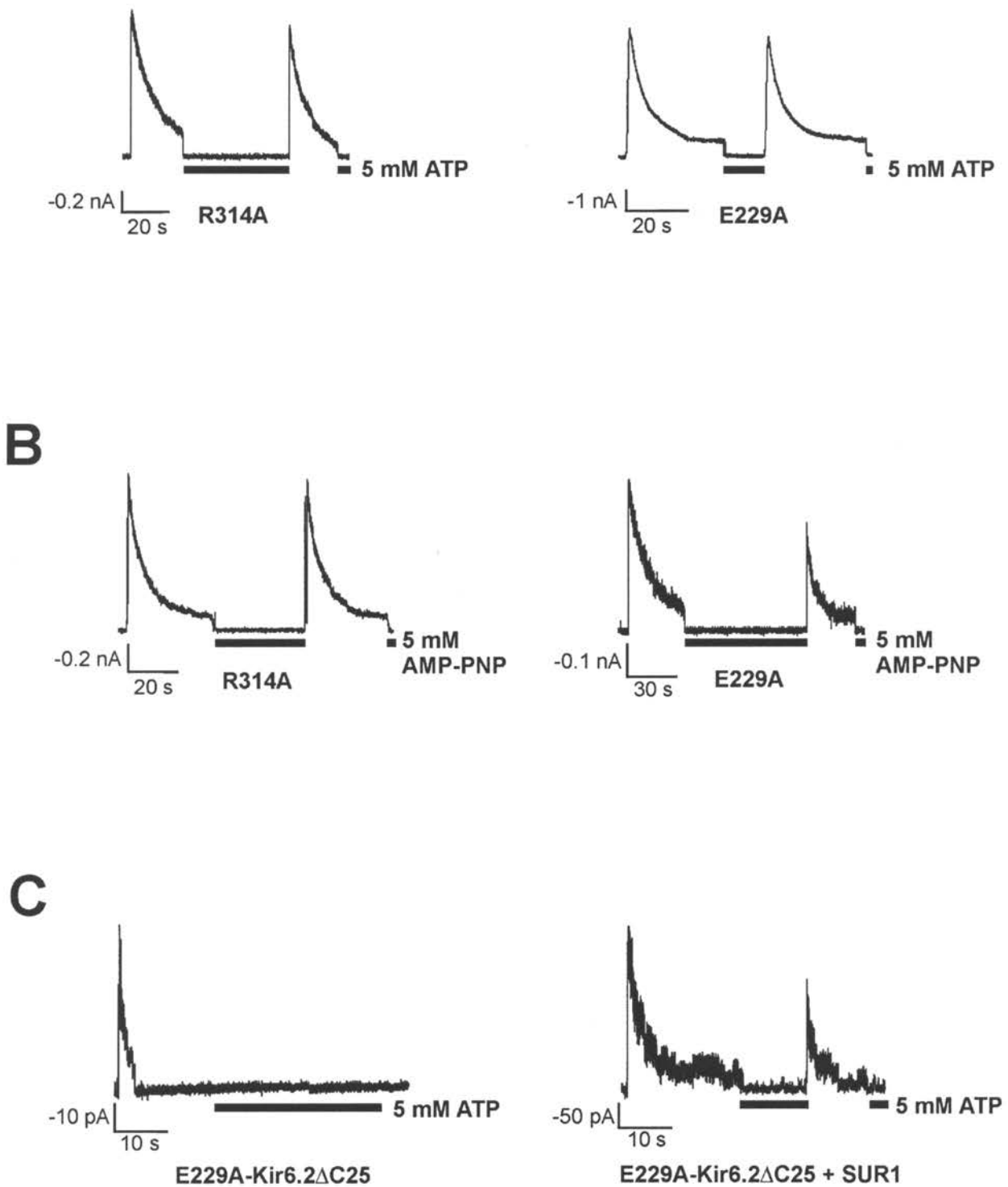

Lin et al. Figure2

Figure 16. Channel inactivation can be recovered by exposure to ATP and subsequent washout of ATP. (A) Inactivated R314A (*left*) and E229A (*right*) channels were reactivated by exposure to ATP (5 mM) and subsequent washout of ATP. (B) A non-hydrolyzable ATP analog, AMP-PNP mimicked the reactivation effect of ATP in both R314A (*left*) and E229A (*right*) channels. (C) The reactivation effect of ATP was not observed in channels formed by E229A-Kir6.2ΔC25 alone (*left*), but was retained in channels formed by E229A-Kir6.2ΔC25 in the presence of SUR1 (*right*).

Figure 17

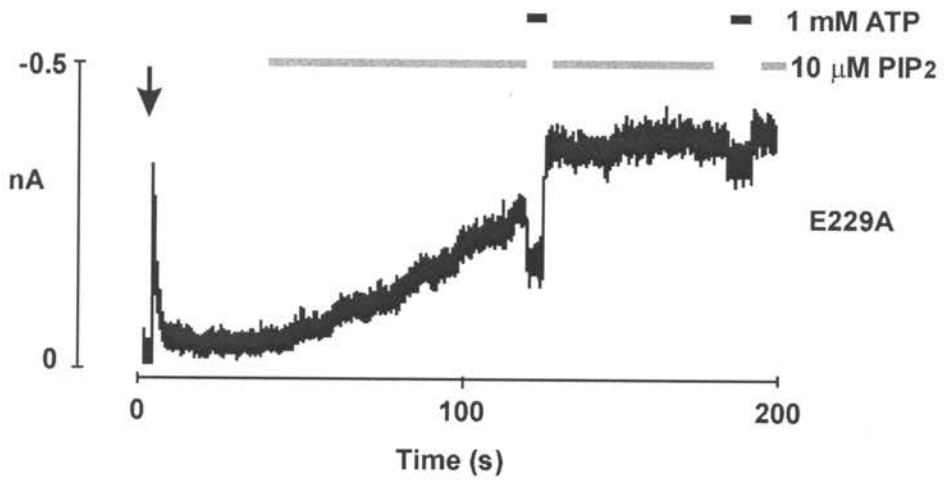

Lin et al., Figure 3

Figure 17. Inactivation of E229A mutant channels is reversed by PIP_2. Application of PIP_2 (10 μM) reversed inactivation and stimulated channel activity; it also decreased the ATP sensitivity of the channel, as was previously reported for WT channels (Baukrowitz et al., 1998; Shyng and Nichols, 1998).

Figure 18

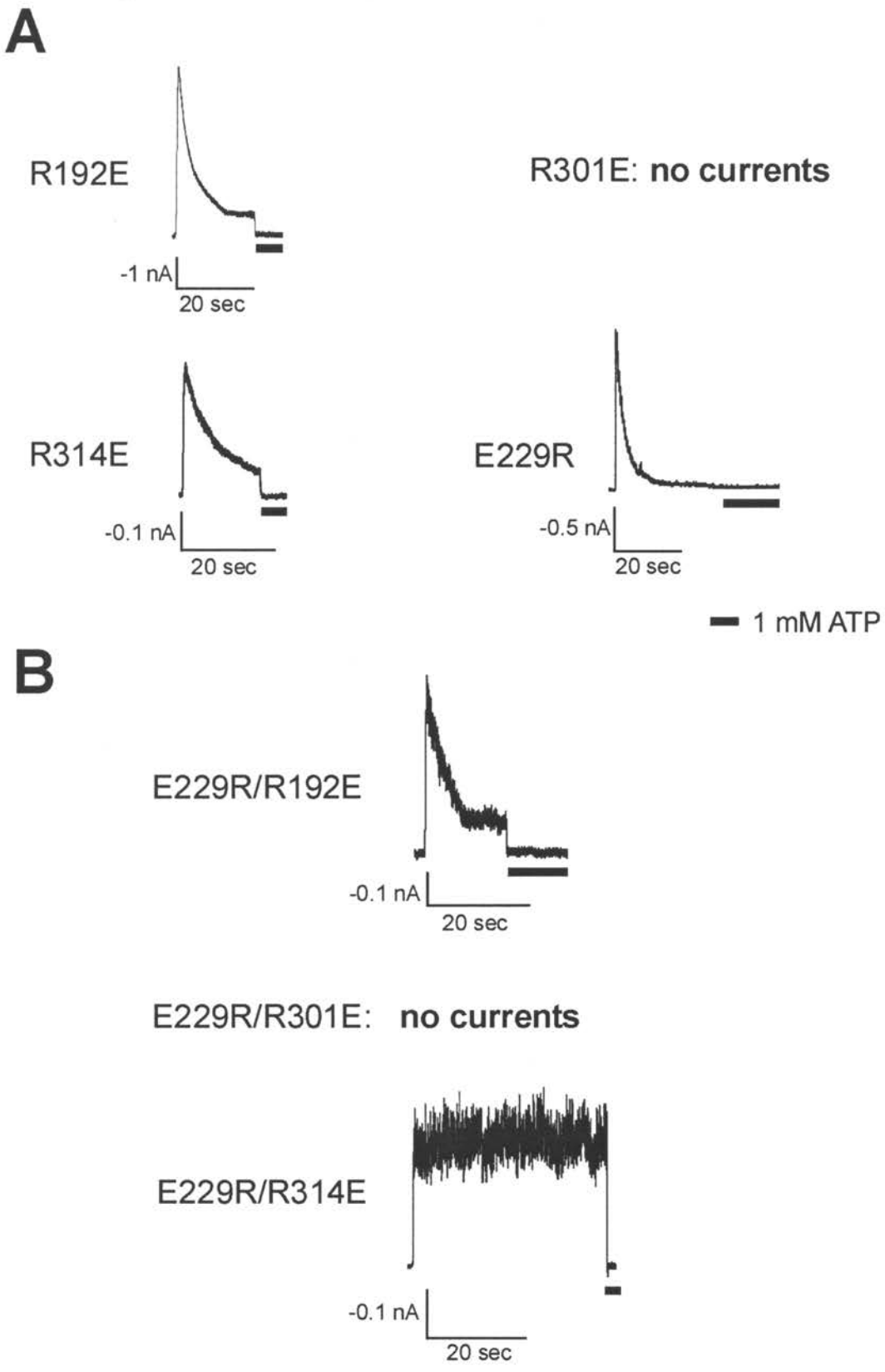

Lin et al. Figure 4

Figure 18. Open state stability is retained in the E229R/R314E double reverse mutant channels. (A) Representative currents recorded from inside-out membrane patches containing R192E, R301E, R314E, or E229R mutant channels. R301E channels did not give rise to measurable currents. All the other three mutant channels exhibited inactivation. (B) Currents recorded from membrane patches isolated from cells expressing the double charge reversal mutant E229R/R192E, E229R/R301E, or E229R/R314E. No currents were detected for the E229R/R301E channels. The E229R/R192E mutant channels still showed inactivation. In contrast, the E229R/R314E double mutant did not inactivate and behaved like WT channels.

Figure 19

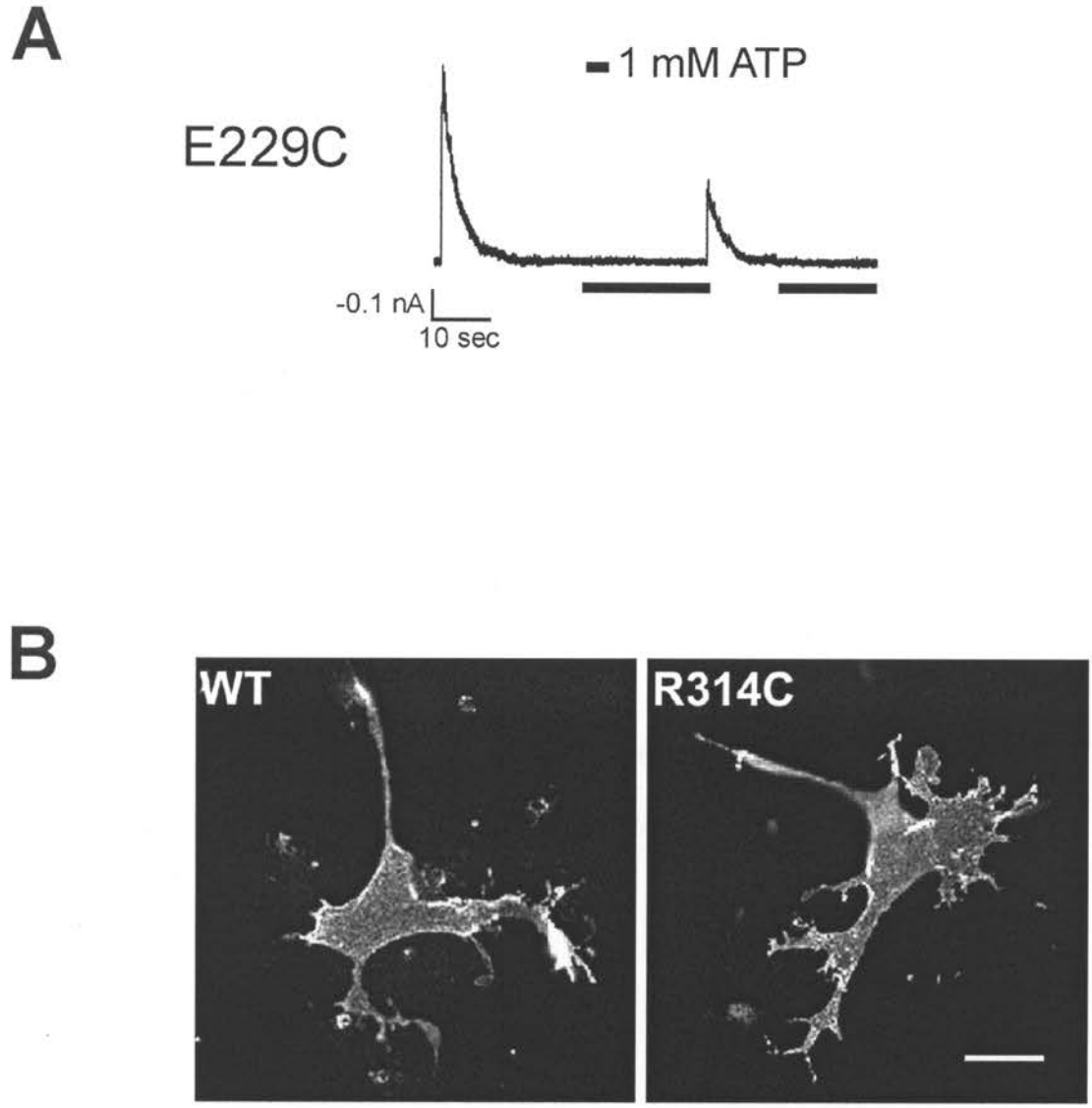

Lin et al. Figure 5

Figure 19. Characterization of the E229C and the R314C mutant channels. (A) A representative current trace recorded from an inside-out membrane patch containing the E229C mutant channels. The channels displayed inactivation similar to that observed in the E229A and E229R channels upon patch excision into the K-INT/EDTA solution. Exposure to 1 mM ATP (indicated by black bars below the recordings) partially reactivated the channels, which again underwent rapid inactivation. (B) The R314C Kir6.2 mutant protein is expressed and incorporated into the K_{ATP} channel complex. Surface immunofluorescent staining of cells co-expressing FLAG-tagged SUR1 and either the WT or the R314C mutant Kir6.2. Immunostaining was carried out in living cells at 4°C using the M2 anti-FLAG monoclonal antibody followed by Cy3-conjugated secondary antibody. Surface labeling of the FLAG-SUR1 was observed in both cells co-expressing the WT or the R314C mutant Kir6.2, demonstrating that the R314C Kir6.2 is properly incorporated into the K_{ATP} channel complex.

Figure 20

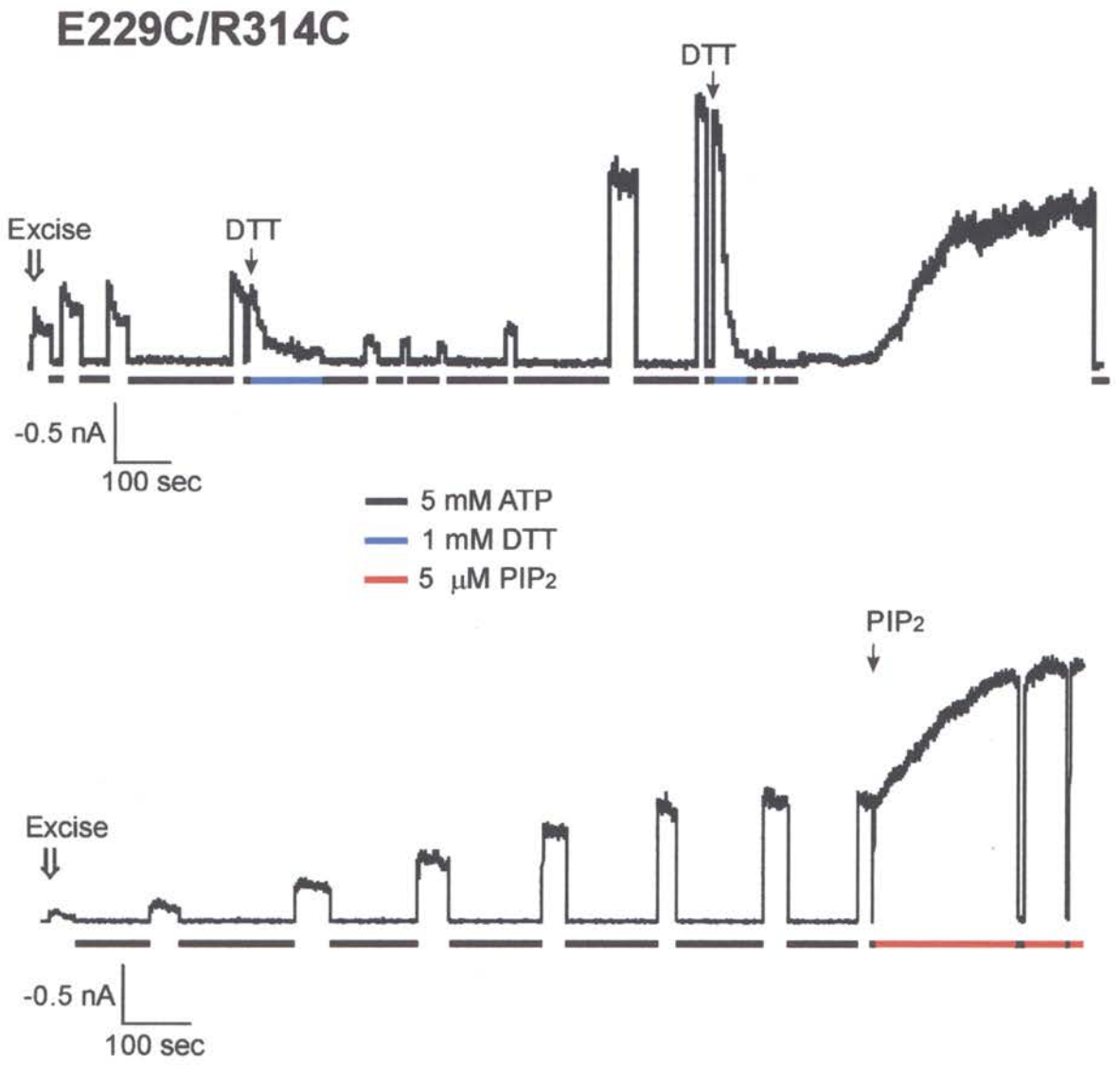

Lin et al. Figure 6

Figure 20. Disulfide bond formation between C229 and C314 in the E229C/R314C mutant channel stabilizes channel opening. Currents recorded from two separate membrane patches containing the E229C/R314C mutant channels. Upon patch excision into K-INT/EDTA, the channel exhibited low open probability and mild inactivation. However, the current gradually increased in amplitude and stability. Exposure of the patch to 5 mM ATP (indicated by the black bars underneath the current traces) accelerated the current reactivation process. *Top trace*: Application of 1 mM DTT (in K-INT/EDTA, indicated by the gray bar) after current stabilization induced rapid inactivation of the channel in a reversible manner, indicating that the current stabilization was due to spontaneous disulfide bond formation. *Bottom trace*: After the current has reached the maximum, application of 5 μM PIP_2 (see Materials and Methods) further stimulated channel activity by ~2-fold.

Figure 21

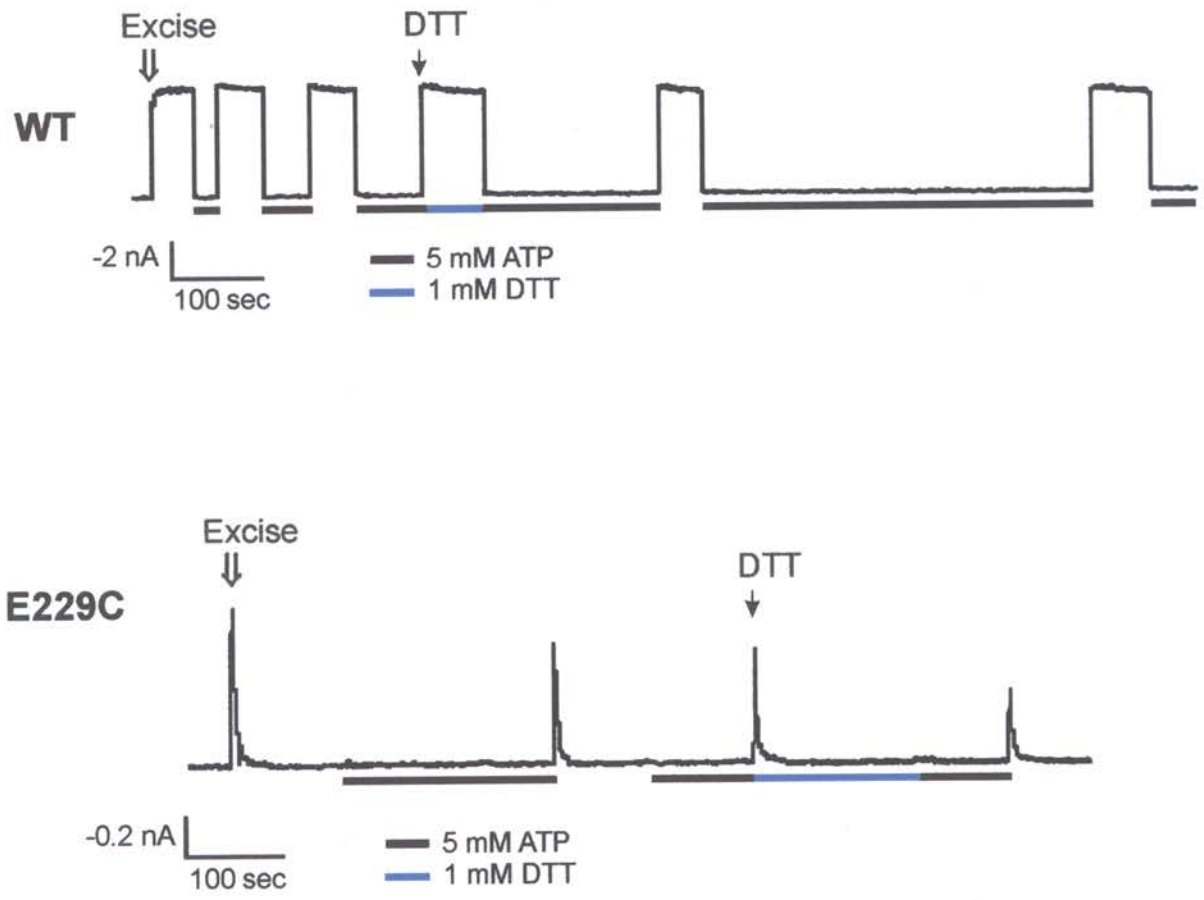

Lin et al. Figure 7

Figure 21. Disulfide bond formation that promotes channel opening in the E229C/R314C mutant does not involve endogenous cysteines. Representative recordings of WT and E229C channels showing the lack of time-dependent current increase in K-INT/EDTA and the lack of response to DTT.

Figure 22

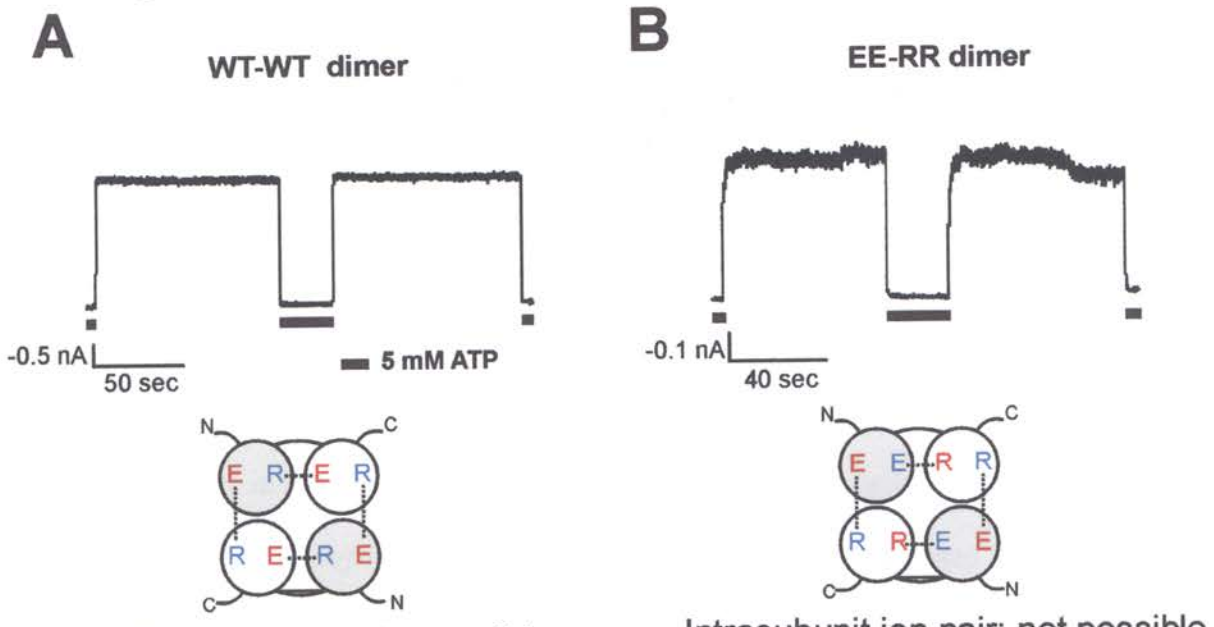

Lin et al. Figure 8

Figure 22. The E229/R314 ion pair is formed between two adjacent Kir6.2 subunits. (A) Currents recorded from a membrane patch containing Kir6.2 WT-WT (or ER-ER) dimer channels in the K-INT/EDTA bath solution. The dimer channel currents were stable and were inhibited by 5 mM ATP. Below the current trace is a cartoon illustrating the expected tetramer formed by the tandem dimer. The 229 residue in each subunit is shown in red and the 314 residue shown in blue. For each tandem dimer, the leading subunit is in grey and the trailing subunit in white. The expected ion pairs are connected by dotted lines. (B) In the EE-RR dimer channels, the possibility of ion pair formation in a single subunit is excluded. The channels behaved similarly to the WT-WT dimer channels; the rate of current decay is only slightly faster (see Table IV). (C) In the AR-AR dimer channels, neither intra- nor inter-subunit ion pair formation is possible. Currents from these channels decayed much faster than the WT-WT dimer channels, as expected. (D) In the RE-ER dimer channels, the possibility of ion pair formation between two adjacent subunits is excluded. Currents from these channels decayed much faster than the WT-WT, or the EE-RR dimer channels (see Table IV).

Figure 23

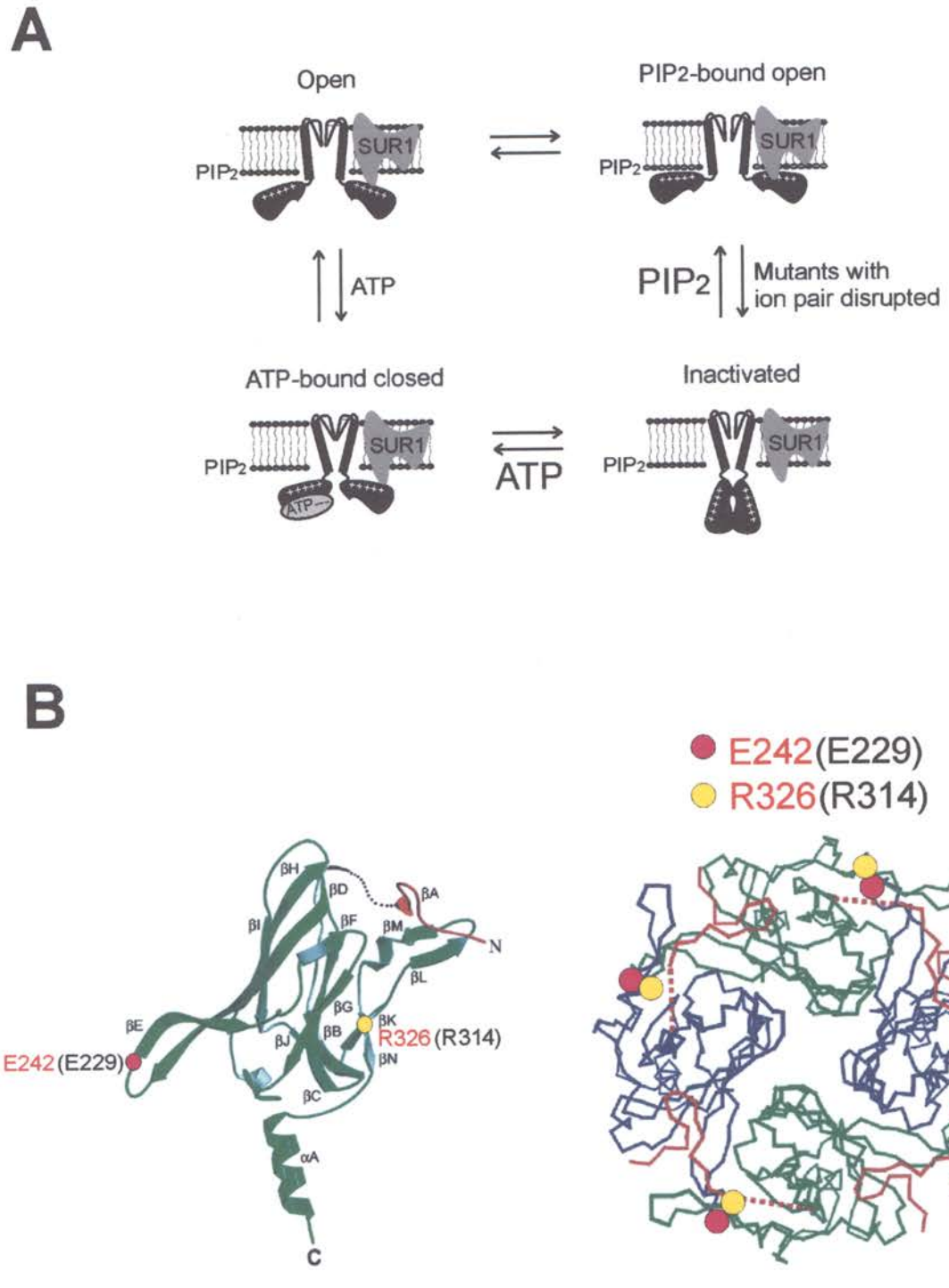

Lin et al. Figure 9

Figure 23. Proposed model for K_{ATP} channel inactivation. (A) Cartoon illustrating proposed physical relationships between the channel, ATP, and PIP_2 in the inactivation mutants. Disruption of the ion pair causes a structural change in the Kir6.2 tetramer, and possibly also a change in Kir6.2/SUR1 interactions, leading to channel inactivation. These structural changes can be overcome by increasing membrane PIP_2, or by ATP binding to the channel in a SUR1-dependent manner. Note that the four states presented should not be taken as detailed kinetic gating states of the channel, and that the transitions between the states are indicated only to illustrate the recovery effects of PIP_2 and ATP on inactivated channels. (B) Positions of the two ion pair-forming corresponding residues in the single (*left*) and tetramer (*right*) GIRK1 channel structures (Nishida and MacKinnon, 2002). Residue numbering in Kir6.2 is in black, and in GIRK1, red. The Kir6.2-E229 corresponding residue is shown as pink circles, and R314 corresponding residues as yellow circles.

CHAPTER THREE

A NOVEL *KCNJ11* MUTATION ASSOCIATED WITH CONGENITAL HYPERINSULINISM REDUCES THE INTRINSIC OPEN PROBABILITY OF β-CELL ATP-SENSITIVE POTASSIUM CHANNELS

Yu-Wen Lin[1], Courtney MacMullen[2], Arupa Ganguly[2], Charles A. Stanley[2], and Show-Ling Shyng [1]

From the Center for Research on Occupational and Environmental Toxicology, Oregon Health & Science University, Portland, OR 97239,[1] and Division of Endocrinology/Diabetes, The Children's Hospital of Philadelphia, Philadelphia, Pennsylvania, 19104. [2]

The work described in this chapter is published in ***Journal of Biological Chemistry*** (281), 2006. Courtney MacMullen and Arupa Ganguly from Dr.Charles A. Stanley's lab did the work of gene screening from patients and identify this novel mutation.

.

ABSTRACT

The β-cell ATP-sensitive potassium (K_{ATP}) channel controls insulin secretion by linking glucose metabolism to membrane excitability. Loss of K_{ATP} channel function due to mutations in *ABCC8* or *KCNJ11*, genes that encode the sulfonylurea receptor 1 or the inward rectifier Kir6.2 subunit of the channel, is a major cause of congenital hyperinsulinism. Here, we report identification of a novel *KCNJ11* mutation associated with the disease that renders a missense mutation, F55L, in the Kir6.2 protein. Mutant channels reconstituted in COS cells exhibited wild-type like surface expression level and normal sensitivity to ATP, MgADP, and diazoxide. However, the intrinsic open probability of the mutant channel was greatly reduced, by ~10-fold. This low open probability defect could be reversed by application of phosphatidylinositol 4,5-bisphosphates or oleoyl CoA to the cytoplasmic face of the channel, indicating that reduced channel response to membrane phospholipids and/or long chain acyl CoAs underlies the low intrinsic open probability in the mutant. Our findings reveal a novel molecular mechanism for loss of K_{ATP} channel function and congenital hyperinsulinism, and support the importance of phospholipids and/or long chain acyl CoAs in setting the physiological activity of β-cell K_{ATP} channels. The F55L mutation is located in the slide helix of Kir6.2. Several permanent neonatal diabetes-associated mutations found in the same structure have the opposite effect of increasing intrinsic channel open probability. Our results also highlight the critical role of the Kir6.2 slide helix in determining the intrinsic open probability of K_{ATP} channels.

INTRODUCTION

Pancreatic ATP-sensitive potassium (K_{ATP}) channels play a key role in glucose-stimulated insulin secretion by coupling glucose metabolism to β-cell excitability (Aguilar-Bryan and Bryan 1999; Ashcroft and Gribble 1999; Huopio, Shyng et al. 2002). Each K_{ATP} channel consists of four pore-forming Kir6.2 subunits encoded by *KCNJ11* and four regulatory sulfonylurea receptor 1 (SUR1) receptors encoded by *ABCC8* (Clement, Kunjilwar et al. 1997; Inagaki, Gonoi et al. 1997; Shyng and Nichols 1997). The activity of K_{ATP} channels is subject to regulation by intracellular nucleotides ATP and ADP (Ashcroft 1988; Aguilar-Bryan and Bryan 1999; Tarasov, Dusonchet et al. 2004). ATP inhibits channel activity by binding to the Kir6.2 subunit, whereas ADP, in complex with Mg^{2+}, stimulates channel activity by interacting with SUR1. Changes in ATP and ADP concentrations during glucose metabolism are thus linked to K_{ATP} channel activity, which in turn controls β-cell membrane potential and insulin secretion. As such, genetic mutations in Kir6.2 or SUR1 that alter channel sensitivity to ATP or MgADP impair the ability of K_{ATP} channels to convert metabolic signals to electrical signal, resulting in insulin secretion diseases. In addition to intracellular nucleotides, both long-chain acyl CoAs and membrane phosphoinositides have been shown to stimulate channel activity and reduce channel sensitivity to ATP inhibition by interacting with Kir6.2 (Baukrowitz, Schulte et al. 1998; Branstrom, Leibiger et al. 1998; Gribble, Proks et al. 1998; Shyng and Nichols 1998; Riedel, Boora et al. 2003;

Schulze, Rapedius et al. 2003; Schulze, Rapedius et al. 2003; Branstrom, Aspinwall et al. 2004; Riedel and Light 2005). However, compared to intracellular nucleotides, the role of membrane phosphoinositides or long-chain acyl CoAs in controlling K_{ATP} channel activity in physiological and pathological conditions is less clear and still under investigation (Tarasov, Dusonchet et al. 2004).

Congenital hyperinsulinism (CHI) is a disease characterized by persistent insulin secretion despite life-threatening hypoglycemia (Glaser 2000; Aguilar-Bryan, Bryan et al. 2001; Huopio, Shyng et al. 2002; Stanley 2002; Dunne, Cosgrove et al. 2004). Dominant or recessive mutations in *ABCC8* or *KCNJ11* that reduce or abolish channel activity are the major genetic cause of the disease (Glaser 2000; Aguilar-Bryan, Bryan et al. 2001; Huopio, Shyng et al. 2002; Stanley 2002; Dunne, Cosgrove et al. 2004). Most mutations identified to date reside in the SUR1 subunit (Nestorowicz, Glaser et al. 1998; Aguilar-Bryan and Bryan 1999; Sharma, Crane et al. 2000; Huopio, Shyng et al. 2002). Functional studies of a considerable number of missense SUR1 mutations have established loss of channel response to MgADP and impaired expression of functional channels at the cell surface as two major defects (Nichols, Shyng et al. 1996; Shyng, Ferrigni et al. 1998; Matsuo, Trapp et al. 2000; Magge, Shyng et al. 2004). Relatively few mutations have been reported in the Kir6.2 subunit (Nestorowicz, Inagaki et al. 1997; Aguilar-Bryan and Bryan 1999); these mutations either introduce a premature stop codon that results in truncated nonfunctional Kir6.2 protein or introduce missense mutations that cause rapid degradation of the protein (Nestorowicz, Inagaki et al. 1997; Crane and Aguilar-Bryan 2004). Here, we report the identification and functional

characterization of a dominant CHI-associated Kir6.2 missense mutation F55L (See Figure 38 for its position on a homologous KirBac1.1 structure). We show that this mutation greatly reduces the open probability of K_{ATP} channels in intact cells without affecting channel expression. The low channel activity is likely due to reduced channel response to membrane phosphoinositides and/or long-chain acyl CoAs, as application of exogenous PIP_2 or oleoyl CoA restores channel activity to that seen in wild-type (WT) channels. Our finding identifies impaired K_{ATP} channel response to phospholipids and/or long-chain acyl CoAs as a novel mechanism underlying congenital hyperinsulinism.

MATERIALS AND METHODS

Clinical and genetic analyses-Tests of acute insulin responses (AIR) to calcium (2 mg/kg), leucine (15 mg/kg), glucose (0.5 gm/kg), and tolbutamide (25 mg/kg) sequentially infused intravenously at intervals of one hour were carried out as previously described (Magge, Shyng et al. 2004). Peripheral blood was obtained for isolation of genomic DNA from the proband, a male infant, and his father. Direct sequencing of DNA from the patient and family members was done as previously described (Magge, Shyng et al. 2004).

Molecular biology - Rat Kir6.2 cDNA is in pCDNAI/Amp vector (a generous gift from Dr. Carol A. Vandenberg) and SUR1 in pECE. Site-directed mutagenesis was carried out using the QuickChange site-directed mutagenesis kit (Strategene) and the mutation

confirmed by sequencing. Mutant clones from two independent PCR reactions were analyzed to avoid false results caused by undesired mutations introduced by PCR.

$^{86}Rb^{+}$ efflux assay - COSm6 cells were plated onto 35 mm culture dishes and transfected with wild-type SUR1 and control or mutant rat Kir6.2 cDNA using FuGene. Cells were incubated for 24 hours in culture medium containing ^{86}RbCl (1μCi/ml) 2 days after transfection. Before measurement of $^{86}Rb^{+}$ efflux, cells were incubated for 30 min at room temperature in Krebs-Ringer solution with metabolic inhibitors (2.5 μg/ml oligomycin and 1 mM 2-deoxy-D-glucose). At selected time points, the solution was aspirated from the cells, and replaced with fresh solution. At the end of a 40 min period, cells were lysed. The $^{86}Rb^{+}$ in the aspirated solution and the cell lysate was counted. The percentage efflux at each time point was calculated as the cumulative counts in the aspirated solution divided by the total counts from the solutions and the cell lysates (Shyng, Ferrigni et al. 1998).

Western blotting and chemiluminescence assay - Cell surface expression level of the mutant channel was assessed by Western blot and by a quantitative chemiluminescence assay using a SUR1 that was tagged with a FLAG-epitope (DYKDDDDK) at the N-terminus (fSUR1), as described previously (Taschenberger, Mougey et al. 2002). COSm6 cells grown in 35 mm dishes were transfected with 0.4 μg rat Kir6.2 and 0.6 μg fSUR1 and lysed 48-72 hours post-transfection in 20 mM HEPES, pH 7.0/5 mM EDTA/150 mM NaCl/1% Nonidet P-40 (IGAPEL) with Complete^{TR} protease inhibitors (Roche Applied Science, Indianapolis, IN). Proteins in the cell lysate were separated by

SDS/PAGE (7.5% for SUR1 and 12% for Kir6.2), transferred to nitrocellulose membrane, and analyzed by incubation with appropriate primary antibodies followed by horseradish peroxidase (HRP)-conjugated secondary antibodies (Amersham Biosciences, Piscataway, NJ), and visualized by enhanced chemiluminescence (Super Signal West Femto; Pierce, Rockford, IL). The primary antibodies used are: M2 mouse monoclonal anti-FLAG antibody for fSUR1 (Sigma, St. Louis, MO) and rabbit polyclonal anti-Kir6.2 for Kir6.2 (from Santa Cruz Biotechnology, Santa Cruz, CA). For chemiluminescence assay, cells were fixed with 2% paraformaldehyde for 30 min at 4°C. Fixed cells were preblocked in PBS+0.1% BSA for 30 min, incubated in M2 anti-FLAG antibody (10 μg/ml) for an hour, washed 4x30 min in PBS+0.1% BSA, incubated in HRP-conjugated anti-mouse (Jackson, 1:1000 dilution) for 20 min, and washed again 4x30 min in PBS+0.1% BSA, all at room temperature. Chemiluminescence of each dish was quantified in a TD-20/20 luminometer (Turner Designs) following 15 sec incubation in Power Signal Elisa luminol solution (Pierce). All steps after fixation were carried out at room temperature.

Electrophysiology - Patch-clamp recordings were performed in the inside-out configuration as previously described (Taschenberger, Mougey et al. 2002). Briefly, COSm6 cells were tranfected with cDNA encoding WT or mutant channel proteins, as well as cDNA for the green fluorescent protein (GFP) to help identify positively transfected cells. Patch-clamp recordings were made 36-72 hours post-transfection. Micropipettes were pulled from non-heparinized Kimble glass (Fisher Scientific) with resistance typically ~1-2 MΩ. The bath (intracellular) and pipette (extracellular)

solution (K-INT) had the following composition: 140 mM KCl, 10 mM K-HEPES, 1 mM K-EGTA, pH 7.3. ATP and ADP were added as the potassium salt. For measuring ATP^{4-} sensitivity, 1 mM EDTA was included in K-INT to prevent channel rundown (Lin, Jia et al. 2003). All currents were measured at a membrane potential of -50 mV (pipette voltage = +50 mV) and inward currents shown as upward deflections. Data were analyzed using pCLAMP software (Axon Instrument). Off-line analysis was performed using Microsoft Excel programs. The MgADP or diazoxide response was calculated as the current in a K-INT solution containing either 0.1 mM ATP and 0.5 mM ADP or 0.1 mM ATP and 0.3 mM diazoxide (both with1 mM free Mg^{2+}), relative to that in plain K-INT solution.

Data Analysis - ATP dose response curve fitting was performed with Origin 6.1. Channel intrinsic P_o was estimated from stationary fluctuation analysis of short recordings (~ 1 second) of macroscopic currents in KINT/EDTA solution or KINT/EDTA plus 5 mM ATP (Neher and Stevens 1977; Sigworth 1980; Shyng, Ferrigni et al. 1997). Currents were filtered at 1 kHz. Mean current (I) and variance (σ^2) in the absence of ATP were obtained by subtraction of the mean current and variance in 5 mM ATP. Single channel current (i) was assumed to be -3.6 pA at –50 mV (corresponding to single channel conductance of 72 pS). P_o was then calculated using the following equation: $P_o = 1 - (\sigma^2/[i*I])$. Statistical analysis was performed using independent two-population two-tailed Student's *t*-test.

RESULTS

Patient history and identification of the F55L missense mutation in Kir6.2

The proband was a male infant diagnosed with persistent hypoglycemia and hyperinsulinism at 12 hours of age (14 μU/ml with a blood glucose level of 31 mg/dL; 13 μU/ml with blood glucose of 24 mg/dL; normal < 3 μU/ml). Tests of acute insulin responses to secretogogues were performed in the proband and his father and results compared to hyperinsulinism patients with recessive ABCC8 null mutations (3992-9G→A and □F1388) and glutamate dehydrogenase (GDH) mutations and normal adult controls (Henwood, Kelly et al. 2005). The proband showed a pattern of responses similar to those seen in patients with recessive ABCC8 mutations, an abnormal positive insulin response to calcium stimulation, as well as possibly diminished responses to glucose and tolbutamide (Table V). The father of the proband had mildly abnormal acute insulin responses, including abnormally increased insulin responses to calcium and leucine, and a lower response to tolbutamide than to glucose stimulation. This pattern of insulin responses resembles that seen in children with hyperinsulinism due to recessive ABCC8 and KCNJ11 mutations which retain partial channel activity (Henwood, Kelly et al. 2005). Subsequent genetic testing revealed that the proband and the father shared a 165C→A mutation in the KCNJ11, resulting in a missense mutation, F55L, in the Kir6.2 subunit of the K_{ATP} channel. Of note, although the father showed mildly abnormal acute insulin responses as well as evidence of protein-sensitive hypoglycemia (blood glucose nadir of 63 mg/dL at 60 min following ingestion of oral protein; normals > 70 mg/dL), he demonstrated normal fasting blood glucose (84 mg/dL after 12 hr fast). The more severe hypoglycemia seen in the proband, at least in the

newborn period, is likely attributed in part to perinatal stress, as has been reported previously (Collins and Leonard 1984; Collins, Leonard et al. 1990).

Treatment with diazoxide at 15 mg/kg/day rapidly improved the hypoglycemia in the proband. Within 4 days, he was able to fast 12 hr without hypoglycemia. Periodic reassessments up to 4 years of age showed that, while on treatment with a low dose of diazoxide at 4 mg/kg/day, the proband was able to fast successfully for 12-15 hours without hypoglycemia and did not develop hypoglycemia in response to an oral protein tolerance test (1 gm/kg).

The F55L mutation reduces open probability of K_{ATP} channels

To investigate how the F55L mutation in Kir6.2 affects channel function, we reconstituted the mutant channels in COS cells by co-expression of F55L-Kir6.2 and SUR1. To first confirm reduction or loss of channel activity in intact cells during glucose deprivation, as one would predict based on the disease phenotype, we performed $^{86}Rb^{+}$ efflux assays to assess channel activity in response to metabolic poisoning. As shown in Fig.24A, homomeric mutant channels are much less active upon metabolic inhibition compared to WT channels. Because the F55L mutation is heterozygous in the patient, we simulated the heterozygous state by co-expressing WT and mutant Kir6.2 at 1:1 cDNA molar ratio with SUR1 (referred to as hetF55L). The hetF55L channels, although are much more active than homomeric F55L mutant channels (referred to as homF55L), are still less active than WT channels. These results demonstrate the causal role of the Kir6.2 F55L mutation in congenital hyperinsulinism.

The reduced activity of the mutant channel upon metabolic inhibition could be due to reduced surface expression or altered gating properties (Huopio, Shyng et al. 2002). To distinguish between these possibilities, we compared the level of surface expression of mutant channels to that of WT channels. Western blots showed that the steady-state mutant Kir6.2 protein level is similar to WT Kir6.2 (Fig.24B, left). Moreover, fSUR1 co-expressed with the F55L mutant Kir6.2 exhibits core-glycosylated as well as complex-glycosylated forms comparable to that observed in fSUR1 co-expressed with WT Kir6.2 (Fig.24B, left), indicating the mutation does not affect surface expression of the channel. Quantification of surface expression by chemiluminescence assays further corroborated the conclusion that the F55L mutation does not affect channel expression (Fig.24B, right).

The above results suggest that the reduced activity seen in the mutant is likely due to altered gating regulation. We therefore carried out detailed electrophysiological analysis using the inside-out patch-clamp recording technique. Upon patch excision into ATP-free solution, WT channels gave averaged currents of ~2 nA at –50 mV with symmetrical potassium concentrations on both sides of the membrane. By contrast, the averaged current amplitude from the F55L mutant channels was only ~0.2 nA. To test whether the reduction in current amplitude results from reduced single channel conductance or channel open probability, we performed single channel recording of the mutant. The F55L mutant exhibited single channel conductance (70.4 ± 1.6 pS) comparable to that of WT channel (68.0 ± 3.1 pS). However, the channel open

probability appears greatly reduced (Fig.24C). These results show that the mutation reduces the ATP-independent open probability (referred to as the intrinsic open probability in this study) of K_{ATP} channels.

Effects of PIP_2 and oleoyl-CoA on the F55L mutant channel

Membrane phosphoinositides, in particular PIP_2, are known to affect the open probability of K_{ATP} channels (Baukrowitz, Schulte et al. 1998; Shyng and Nichols 1998; Enkvetchakul, Loussouarn et al. 2000). Recently, we reported that expression of Kir6.2 constructs with deliberate mutations that abolish channel sensitivity to PIP_2 (R176A, R177A, R206A) in the insulin secreting cell INS-1 results in phenotypes mimicking those seen in congenital hyperinsulinism. These include reduced K_{ATP} channel activity, depolarized membrane potential, and excessive insulin secretion, at basal glucose concentration. We therefore hypothesize that the reduced channel open probability observed in the F55L mutant could be due to attenuated channel response to PIP_2. Supporting this hypothesis, we found that in inside-out patch-clamp recordings application of exogenous PIP_2 (5 μM) to the cytoplasmic face of the membrane markedly increased the current amplitude of the F55L mutant channels (Fig.25A). The fold increase in current amplitude upon PIP_2 stimulation for WT, hetF55L, and homF55L channels are 1.27 ± 0.08, 2.27 ± 0.34, and 10.02 ± 2.39, respectively (Table VI). Based on the fold increase in current amplitude, we expect the P_o of WT, hetF55L, and homF55L channels to be ~0.78, 0.44, and 0.1, respectively, assuming the maximal P_o after PIP_2 stimulation is near 1 for all channels. Using noise analysis (Sigworth 1980; Shyng, Ferrigni et al. 1997) we estimated the P_o of WT, hetF55L, and homF55L

channels before and after PIP_2 stimulation. As shown in Table V, the P_o for WT, hetF55L, and homF55L channels prior to PIP_2 application was 0.81 ± 0.02, 0.66 ± 0.04, and 0.11 ± 0.01, respectively. After PIP_2 stimulation, the P_o for WT, hetF55L, and homF55L channels increased to 0.94 ± 0.01, 0.89 ± 0.02, and 0.72 ± 0.04. These numbers are in general agreement with the trend expected based on macroscopic current amplitude increase. However, note that the P_o estimated by the noise analysis is likely higher because underestimation of the noise due to filtering (Neher and Stevens 1977; Sigworth 1980; Shyng, Ferrigni et al. 1997; Cukras, Jeliazkova et al. 2002). Also, the maximal P_o estimated by noise analysis after PIP_2 stimulation for homF55L mutant channels is 0.72, significantly lower than 1. Therefore the intrinsic P_o of the homF55L mutant channel is likely below 0.1 (based on a ~10-fold increase in macroscopic currents after PIP_2 stimulation and the estimated maximal P_o of 0.72).

Long-chain acyl CoAs, like PIP_2, stimulate K_{ATP} channel activity by interacting with Kir6.2 and have been proposed to play a role in modulating channel activity in □-cells (Branstrom, Leibiger et al. 1998; Gribble, Proks et al. 1998; Branstrom, Aspinwall et al. 2004; Manning Fox, Nichols et al. 2004). At 5 μM, oleoyl CoA stimulated F55L channel activity to a similar extent (13.12 ± 2.18 fold increase) as 5 μM PIP_2 (Fig.25B, Table V). However, in a given patch, the time course of stimulation is faster with oleoyl CoA than with PIP_2 (Fig.25C). In addition, unlike the effect of PIP_2, the effect of oleoyl CoA is readily reversible (Fig.25C). Taken together, these results are consistent with the notion that the F55L mutation renders the channel less responsive to endogenous

membrane phosphoinositides and/or long-chain acyl CoAs, leading to lower channel open probability, thereby persistent membrane depolarization and hyperinsulinism.

Reduced channel sensitivity to phosphoinositides/long-chain acyl CoAs could result from reduced binding to these ligands or impaired gating movements following ligand binding. To gain further insight into the mechanism, we substituted F55 with additional amino acids with distinct biophysical properties. We reasoned that if the residue is directly involved in lipid binding, mutation to positively charged residue should increase channel activity whereas mutation to negatively charged residue should decrease channel activity, as shown previously for other PIP_2/CoA binding residues (Baukrowitz, Schulte et al. 1998; Shyng, Cukras et al. 2000; Schulze, Krauter et al. 2003; Manning Fox, Nichols et al. 2004). Mutation of F55 to either positively charged lysine or negatively charged glutamate yielded channels with very low activity, which increased markedly upon exposure to oleoyl CoA (Fig.26) or PIP_2 (not shown). The current increase after 5 μM oleoyl CoA stimulation was > 20-folds for both F55E and F55K (n = 3; Fig.26). In comparison, mutation of F55 to hydrophobic methionine yielded channels whose intrinsic open probabilities are lower than WT but higher than F55L, with the fold-increase in macroscopic current upon stimulation by 5μM oleoyl CoA for F55M being 3.11 ± 0.18 (n =5). By contrast, introduction of aromatic amino acids tryptophan or tyrosine at this position had very mild or no effect on channel activity. The fold-increase in macroscopic current after oleoyl CoA stimulation for F55W and F55Y are 1.65 ± 0.01 (n = 3) and 1.14 ± 0.06 (n = 4), respectively. These

results suggest that the aromatic side-chain rather than charge at this amino acid position is important for the slide helix structure and function of the channel (see Discussion).

Nucleotide sensitivity and diazoxide response of F55L mutant channels

To test whether the F55L mutation also affects channel sensitivity to intracellular nucleotides, we examined mutant channel response to ATP and MgADP. ATP-dose response curves were constructed by exposing channels to various concentrations of ATP^{4-} in K-INT plus 1 mM EDTA solution (see Materials and Methods); EDTA was used as it effectively prevents channel rundown, allowing for more accurate measurement of ATP sensitivity (Lin, Jia et al. 2003). The half maximal inhibition concentration (IC_{50}) for WT, hetF55L, and homF55L channels are 23.4 ± 1.4, 17.4 ± 0.3, and 14.5 ± 0.5 μM, respectively (Fig.27A); the IC_{50} of homF55L channels is slightly although significantly lower than that of WT channels ($p < 0.01$). Next, the response of the F55L mutant channel to MgADP stimulation was examined. In these experiments, we compared the current in 0.1 mM ATP with that in 0.1 mM ATP and 0.5 mM ADP (free Mg^{2+} concentration ~1 mM). In WT channels, 0.5 mM ADP in the presence of Mg^{2+} antagonized the inhibitory effect of 0.1 mM ATP and stimulated channel activity (Fig.27B). This stimulatory effect was fully retained in the F55L mutant channel (Fig.27B), indicating the mutation does not disrupt the coupling between SUR1 and Kir6.2. As described above, the patient carrying the F55L mutation responded to treatment by the potassium channel opener diazoxide. Because the mutation is heterozygous, the diazoxide response could simply be conferred by the WT allele. We therefore examined whether the F55L mutation in Kir6.2 affects diazoxide

sensitivity. Under the same experimental paradigm, the response of homF55L mutant channel to diazoxide stimulation was comparable to that seen in WT channels (Fig.27C). Thus, the F55L mutation does not affect the channel's ability to respond to diazoxide. It is worth noting however, that while both MgADP and diazoxide stimulated mutant channel activity, the current amplitude at maximal stimulation even after prolonged exposure (> 10 min; not shown) did not exceed the initial current observed in K-INT solution (Fig.27B, C). These results indicate the nucleotide stimulatory effect of SUR1 cannot overcome the low intrinsic open probability defect caused by the F55L mutation in Kir6.2.

DISCUSSION

Because the linkage between K_{ATP} channel mutations and congenital hyperinsulinism was established a decade ago, much effort has been devoted to understanding the molecular and cellular mechanisms by which mutations alter channel function, as this information is necessary for developing pharmacological strategies towards disease treatment (Thomas, Cote et al. 1995; Aguilar-Bryan and Bryan 1999; Huopio, Shyng et al. 2002; Dunne, Cosgrove et al. 2004). Studies thus far, mostly from SUR1 mutations, have shown loss of surface channel expression due to defects in channel biogenesis or trafficking and loss of channel sensitivity to MgADP as two major mechanisms leading to channel dysfunction (Huopio, Shyng et al. 2002). In this work, we have identified a *KCNJ11* mutation 165C→A that results in a missense mutation, F55L, in Kir6.2. Functional analysis of the mutant channel revealed a novel defect. Unlike previously reported disease mutations, the missense F55L mutation in

Kir6.2 does not affect channel expression nor channel response to MgADP. Instead, it renders the channel much less active by decreasing the intrinsic channel open probability, by at least 10-fold. The reduced channel open probability is consistent with the mutation playing a causal role in the disease.

Mechanisms underlying the reduced open probability of F55L mutant channels

In the absence of nucleotides, WT K_{ATP} channels have reported open probability of ~0.5-0.8 (Drain, Li et al. 1998; Babenko, Gonzalez et al. 1999; Enkvetchakul, Loussouarn et al. 2000; Proks, Capener et al. 2001). The level of phosphoinositides such as PIP_2 in the plasma membrane has been positively correlated with the intrinsic open probability of K_{ATP} channels (Baukrowitz, Schulte et al. 1998; Shyng and Nichols 1998; Enkvetchakul, Loussouarn et al. 2000). The fact that the F55L mutant channel activity is markedly increased by application of exogenous PIP_2 supports the notion that reduced channel sensitivity to PIP_2 accounts for the reduced open probability seen in the mutant. Currently available experimental approaches do not allow for definitive tests of whether the mutation reduces channel sensitivity to PIP_2 by directly affecting binding, indirectly affecting the gating steps following PIP_2 binding, or both. Several positively charged residues in the cytoplasmic domain of Kir6.2 have been proposed as PIP_2 binding residues, including R54, which is immediately adjacent to F55 (Baukrowitz, Schulte et al. 1998; Shyng, Cukras et al. 2000; Cukras, Jeliazkova et al. 2002; Schulze, Krauter et al. 2003). Deliberate mutation of R54 to neutral alanine or glutamine or to negatively charged glutamate results in channels with reduced PIP_2 response and low open probability similar to the F55L mutant (Cukras, Jeliazkova et al. 2002; Schulze, Krauter

et al. 2003), whereas mutation to positively charged lysine results in a channel with WT-like phenotype (Schulze, Krauter et al. 2003). These observations have led to the proposal that R54 may be directly involved in PIP_2 binding (Schulze, Krauter et al. 2003). F55 is the first amino acid in the predicted amphipathic "slide helix" that runs parallel to the lipid bilayer; the slide helix has been proposed to move laterally along the membrane during channel gating (Kuo, Gulbis et al. 2003). Given our results that substitution of F55 by either lysine or glutamate both greatly reduced channel open probability whereas mutation of F55 to tryptophan or tyrosine, two other amino acids also containing an aromatic side chain, gave rise to channels resembling WT, F55 is unlikely a PIP_2/CoA-binding residue. Rather, our data suggest that the reduced sensitivity to PIP_2/CoA seen in the F55L mutant may be due to impaired transduction steps following PIP_2 binding. The leucine mutation may disrupt the amphipathic helical structure and interfere with the ability of the helix to move along the membrane during gating. Alternatively, F55L may interfere with PIP_2/CoA binding indirectly by preventing other residues from interacting with PIP_2/CoA.

In addition to reduced PIP_2 sensitivity and reduced open probability, a slightly increased ATP sensitivity was also observed in the F55L mutant. We do not believe this increased ATP sensitivity is a result of increased ATP binding affinity but a consequence of allosteric effect. This is consistent with previous studies showing that channel open probability is negatively correlated with ATP sensitivity (Enkvetchakul, Loussouarn et al. 2000). The increased ATP sensitivity is not likely to contribute to the disease since at physiological concentrations of ATP (mM range) most WT channels are

already closed (Cook, Satin et al. 1988). Some mutations in Kir6.2 that reduce channel sensitivity to PIP_2, such as R176C and R177C, have been reported to cause uncoupling between SUR1 and Kir6.2 and abolish channel response to MgADP (John, Weiss et al. 2001). This is not the case for F55L, as the channel exhibits normal response to both MgADP and diazoxide. Since both R176C and R177C are believed to directly reduce PIP_2 binding affinity, the distinction between these two mutants and F55L is consistent with our above suggestion that F55L reduces channel sensitivity to PIP_2 via a different mechanism.

The reduced intrinsic channel open probability caused by the F55L mutation in Kir6.2 is in direct contrast to the increased intrinsic channel open probability reported in a group of neonatal diabetes-causing Kir6.2 mutations including V59G which is also located in the slide helix of Kir6.2 (Proks, Antcliff et al. 2004; Proks, Girard et al. 2005). The V59G mutation results in channels with very high intrinsic open probability that cannot be reversed by prolonged incubation with the PIP_2-binding polycation neomycin, suggesting that the mutant channel is locked in an open state (Proks, Antcliff et al. 2004). These studies show that disruption of the slide helix structure by mutations can lead to either gain or loss of channel open probability, highlighting the critical role of the slide helix in K_{ATP} channel gating.

Membrane phosphoinositides and long-chain CoAs in K_{ATP} channel regulation

The gating effects of membrane phosphoinositides and long-chain CoAs on K_{ATP} channels in isolated membranes have been well documented (Baukrowitz, Schulte et al. 1998; Branstrom, Leibiger et al. 1998; Gribble, Proks et al. 1998; Shyng and Nichols

1998; Riedel, Boora et al. 2003; Schulze, Rapedius et al. 2003; Schulze, Rapedius et al. 2003; Branstrom, Aspinwall et al. 2004; Riedel and Light 2005). Structure-functional studies indicate that modulation of channel activity by the two classes of lipid molecules involve the same set of Kir6.2 residues (Branstrom, Leibiger et al. 1998; Gribble, Proks et al. 1998; Schulze, Rapedius et al. 2003; Manning Fox, Nichols et al. 2004). Our results that both PIP_2 and oleoyl-CoA rescue the P_o defect of the F55L mutant channel are consistent with this notion. However, because phosphoinsotides and long-chain CoAs appear to share the same gating mechanism, it has been difficult to study the relative role of the two classes of lipids in determining channel activity in physiological or pathological conditions (Larsson, Barker et al. 2000; Tarasov, Dusonchet et al. 2004). Recently, we reported that manipulations of channel-PIP_2 interactions in the insulin-secreting cell line INS-1 have profound effects on channel activity and the coupling between glucose and insulin secretion (Lin, Yan et al. 2005). A Kir6.2 polymorphism, E23K/I337V, that has been implicated in type II diabetes was recently shown to increase channel sensitivity to long-chain CoAs (Riedel, Boora et al. 2003; Riedel and Light 2005; Riedel, Steckley et al. 2005).Our study presented here demonstrates that a naturally occurring mutation in human that reduces channel response to PIP_2/CoA results in congenital hyperinsulinism. Together, these studies are consistent with both classes of lipid molecules playing a role in controlling channel activity. They raise the possibility that membrane phosphoinositides and long chain CoAs could serve as potential pharmacological targets for treating insulin secretion disorders caused by K_{ATP} channel mutations.

ACKNOWLEDGEMENTS

We thank Dr. Carol A.Vandenberg for the rat Kir6.2 clone and Jillene Casey from the Shyng lab for technical assistance. We are grateful to the patients, the General Clinical Research Center staff and the Children's Hospital of Philadelphia nurses without whom this work would not have been possible. This work was supported by NIH Grant R01DK57699 to S.-L. Shyng, R01DK56268 and 5-MO1-RR-000240 to C. A. Stanley, and a Predoctoral Fellowship from the American Heart Association to Y.-W. Lin.

Keywords: K_{ATP} channel, KCNJ11, PIP_2, long chain-CoA, congenital hyperinsulinism

Table V In vivo islet phenotype (Acute Insulin Responses)

Acute insulin responses to secretogogues in proband with F55L mutation of KCNJ11 (μU/mL, mean ± SD).				
	Calcium	Leucine	Glucose	Tolbutamide
Proband (17 days old)	36	5	25	16
Father of proband	9	13	114	44
Hyperinsulinism due to recessive ABCC8 (SUR1) mutations[a] (n=7)	28 ± 16	5 ± 8	12 ± 9	4 ± 6
Hyperinsulinism due to dominant GLUD1 mutations (n=7)	2.3 ± 5.4	42 ± 27	120 ± 52	94 ± 65
Normal adult controls (n=6)	3 ± 4	1.4 ± 2.8	56 ± 26	48 ± 32

[a] Common Ashkenazi Jewish mutation: 3992-9 G→A or ΔF1388 (55).

Table VI. Effects of PIP_2 and Oleoyl CoA on channel activity

Channel	Intrinsic P_o[a]	P_o[a] after 5 μM PIP_2	P_o[a] after 5 μM Oleoyl CoA	Current increase after 5 μM PIP_2 (fold)	Current increase after 5 μM Oleoyl CoA (fold)
WT	0.81 ± 0.02 (n = 13)	0.94 ± 0.01 (n = 6)	0.94 ± 0.01 (n = 7)	1.27 ± 0.08 (n = 6)	1.18 ± 0.03 (n = 7)
F55L	0.11 ± 0.01 (n = 25)	0.72 ± 0.04 (n = 10)	0.66 ± 0.05 (n = 15)	10.02 ± 2.39 (n = 10)	13.12 ± 2.48 (n = 15)
WT + F55L	0.66 ± 0.04 (n = 8)	0.89 ± 0.02 (n = 3)	0.88 ± 0.04 (n = 5)	2.27 ± 0.34 (n = 3)	2.01 ± 0.22 (n = 5)

[a]Values derived from noise analysis.

Figure 24

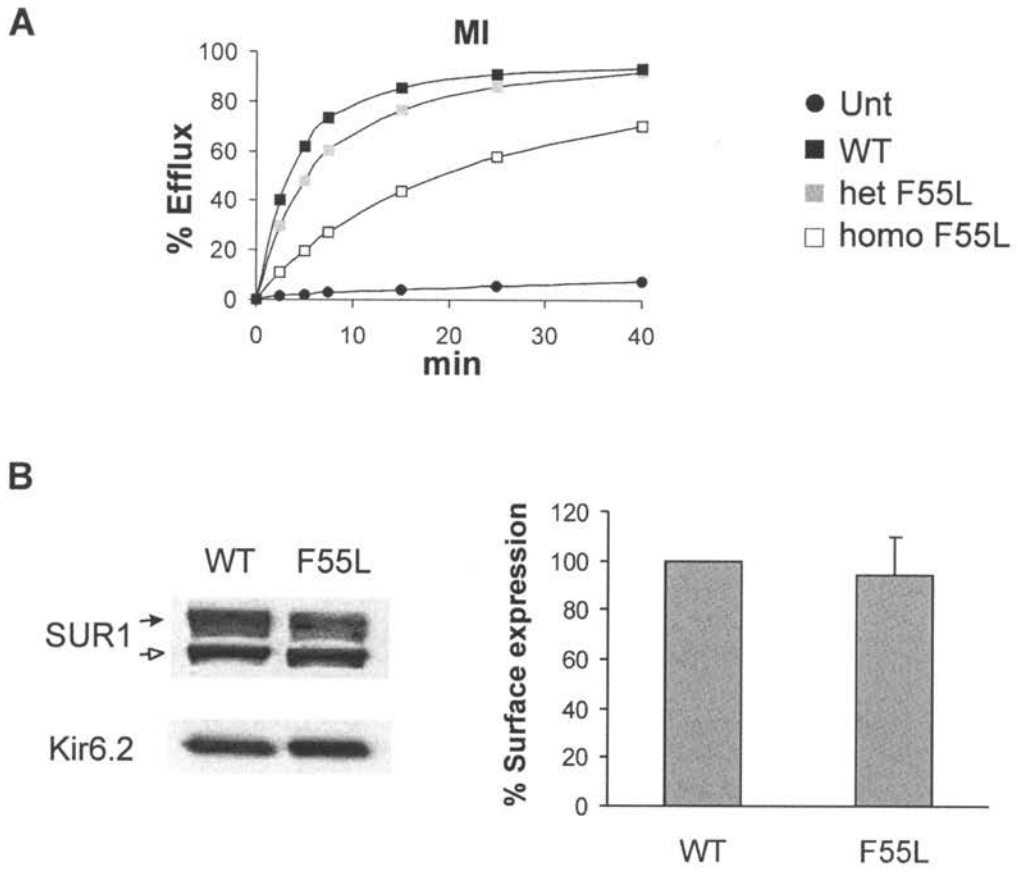

Lin et al. Figure 1

Fig. 24 Analyses of mutant channel activity, expression and single channel properties.

(A) Reduced activity of mutant K_{ATP} channels reconstituted in COSm6 cells in response to metabolic inhibition. COSm6 cells expressing wild-type (WT), homF55L (F55L), or hetF55L (WT+F55L) channels were subjected to $^{86}Rb^{+}$ efflux assays as described previously (Shyng, Ferrigni et al. 1998). Metabolic inhibition activated WT channels with $^{86}Rb^{+}$ efflux reaching >90% in a 40-min period. By comparison, WT+F55L channels were less active, and F55L still less active. In the absence of metabolic inhibition, both WT and mutant channels exhibited background efflux indistinguishable from untransfected cells (not shown). (B) *Left*, Western blots of fSUR1 (*upper panel*) and Kir6.2 (*lower panel*) in COSm6 cells coexpressing fSUR1 and WT Kir6.2 or fSUR1 and F55L Kir6.2. The complex-glycosylated fSUR1 is indicated by the solid arrow and the core-glycosylated form the open arrow. Comparable expression of both fSUR1 and Kir6.2 was observed in cells expressing WT or mutant K_{ATP} channels. *Right*, cell surface expression quantified using chemiluminescence assays. Expression of the mutant is normalized to that of WT. Data represent mean ± S.E. of 3 independent experiments (dishes in duplicates or triplicates for each experiment). There is no statistically significant difference between the expression of WT and the mutant ($p > 0.1$). (C) Single-channel recordings of WT and the F55L mutant. O: open; C: closed. Recordings were made at +50 mV pipette potential with symmetrical K-INT/EDTA solution on both sides of the membrane patch. Inward currents are shown as upward deflection.

Figure 25

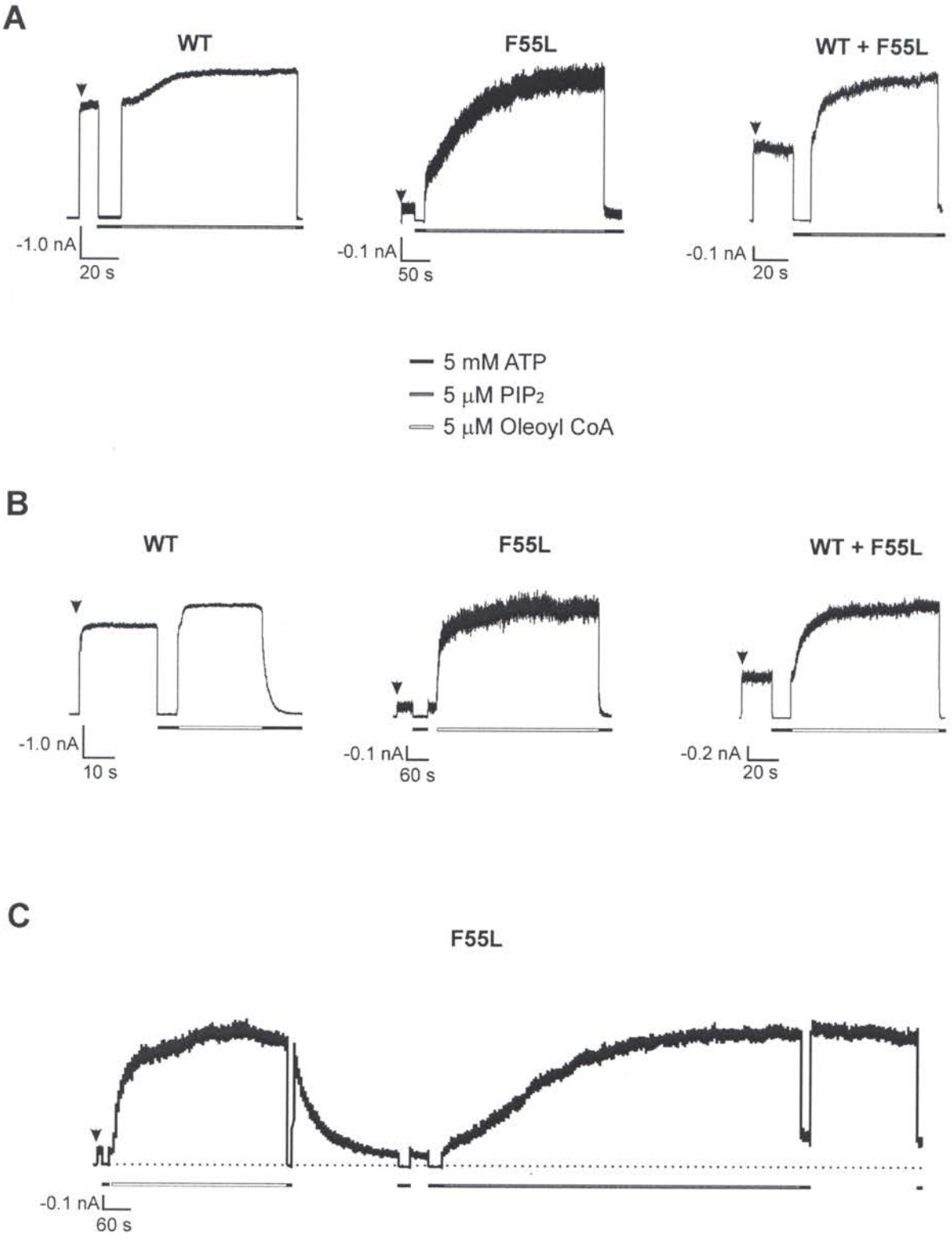

Lin et al. Figure 2

Fig. 25 Reduced sensitivity of F55L mutant channels to PIP_2 and oleoyl CoA.

(A) Representative inside-out patch-clamp recordings from cells expressing wild-type (WT; n = 6), homF55L (F55L; n = 10), or hetF55L (WT + F55L; n = 3). Note the very low activity of the homomeric F55L mutant channel upon patch excision and the large increase in current amplitude upon exposure to PIP_2. (B) Same as (A) except that channels were exposed to 5 μM oleoyl CoA (n = 7, 15, and 5 for WT, WT+F55L, and F55L, respectively). (C) Direct comparison of F55L mutant channel response to oleoyl CoA and PIP_2 in the same patch (an example from a total of four such recordings). Note the effect of oleoyl CoA could be easily washed out whereas the effect of PIP_2 was irreversible. Also, some patches showed obvious reduction in sensitivity to inhibition by 5 mM ATP, as previously reported (Baukrowitz, Schulte et al. 1998; Shyng and Nichols 1998). All recordings were made at +50 mV pipette potential with symmetrical K-INT/EDTA solution on both sides of the membrane patch. Inward currents are shown as upward deflection.

Figure 26

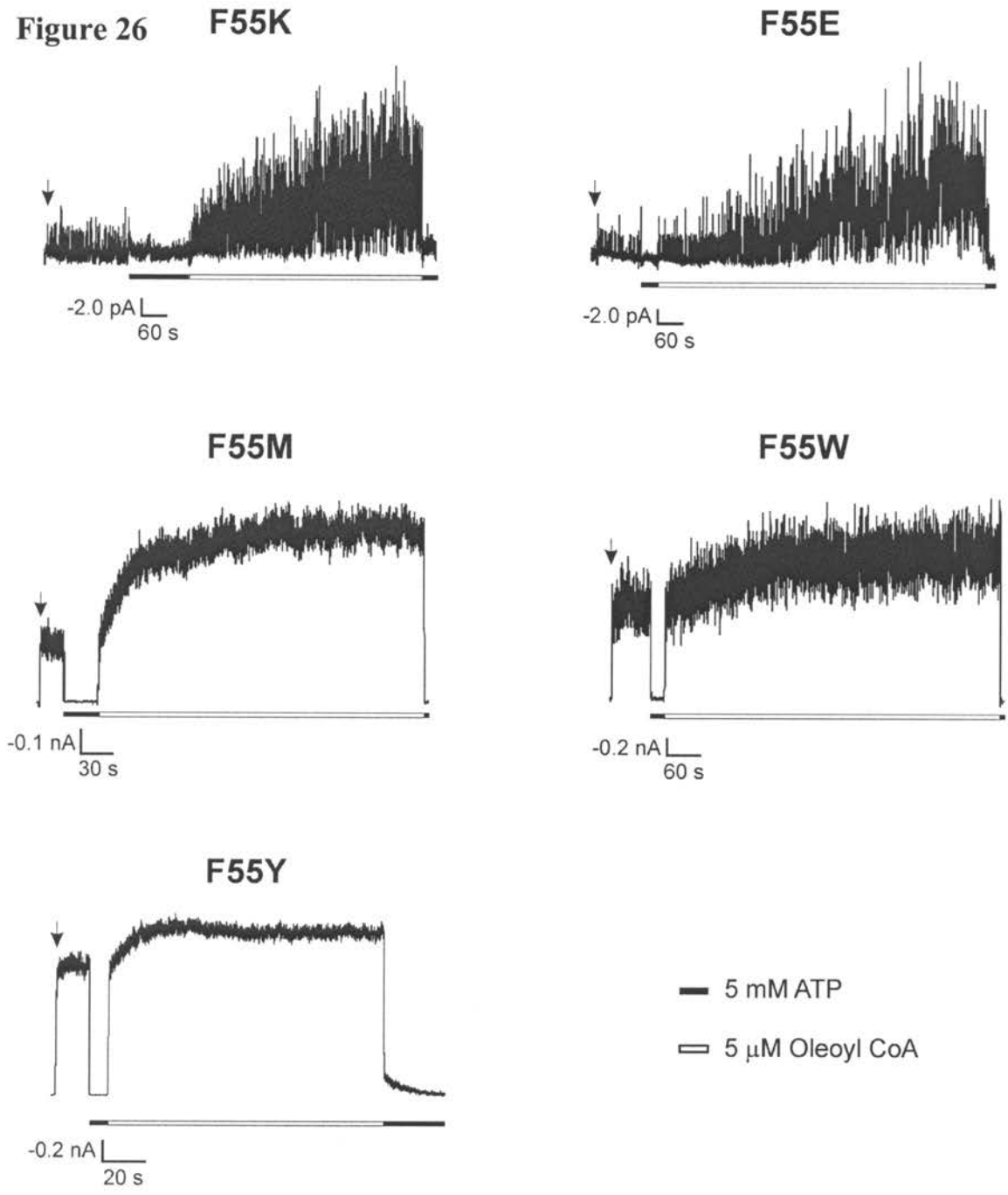

Lin et al. Figure 3

Fig. 26 Mutation of Kir6.2 residue F55 to other amino acids: effects on channel response to oleoyl-CoA. Representative inside-out patch-clamp recordings from cells coexpressing SUR1 and Kir6.2 with phenylalanine at position 55 mutated to lysine (F55K), glutamate (F55E), methionine (F55M), tryptophan (F55W), or tyrosine (F55Y). Recording conditions were as described in Fig.25. Response of the various mutant channels to PIP_2 was similar to their response to oleoyl CoA (not shown).

Figure 27

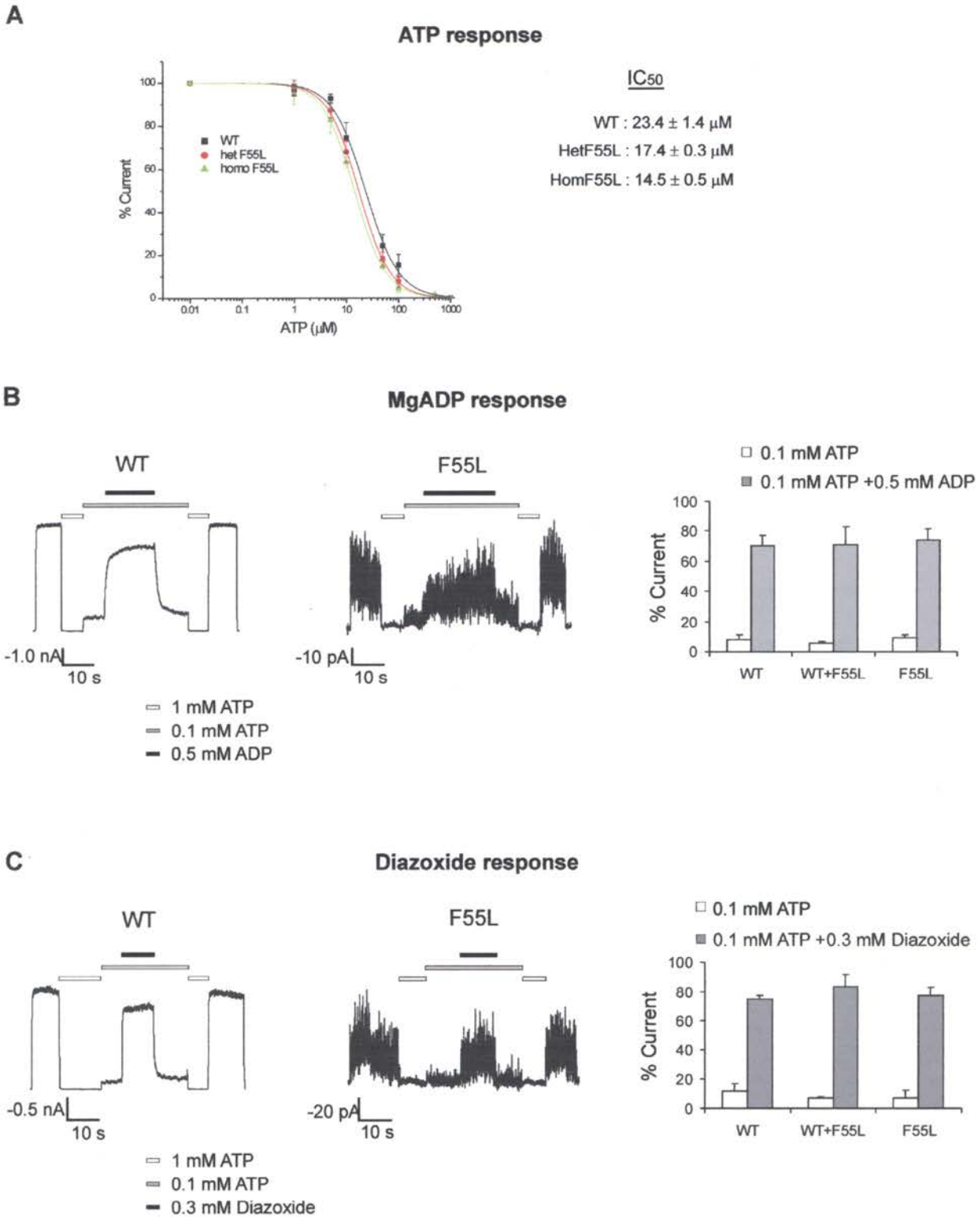

Lin et al. Fig.4

Fig. 27 Analyses of response of the F55L mutant channel to ATP, MgADP, and diazoxide. (A) ATP dose response curve of WT, hetF55L, and homF55L channels. Channels in inside-out patches were exposed to varying concentrations of ATP in KINT/EDTA solution. Channel activity was normalized to that seen in the absence of ATP. The curves were fit by the Hill equation ($I_{rel} = 1/(1+([ATP]/IC_{50})^H)$; I_{rel} = current in [ATP]/current in zero ATP; H = Hill coefficient; IC_{50} = [ATP] causing half-maximal inhibition) to averaged data. The Hill coefficients are 1.37, 1.45, and 1.45 for WT, homF55L, and hetF55L, respectively. Each data point is the average of 5-7 patches. (B) Channel response to MgADP. Representative inside-out patch clamp recordings of WT or homF55L channels are shown (*left and middle*). Patches were exposed to 1 mM ATP, 0.1 mM ATP, or 0.1 mM ATP plus 0.5 mM ADP, with free Mg^{2+} concentration at ~1 mM in all solutions. Currents in 0.1 mM ATP or 0.1 mM ATP plus 0.5 mM ADP were normalized to currents in nucleotide-free solution for WT, homF55L, and hetF55L channels. Each bar is the mean ± S.E. of 5-8 patches. (C) Same as (B) except that channels were tested for their response to 0.3 mM diazoxide. Each bar is the mean ± S.E. of 4-11 patches.

CHAPTER FOUR

Kir6.2 mutations associated with neonatal diabetes reduce expression of K_{ATP} channels: implications in disease mechanism and sulfonylurea therapy

Chia-Wei Lin, Yu-Wen Lin, Fei-Fei Yan, Jillene Casey, Malini Kochhar, Emily B. Pratt, and Show-Ling Shyng ¶

Center for Research on Occupational and Environmental Toxicology, Oregon Health & Science University, Portland, OR 97239.

The work described in this chapter was accepted by the journal ***Diabetes***. Chia-Wei Lin carried out the electrophysiological characterization of these PNDM mutants and made the viral construct. I constructed the Q52R, V59M and V59G mutants, made the ATP dose response curve of V59M and characterized the surface expression of these mutants. Fei-Fei Yan conducted the insulin secretion assay and Emily B. Pratt carried out some of the western blots for the unfolded protein response. Jillene Casey and Malini Kochhar made the rest of the mutants and repeated the surface expression assay.

ABSTRACT

Heterozygous mis-sense mutations in the pore-forming subunit Kir6.2 of ATP-sensitive potassium (K_{ATP}) channels have recently been shown to cause permanent neonatal diabetes mellitus (PNDM). Functional studies demonstrated that PNDM mutations reduce K_{ATP} channel sensitivity to ATP inhibition, resulting in gain of channel function. However, the impact of these mutations on channel expression has not been examined. Here, we show that PNDM mutations, including Q52R, V59G, V59M, R201C, R201H, and I296L, not only reduce channel ATP sensitivity but also impair channel expression at the cell surface to varying degrees. By tagging the PNDM Kir6.2 mutant V59G or R201H with an additional mutation, N160D, that confers voltage-dependent polyamine block of K_{ATP} channels, we demonstrate that in simulated heterozygous state, all surface channels are either wild-type or heteromeric channels containing both wild-type and mutant Kir6.2 subunits. Comparison of the various PNDM mutations in their effects on channel ATP sensitivity, expression, as well as disease phenotype suggests that both channel gating defect and expression level may play a role in determining disease severity. Interestingly, sulfonylureas significantly increase surface expression of a number of PNDM mutant channels, raising new questions about the use of these drugs in treatment of PNDM caused by Kir6.2 mutations.

INTRODUCTION

Pancreatic ATP-sensitive potassium (K_{ATP}) channels, each consisting of four pore-forming Kir6.2 subunits and four regulatory sulfonylurea receptor 1 (SUR1) receptors, link β-cell metabolism to insulin secretion (Aguilar-Bryan and Bryan 1999; Ashcroft and Gribble 1999; Huopio, Shyng et al. 2002). The activity of K_{ATP} channels is governed mainly by intracellular nucleotides ATP and ADP, derivatives of glucose metabolism (Ashcroft 1988; Aguilar-Bryan and Bryan 1999; Tarasov, Dusonchet et al. 2004). Both nucleotides can stimulate or inhibit channel activity depending on their relative concentrations and whether Mg^{2+} is present. Inhibition of channels by nucleotides is mediated by the Kir6.2 subunit and does not require Mg^{2+} (Tucker, Gribble et al. 1997; Ashcroft and Gribble 1998), whereas nucleotide stimulation is conferred by the SUR1 subunit and requires Mg^{2+} (Nichols, Shyng et al. 1996; Gribble, Tucker et al. 1998; Zingman, Alekseev et al. 2001). The physiological activity of K_{ATP} channels in β-cells is thus a balance between nucleotide inhibition and nucleotide stimulation. As glucose rises, ATP concentrations increase and ADP concentrations decrease, resulting in K_{ATP} channel closure. Because K_{ATP} channels carry the dominant conductance in high- input resistance β -cells at resting state, closure of K_{ATP} channels leads to membrane depolarization, which in turn leads to opening of voltage-gated calcium channels, calcium influx, and insulin release. On the other hand, when glucose falls, the concentration ratio of ATP to ADP decreases, leading to K_{ATP} channel opening, membrane hyperpolarization, and termination of insulin secretion.

Recent studies have established heterozygous missense mutations in Kir6.2 as a major cause underlying permanent neonatal diabetes mellitus (PNDM) (Edghill, Gloyn et al. 2004; Gloyn, Cummings et al. 2004; Gloyn, Pearson et al. 2004; Sagen, Raeder et al. 2004; Vaxillaire, Populaire et al. 2004; Ashcroft 2005; Koster, Permutt et al. 2005; Massa, Iafusco et al. 2005). As Kir6.2 is also a constituent of other K_{ATP} channel subtypes expressed outside of pancreas, including cardiac muscle, skeletal muscle, and brain, some mutations have been reported to cause developmental delay, muscle weakness, epilepsy, dysmorphic features, in addition to neonatal diabetes (referred to as DEND syndrome) (Ashcroft 2005; Hattersley and Ashcroft 2005). Functional studies of mutant channels have revealed reduced ATP sensitivity as a common defect (Gloyn, Pearson et al. 2004; Proks, Antcliff et al. 2004; Proks, Girard et al. 2005). While reduced channel sensitivity to ATP provides an explanation for how these mutations lead to K_{ATP} channel overactivity in β-cells at high glucose, thereby diabetes (Koster, Marshall et al. 2000; Gribble and Reimann 2004), some puzzles remain. For example, in some mutations, such as R201C and R201H, reduced ATP sensitivity was clearly observed in homomeric mutant channels, however no significant difference in ATP sensitivity from WT channels could be detected under the condition that simulates heterozygous expression in patients (by injecting WT and mutant Kir6.2 at 1:1 mRNA ratio into *Xenopus* oocyte) (Gloyn, Pearson et al. 2004; Gribble and Reimann 2004; Proks, Antcliff et al. 2004). A potential explanation for the lack of detectable difference could be that the mutant is not expressed as efficiently as the WT Kir6.2, a hypothesis that has not been tested. Furthermore, the extent of ATP sensitivity reduction seen in the different mutant

channels does not always match well with disease severity. For example, the mutation V59M results in channels much more sensitive to ATP than R201C or R201H, yet it is associated with more severe disease phenotype. These observations suggest to us that additional factors might contribute to the pathogenic potency of a mutation.

In this study, we examined the effects of several PNDM mutations, including Q52R, V59G, V59M, R201C, R201H, and I296L, on K_{ATP} channel expression. We found that all of them lead to reduced surface expression, to varying degrees, of K_{ATP} channels reconstituted in three different mammalian cell lines. By tagging the V59G or R201H mutant Kir6.2 with the N160D inward rectification mutation, which confers voltage-dependent spermine block of K_{ATP} channels (Shyng, Ferrigni et al. 1997), we demonstrate that in simulated heterozygous expression condition, nearly all channels present at the cell surface are either pure wild-type (WT) or heteromeric channels containing a mixture of WT and mutant Kir6.2. We present evidence that the expression level of a mutation plays a role in determining the extent of abnormality in □-cell response to glucose stimulation. Moreover, we show that sulfonylureas significantly enhanced surface expression of some PNDM mutant channels, suggesting that the efficacy of sulfonylurea therapy may be compromised by its effect on channel expression.

RESEARCH DESIGN AND METHODS

Molecular biology.

Rat Kir6.2 cDNA is in pCDNAI/Amp vector (a generous gift from Dr. Carol A.

Vandenberg) and SUR1 in pECE. Site-directed mutagenesis was carried out using the QuickChange site-directed mutagenesis kit (Strategene) and the mutation confirmed by sequencing. Mutant clones from at least two independent PCR reactions were analyzed to avoid false results caused by undesired mutations introduced by PCR. Construction of adenovirus carrying R201H Kir6.2 cDNA is as described previously (Lin, Yan et al. 2005).

Western blotting.

COSm6 cells grown in 35 mm dishes were transfected with 0.4 μg rat Kir6.2 and 0.6 μg of a previously described SUR1 (Cartier, Conti et al. 2001) tagged with a FLAG-epitope (DYKDDDDK) at the N-terminus (referred to as fSUR1) using FuGene6 (Roche Applied Science, Indianapolis, IN). The fSUR1 has been shown in previous studies to behave as WT SUR1 and was used in this study to facilitate detection of SUR1 (Cartier, Conti et al. 2001). Cells were lysed 48-72 hours post-transfection in 20 mM HEPES, pH 7.0/5 mM EDTA/150 mM NaCl/1% Nonidet P-40 (IGAPEL) with Complete^{TR} protease inhibitors (Roche Applied Science, Indianapolis, IN). Proteins in the cell lysate were separated by SDS/PAGE (7.5% for SUR1 and 12% for Kir6.2), transferred to nitrocellulose membrane, and analyzed by incubation with appropriate primary antibodies followed by horseradish peroxidase (HRP)-conjugated secondary antibodies (Amersham Biosciences, Piscataway, NJ), and visualized by enhanced chemiluminescence (Super Signal West Femto; Pierce, Rockford, IL). Mouse monoclonal antibodies for FLAG (M2) and α-tubulin are from Sigma (St. Louis, MO). Rabbit polyclonal antibodies for Kir6.2 and mouse monoclonal antibody for CHOP are from Santa Cruz Biotechnology (Santa

Cruz, CA). Mouse monoclonal antibody for BiP is from BD Transduction Laboratories (San Diego, CA).

Chemiluminescence assay

COS cells in 35 mm dishes were transfected as described above. For homozygous expression, 0.4 μg of indicated Kir6.2 and 0.6 μg of fSUR1 were used. To simulate heterozygous expression, 0.2 μg each of WT and mutant Kir6.2 were combined with 0.6 μg of fSUR1. Chemiluminescence assays were carried out as previously described (Taschenberger, Mougey et al. 2002; Yan, Lin et al. 2004). Cells were fixed with 2% paraformaldehyde for 20 min at room temperature 48-72 hours post transfection. Fixed cells were pre-blocked in phosphate buffered saline (PBS) +0.5 % bovine serum albumin (BSA) for one hour, incubated in M2 anti-FLAG antibody (10 μg/ml) for an hour, washed 4 x 30 min in PBS + 0.5% BSA, incubated in HRP-conjugated anti-mouse secondary antibodies (Amersham, 1:1000 dilution) for 20 min, washed again 4 x 30 min in PBS +0.1% BSA, and 2 x 5 min in PBS. Chemiluminescence signal was read in a TD-20/20 luminometer (Turner Designs) following 10 sec incubation in SuperSignal Elisa Femto luminol solution (Pierce, Rockford, IL). Results of each experiment are the average of 2-3 dishes and each data point shown in figures is the average of 3-5 independent experiments.

Virus infection.

For expression of Kir6.2 in INS-1 cells [clone 832/13, a gift from Dr. Chris Newgard (Hohmeier, Mulder et al. 2000)], recombinant adenoviruses containing WT or R201H Kir6.2 with desired titers were used for infection as previously described (Lin,

Yan et al. 2005). Briefly, INS-1 cells were plated in 24-well tissue culture plates and cultured in RPMI-1640 with 11.1 mM D-glucose (Invitrogen) supplemented with 10% FBS, 100U/ml penicillin, 100μg/ml streptomycin, 10 mM HEPES, 2 mM glutamine, 1 mM sodium pyruvate, and 50 μM β-mercaptoethanol. Twenty-four hours later, cells were infected with appropriate titer of each adenovirus diluted in 1 ml of OptiMEM at 37°C for 1.5 hours. One ml of RPMI-1640 with 2x supplement was then added to each dish for overnight incubation. The next day, the infection medium was replaced with regular medium and incubated for another day before experiments.

Insulin secretion assay

INS-1 cells infected with or without viruses were subject to insulin secretion assays as described previously (Lin, Yan et al. 2005). Twenty-four hours post-virus infection, the culture medium was replaced by RPMI 1640 with 5 mM glucose and cells incubated for at least 18 hours. Insulin secretion was assayed in HEPES balanced salt solution (HBSS) consisting of (in mM) 114 NaCl, 4.7 KCl, 1 $MgCl_2$, 1.2 KH_2PO_4, 1.16 $MgSO_4$, 20 HEPES, 2.5 $CaCl_2$, 25.5 $NaHCO_3$, and 0.2% bovine serum albumin (pH ~ 7.2) (Hohmeier, Mulder et al. 2000). Cells were washed twice with pre-warmed (37°C) HBSS buffer with 3 mM glucose followed by 2-hour incubation in the same buffer prior to stimulation with 0.8 ml/well pre-warmed HBSS buffer containing 3 or 12 mM glucose for 2 hours. The medium was harvested and insulin content determined using Immunochem coated-tube insulin radioimmunoassay (RIA) from ICN Pharmaceuticals (Costa Mesa, CA). Insulin release at 12 mM glucose was normalized to that observed at 3 mM glucose and expressed as fold-increase.

Electrophysiology

For experiments shown in Fig.30, 31 and the Appendix, standard inside-out patch clamp technique was used in COSm6 cells expressing WT or mutant K_{ATP} channels. The recording pipettes had average resistance ~ 1.0~1.5 MΩ. All recordings were performed with the Axopatch 1D amplifier and Clampex 8.1 (Axon Inc., Foster City, CA) at room temperature at –50 mV with symmetrical K-INT solution containing (in mM): 140KCl, 10 K-HEPES and 1 KEGTA (pH 7.2 with KOH). For measuring ATP^{4-} sensitivity, 1 mM EDTA was included in K-INT to avoid channel rundown (Lin, Jia et al. 2003). For measuring MgATP sensitivity, $MgCl_2$ (at concentration equal to that of ATP) was added to K-INT as Mg^{2+} source. For spermine block experiments, 20μM spermine (Sigma) was added to K-INT (prepared immediately prior to the experiments from a stock solution). Excised patches were subjected to voltage ramps (200 ms) between +100 mV and –100 mV, with each ramp preceded by 20 ms holding potential at +140 mV to saturate channels with spermine. (Shyng and Nichols 1997). Currents obtained in the presence of 10 mM ATP were taken as leakage and subtracted from the total currents for analysis. Only patches with current amplitudes greater than 1 nA (at –50 mV) were included in the analysis.

For measuring INS-1 cell resting membrane potential (RMP), the whole-cell patch clamp recording technique was adopted as previously described (Lin, Yan et al. 2005). Cells were pre-incubated in 12 mM glucose for three hours prior to recording. During recording, cells were bathed in Tyrode's solution consisting of (in mM): 137

NaCl, 5.4 KCl, 1.8 $CaCl_2$, 0.5 $MgCl_2$, 5 HEPES, 3 $NaHCO_3$, 0.16 NaH_2PO_4, with glucose as specified in figure legends. Pipette solution contained (in mM) 10 KCl, 130 Kgluconate, 10 HEPES, 1 EGTA, 3 $MgCl_2$, and 5 ATP.

Data Analysis. Data fitting was performed with Origin 6.1. For estimating expression ratio of WT and N160D-tagged mutant subunit, the Grel/V curve obtained in the presence of spermine was fitted as described previously (Shyng and Nichols 1997) with the sum of 5 individual Boltzmann equations:

$$G_{rel} = \Sigma_{i=1}^{5} A_i \cdot \{ 1 + \exp [(F/RT) \cdot z_i \cdot (V - V_i)] \}^{-1}$$

where A_i, V_i, and z_i are the amplitude, voltage of half-maximal inhibition, and effective valency, respectively, of the i^{th} component (with 0, 1, 2, 3, or 4 mutant subunits). We assumed that the fitted amiplitude (A_i) corresponds to the probability (p_x) of formation of each channel component, with WT and mutant Kir6.2 subunits having equal probability of being incorporated into the channel complex, following the binomial distribution:

$$p_X = \binom{n}{x} \cdot P^x \cdot (1 - P)^{n-x}$$

where n is the number of Kir6.2 subunits in a channel, x is the number, 0 to n, of WT subunits in a given channel component, P is the probability of inclusion of a WT subunit and $(1 - P)$ the probability of inclusion of a mutant subunit. The P value that gave the best fit was taken as the fraction of WT subunits present in the channel population in a given patch.

RESULTS

Effects of PNDM mutations on K_{ATP} channel expression

To study K_{ATP} channel expression, we chose the following Kir6.2 mutations: Q52R, V59G, V59M, R201C, R201H, and I296L, to include both the mild PNDM disease phenotype and the more severe DEND phenotype. Although a large amount of functional data reported to date has been obtained using the *Xenopus* oocyte expression system (Gloyn, Pearson et al. 2004; Proks, Antcliff et al. 2004), this system is less suitable for studying channel maturation and trafficking since many misfolded proteins which fail to mature in mammalian cells are tolerated in *Xenopus* oocytes (Drumm, Wilkinson et al. 1991; Yang, Fang et al. 2005). We therefore examined channel expression in the mammalian cell line COSm6. Western blot analysis was used to assess steady-state channel protein expression level in cells co-transfected with Kir6.2 and fSUR1 (see Research Design and Methods). Channel assembly occurs in the endoplasmic reticulum (ER). As the correctly assembled channel complex exits the ER and travels through the Golgi, the two N-linked glycosylation sites in SUR1 are further modified to give rise to the complex-glycosylated form that migrates slower on the SDS gel (referred to as the upper band) than the core-glycosylated form (referred to as the lower band). The intensity of the upper fSUR1 band is thus indicative of the level of successfully assembled channel complexes that have trafficked beyond the medial Golgi. As shown in Fig.28A, many of the mutants exhibited reduced upper fSUR1 band compared with WT. In addition, a reduced steady-state level of Kir6.2 protein was apparent in R201C and R201H, suggesting these mutants may be rapidly degraded. To ensure that the reduced expression is not unique to COSm6 cells, we also examined mutant channel expression in HEK293 cells and a neuroblastoma cell line N2a.

Fig.28B and 28C show that the expression of the R201H mutant in these two cell lines was similarly reduced (other mutants also exhibited reduced expression, not shown). Surface expression of various mutant channels was further quantified using a previously described chemiluminescence-based immunoassay (Taschenberger, Mougey et al. 2002; Yan, Lin et al. 2004). Consistent with results from Western blot analysis, mutant channels expressed in COS cells exhibited reduced surface expression to varying degrees, with Q52R, V59G, R201C, R201H, and I296L reduced by ~80%, and V59M moderately reduced by ~50% (Fig.28D).

One possible mechanism of reduced channel surface expression is that the mutant Kir6.2 proteins are unable to fold correctly. In such case, expression of the mutant protein may elicit unfolded protein response (UPR) and may even trigger apoptosis (Schroder and Kaufman 2005). To test this idea, we examined two marker proteins, BiP (GRP78), an ER chaperone protein, and CHOP (GADD153), an ER stress-associated apoptosis transcription factor, whose levels are known to be upregulated during UPR and UPR-induced apoptosis (Araki, Oyadomari et al. 2003). No difference in either BiP or CHOP protein level could be detected between control COSm6 cells, cells expressing WT K_{ATP} channels and cells expressing PNDM mutant channels (Fig.29). In contrast, cells treated with tunicamycin, which blocks N-linked protein glycosylation and induces UPR, exhibited significantly increased level of both BiP and CHOP (Sato, Urano et al. 2000). These results indicate that expression of the mutant proteins does not cause significant ER stress, at least in COSm6 cells, within the time course of our experiments.

Assessing the relative abundance of WT and mutant Kir6.2 in surface channels in simulated heterozygous expression by N160D mutation-dependent and voltage-dependent spermine block

The reduced surface expression of the mutant channels observed above suggests that under heterozygous expression condition as seen in patients few surface channels would be pure (homomeric) mutant channels. To test this, we monitored the relative number of surface channels containing 0, 1, 2, 3, or all 4 mutant subunits in heterozygous expression by tagging the mutant Kir6.2 subunits with the N160D mutation, which confers strong inward rectification in the presence of spermine (Shyng, Ferrigni et al. 1997; Shyng and Nichols 1997). Previous studies have shown that the extent of rectification depends on the number of Kir6.2 subunits carrying the N160D mutation and that the relative conductance-voltage (Grel-V) curve of each channel population containing 0, 1, 2, 3, or 4 N160D subunits can be fitted by a single Boltzmann function (Shyng, Ferrigni et al. 1997). In simulated heterozygous expression, the overall Grel-V curve will therefore be the sum of the five individual Boltzmann functions with the relative conductance amplitude of each Boltzmann function corresponding to the relative abundance of each channel population (Shyng and Nichols 1997). Assuming WT and mutant Kir6.2 protein have equal probability of being incorporated into the channel complex, the distribution of the five channel populations should be binomial with the relative abundance of each channel population dictated by the relative amount of the WT versus mutant Kir6.2 proteins. This approach can thus be used to estimate the ratio of WT to mutant Kir6.2 in a single membrane patch. In cells expressing WT and R201H/N160D Kir6.2 at 1:1 cDNA ratio, the patches consistently contained ~ 83 % of WT protein and ~ 17 % of R201H/N160D protein (n = 7), in good

agreement with biochemical data that R201H Kir6.2 is not equally expressed as WT Kir6.2 (see Fig.28). Control experiments confirmed that the N160D mutation does not affect expression of the R201H channels (not shown). Increasing cDNA ratio of WT to mutant Kir6.2 to 1:2 or 1:4 resulted in concordant change in the estimated protein ratio (WT : mutant of 0.72 : 0.28 for cDNA ratio of 1:2, n =6, and 0.60 : 0.40 for cDNA ratio of 1:4, n = 7), as evidenced by the more severe inward-rectification in intracellular 20 μM spermine (an example of 1:4 cDNA ratio expression experiment is shown in Fig. 30). Thus, in simulated heterozygous state, although the cDNA ratio of WT to mutant is 1:1, the protein ratio is only ~1: 0.2. These results led us to conclude that in simulated heterozygous expression, most surface channels are either pure WT or contain a mixture of WT and R201H mutant Kir6.2 subunits, with the population of homR201H mutant channels being less than 0.1% [$(0.17)^4$]. Examination of cells co-expressing WT and V59G/N160D Kir6.2 at 1:1 cDNA ratio in the spermine block experiments similar to those described for R201H also confirmed reduced expression of the V59G mutant in the surface membrane (WT : V59G/N160D protein ratio of 0.83 : 0.17, n = 7). The above functional data further corroborate the results from Western blots and chemiluminescence assays that many PNDM mutations render reduced surface expression efficiency of K_{ATP} channels.

Heterozygous expression of R201H results in channels that are overactive in physiological concentrations of MgATP

If only less than 0.1% of homR201H mutant channels are expressed at the cell surface, how could heterozygous R201H mutation increase the physiological activity of β-cell K_{ATP} channels? We reasoned that in cells, most ATP is complexed with Mg^{2+} (Romani

and Scarpa 2000). In the presence of Mg^{2+}, ATP is hydrolyzed by SUR1; this leads to channel activation and effectively reduces the sensitivity of Kir6.2 to ATP inhibition (Nichols, Shyng et al. 1996; Aguilar-Bryan and Bryan 1999; Tarasov, Dusonchet et al. 2004). We therefore tested whether heterozygous R201H mutation might significantly affect channel sensitivity to MgATP. Indeed, we found that in simulated heterozygous expression (cDNA ratio of WT to mutant = 1:1, i.e. protein ratio of ~0.83:0.17 as shown in Fig.29), the resulting channel population exhibits significantly increased channel activity in mM range of MgATP compared to pure WT channels (Fig.31A). These observations are consistent with those recently reported by Gloyn *et al.* and Proks *et al.* (Gloyn, Reimann et al. 2005; Proks, Girard et al. 2005). Since the number of pure R201H mutant channels is close to 0 in heterozygous expression, based on the estimation that the number of surface K_{ATP} channels in a single human β-cell is fewer than 500 (Branstrom, Aspinwall et al. 2004; Dunne, Cosgrove et al. 2004), we conclude that the active channels in mM MgATP concentration range are those containing 1, 2, or 3 R201H mutant Kir6.2 subunits (Fig.31B).

Effect of R201H-Kir6.2 expression level on INS-1 cell membrane potential and insulin secretion response

A question that arises from our observation of the varied expression efficiency of PNDM mutants (Fig.28D) is whether the expression level plays a role in determining the extent of β-cell dysfunction. To address this issue, we expressed the R201H-Kir6.2 mutant in the insulin secreting cell line INS-1 by infection with a recombinant adenovirus containing R201H-Kir6.2 cDNA. We chose two virus titers that gave 1- or 3-fold excess of mutant protein expression compared to endogenous WT Kir6.2 protein (Fig.32A). To ensure

that cells expressing the mutant protein were not under severe ER stress or undergoing apoptosis, which could reduce insulin secretion, we again checked the level of BiP and CHOP. Similar to what we found in COS cells (Fig.29), no change in either BiP or CHOP was detected during the time course of our experiments (Fig.32B). Next, membrane potential and insulin secretion response to glucose stimulation (12 mM) were measured by whole-cell patch-clamp recording and insulin radioimmunoassay. Fig.32C shows that the membrane potential of cells infected with R201H-Kir6.2 at 12 mM glucose was more hyperpolarized, in an expression level-dependent manner, than uninfected controls cells or cells expressing similar levels of exogenous WT Kir6.2. Moreover, cells infected with the R201H-Kir6.2 virus had reduced insulin secretion response to 12 mM glucose stimulation, again in an expression level-dependent manner (Fig.32D). These results demonstrate directly the causal role of the R201H mutation in impairing glucose-stimulated insulin secretion. In addition, they provide evidence that the expression level of a PNDM mutant Kir6.2 indeed affects the extent of β-cell dysfunction.

Effects of sulfonylureas on surface expression of PNDM mutant channels

Sulfonylurea therapy has been proposed as an alternative to insulin injection in PNDM patients with Kir6.2 mutations. We have previously shown that sulfonylureas increase surface expression of mutant channels with reduced surface expression due to SUR1 mutations associated with congenital hyperinsulinism (Yan, Lin et al. 2004; Yan, Lin et al. 2005). We asked whether sulfonylureas might also affect the expression efficiency of PNDM mutant channels. Interestingly, surface expression level was indeed increased when COSm6 cells transfected with PNDM channel subunits were treated with glibenclamide (5 μM for 24 hours, Fig.33). The degree of increase appeared more pronounced in mutants

with more severe expression defect. These results reveal the complex effects of sulfonylureas on not only gating but also expression of PNDM mutants.

DISCUSSION

In this study, we used both biochemical and electrophysiological approaches to demonstrate that many PNDM-associated Kir6.2 mutations reduce K_{ATP} channel surface expression, in addition to their well-documented effects on reducing channel ATP sensitivity (Gloyn, Pearson et al. 2004; Proks, Antcliff et al. 2004; Sagen, Raeder et al. 2004; Antcliff, Haider et al. 2005; Gloyn, Reimann et al. 2005; Massa, Iafusco et al. 2005). Detailed analyses of the R201H mutation show that in simulated heterozygous state (WT: mutant cDNA ratio of 1:1), the fraction of mutant Kir6.2 present in the plasma membrane is only ~17% of the total surface Kir6.2 protein pool. The findings suggest that in patients, the number of homomeric mutant channels in a □-cell is almost zero and overactivity of K_{ATP} channels is therefore likely attributed to heteromeric channels containing both WT and mutant Kir6.2 subunits (Fig.31). Interestingly, earlier studies have shown that while reduced ATP sensitivity was obvious in homomeric R201H mutant channels, no significant change in ATP sensitivity was detectable in channels from the simulated heterozygous expression condition. Our observation that R201H homomeric channels are poorly expressed (or non-existent) at the cell surface may help explain why little change in channel ATP sensitivity was detected under heterozygous expression (Gloyn, Pearson et al. 2004; Gribble and Reimann 2004; Proks, Antcliff et al. 2004). The R201 residue is thought to be involved in ATP binding (John, Weiss et al. 2003; Antcliff, Haider et al. 2005). Markworth *et al.* have previously reported that only one of the four ATP binding sites in a Kir6.2 tetramer is necessary for ATP-induced

channel closure (Markworth, Schwanstecher et al. 2000); the WT subunit in heteromeric channels may thus be sufficient to confer WT-like ATP sensitivity. This interpretation, however, may not apply to other mutations, such as Q52R and V59G, that render channel insensitive to ATP by increasing the intrinsic channel open probability rather than affecting ATP binding (Proks, Antcliff et al. 2004). In these mutants, it is possible that even one mutant subunit in the tetramer can increase channel open probability and indirectly reduce ATP sensitivity. Although heterozygous expression of R201H does not lead to significant reduction in ATP sensitivity, it does lead to significantly higher channel activity in physiological concentration range of MgATP (Fig.31A), consistent with that reported recently by Gloyn et al. and Proks et al (Gloyn, Reimann et al. 2005; Proks, Girard et al. 2005). Our analyses of other mutants also showed much more pronounced channel overactivity in MgATP than in ATP (see Appendix). Taken together, these results lead us to conclude that for mutations included in this study (Q52R, V59G, V59M, R201C, R201H, and R296L), the heteromeric channel population containing both WT and mutant Kir6.2 subunits plays a dominant role in causing disease by rendering the channel more active in physiological concentration of MgATP.

Channel expression and disease

Reduced surface expression of K_{ATP} channels due to mutations in the channel genes has been recognized in recent years as a significant mechanism contributing to loss of channel function in congenital hyperinsulinism (Cartier, Conti et al. 2001; Huopio, Shyng et al. 2002; Chan, Zhang et al. 2003; Crane and Aguilar-Bryan 2004), a disease characterized by excessive insulin secretion despite severe hypoglycemia (Stanley 2002).

Somewhat unexpectedly, all of the neonatal diabetes-causing mutations we examined in this study also reduce surface expression of the channel to varying degrees. While intuitively one might predict that reduced surface expression should lead to loss of channel function, in the case of PNDM mutations the effect on expression is overruled by the effect of the mutations on gating (reduced ATP sensitivity), leading to an overall "gain of channel function" phenotype. This is not surprising considering that the activity of K_{ATP} channels in cells (I) is the product of the number of channels in the plasma membrane (N) and the open probability of channel under physiological environment (P_o), i.e. $I = N * P_o$. The finding that PNDM mutations affect channel expression at the cell surface also raises the question of whether the expression level of a mutant plays a role in its clinical manifestation. In this regard, our study examining the effect of R201H-Kir6.2 expression in the islet β-cell line INS-1 demonstrates that indeed the extent of cell dysfunction, as assessed by the ability of the cell to depolarize and secrete insulin upon glucose stimulation, is correlated with the expression level of the mutant. Among the PNDM mutations we examined, V59M stands out as the one with the highest expression level (Fig.28). It is interesting to note that V59M channels exhibit the least change in ATP and MgATP sensitivities (see comparison of IC_{50} in Table VII of the Appendix), yet the mutation is associated with intermediate DEND that is more severe than the PNDM phenotype seen in patients carrying another mutation, R201H, which causes much more reduced ATP sensitivity. We recognize that many factors are likely involved in determining the clinical phenotypes in patients; for instance, the R201C mutation has been reported to cause PNDM in some individuals but DEND in others (Gloyn, Pearson et al. 2004; Vaxillaire, Populaire et al. 2004; Massa, Iafusco et al. 2005). Nevertheless, it

is tempting to speculate that the more severe phenotype seen in the V59M patients might be due in part to its higher expression level.

Implications for sulfonylurea therapy

The discovery that PNDM could be caused by overactive K_{ATP} channels has led to the proposal that sulfonylureas might be used as an alternative therapy to insulin injection in patients carrying Kir6.2 mutations (Gloyn, Pearson et al. 2004). Indeed, several studies have reported successful treatment of patients with mutations that cause PNDM alone using sulfonylureas (Gloyn, Pearson et al. 2004; Sagen, Raeder et al. 2004; Zung, Glaser et al. 2004; Klupa, Edghill et al. 2005), although the long term effectiveness of such treatment remains to be determined. We have previously shown that sulfonylureas markedly increase surface channel expression in two congenital hyperinsulinism-causing SUR1 mutations (Yan, Lin et al. 2004). In this study, we found that sulfonylureas also markedly increase surface expression level of several PNDM associated mutant channels. While we don't yet understand the mechanism by which sulfonylureas exert their effects on PNDM channel expression, our finding raises new concerns about sulfonylurea therapy in neonatal diabetes patients with Kir6.2 mutations. On the one hand, sulfonylureas may reduce channel activity via their effects on channel gating; on the other hand, they may increase mutant channel expression and increase channel activity. Our finding, together with previous studies showing that some PNDM Kir6.2 mutations render the channel less sensitive to sulfonylurea inhibition (Proks, Antcliff et al. 2004; Koster, Remedi et al. 2005), point to the complex effects of sulfonylureas on K_{ATP} channel biology and the need to further evaluate the efficacy of sulfonylurea therapy in patients carrying Kir6.2 mutations.

ACKNOWLEDGEMENTS

We thank Dr. Carol A.Vandenberg for providing the rat Kir6.2 clone and Dr. Chris Newgard for INS-1 cells clone 832/13. This work was supported by National Institutes of Health Grant DK57699 (to S.-L. S.) and a Predoctoral Fellowship from the American Heart Association (to Y.-W. L.).

Figure 28

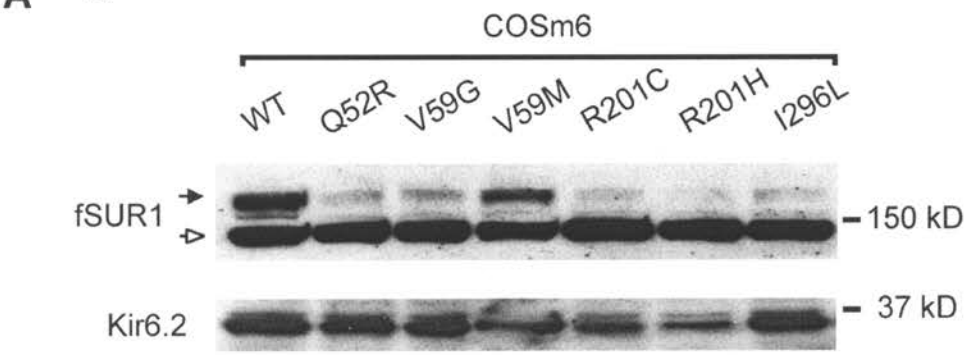

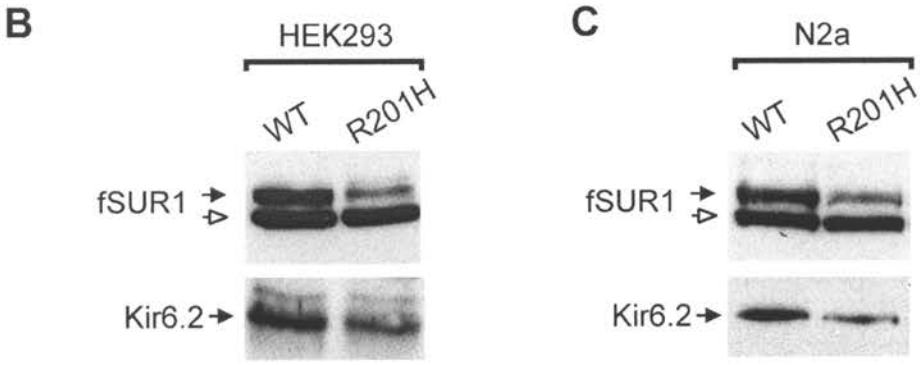

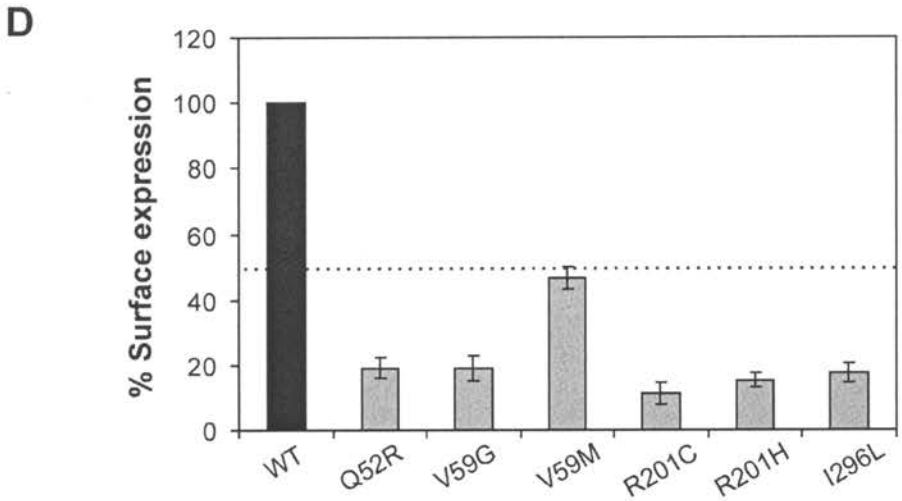

Lin et al. Figure 1

Fig. 28 PMDM-associated Kir6.2 mutations reduce surface expression of K_{ATP} channels. (A) Western blots of WT fSUR1 (upper panel) and WT or mutant Kir6.2 (lower panel) coexpressed in COSm6 cells. The complex-glycosylated form of fSUR1 is indicated by the solid arrow and the core-glycosylated form the open arrow. Note the upper band fSUR1 is reduced in all PNDM mutants compared with WT, indicating reduced surface expression. In some mutants, reduced steady state Kir6.2 protein level was also apparent. The faint band right above monomeric Kir6.2 is nonspecific. Reduced complex-glycosylated fSUR1 band and R201H Kir6.2 protein was also seen in HEK293 cells (B) and N2a cells (C). (D) Quantification of surface expression of mutant channels in COSm6 cells using chemiluminescence assays. Expression level was normalized to that of WT channels. Each value is the average of 6-9 independent experiments. The error bar represents the stardard error of the mean (s.e.m.).

Figure 29

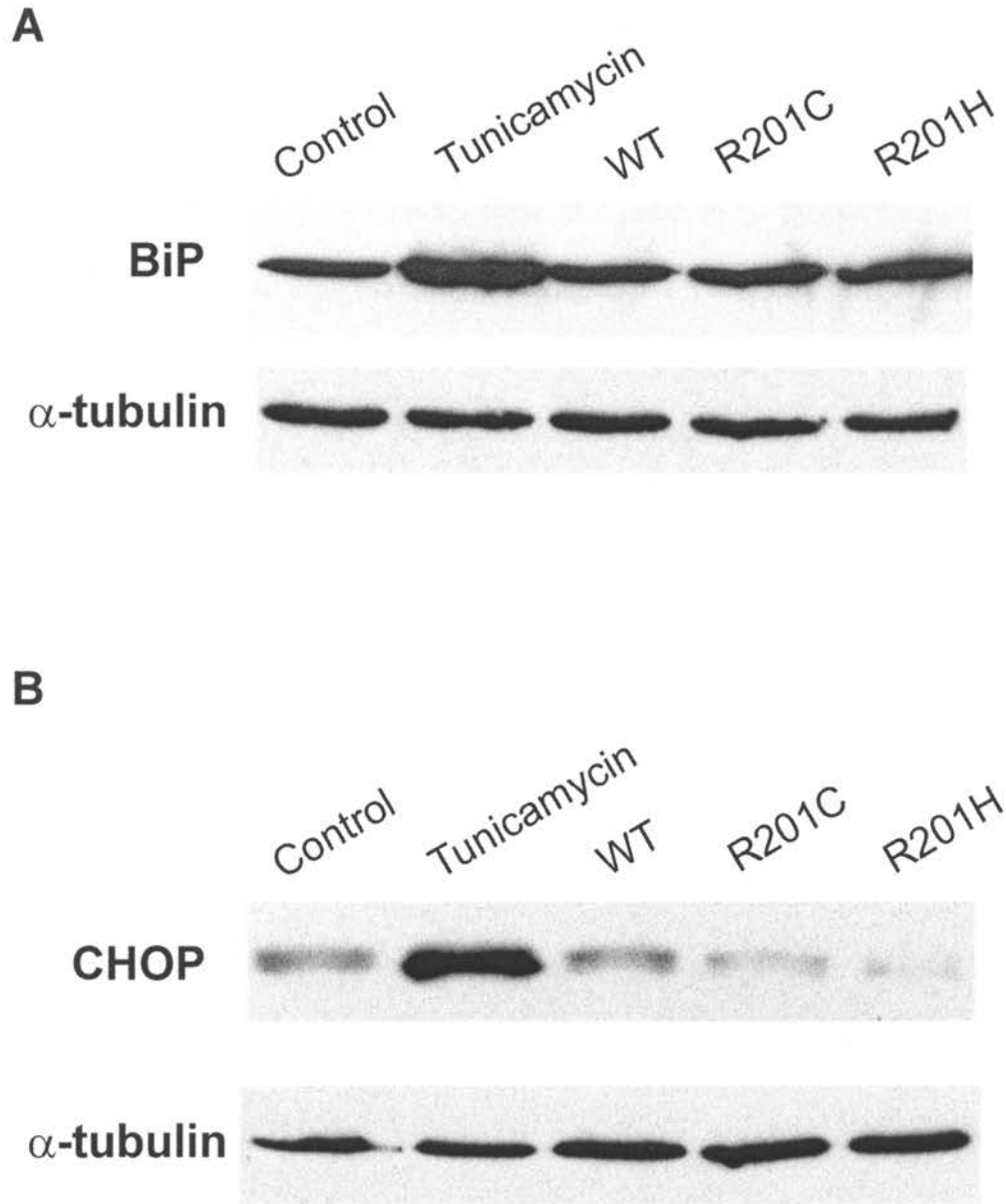

Lin et al. Figure 2

Fig. 29 Expression of mutant Kir6.2 in COSm6 cells does not induce unfolded protein response or apoptosis. Western blots of BiP (A) or CHOP (B) from COSm6 cells expressing WT or mutant K_{ATP} channel proteins (WT SUR1 plus WT or mutant Kir6.2). Cells treated with tunicamycin (1 μg/ml for 8 hours), a drug known to induce the expression of BiP and CHOP, were included as positive control. The same blots were probed for □-tubulin to show that the amount of protein loaded in each lane was similar.

Figure 30

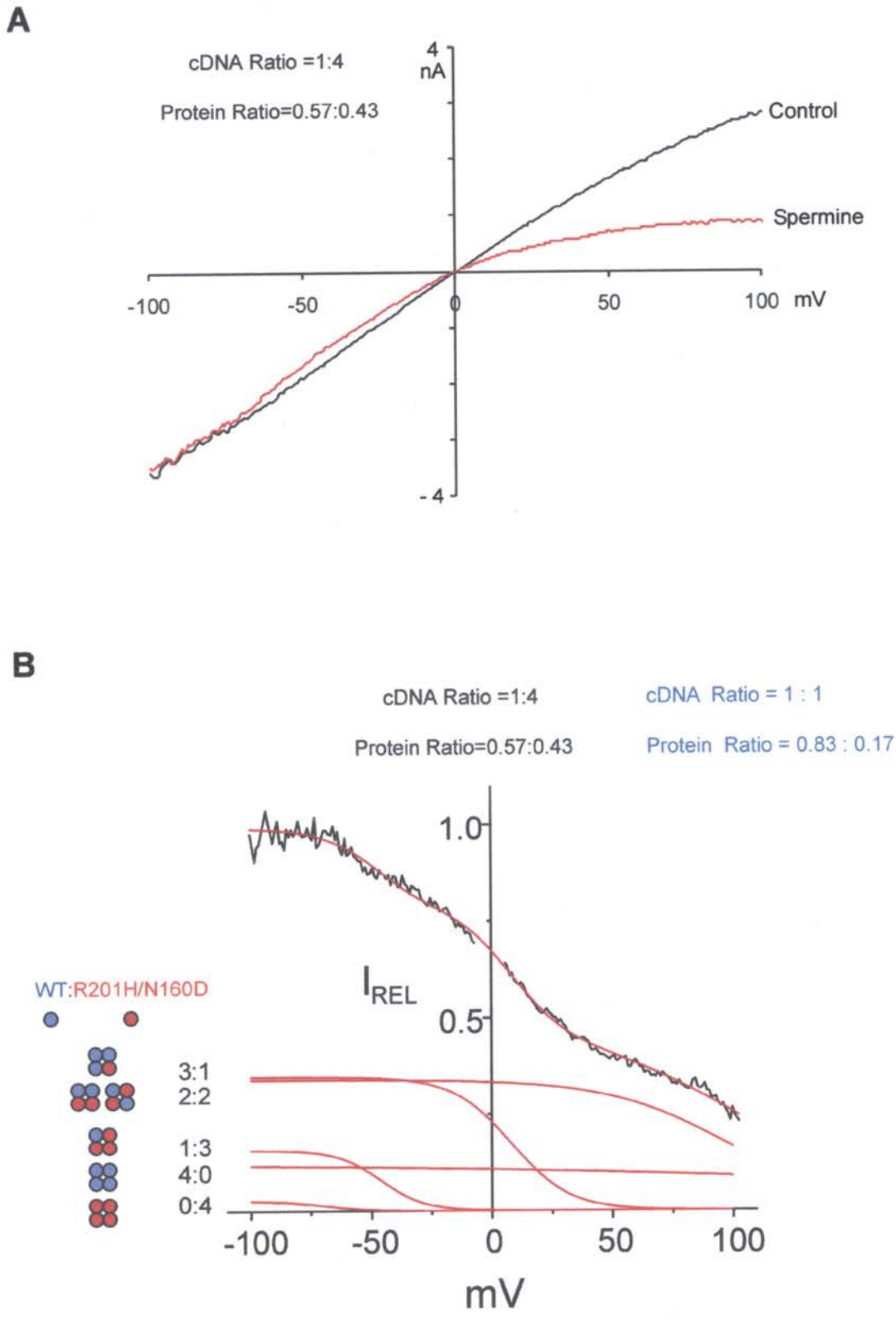

Lin et al. Figure 3

Fig. 30 Monitoring the relative abundance of WT and R201H mutant Kir6.2 subunits in surface K_{ATP} channels in simulated heterozygous expression using voltage-dependent spermine block. R201H mutant Kir6.2 was tagged with the N160D mutation, which confers channel sensitivity to voltage-dependent spermine block. (A) Current-voltage relationships of K_{ATP} channels in the absence (control) or presence of spermine (20 μM). (B) Relative conductance (Grel)-voltage relationships from the data shown in *A*. Note for illustration purposes, the curves presented in this figure are from an experiment where WT and R201H/N160D Kir6.2 were coexpressed at a cDNA ratio of 1:4. At this cDNA ratio, the protein ratio is close to 1:1 (0.57 : 0.43 for the patch shown) such that the five different channel populations (shown as the five individual Boltzmann function plots with the contributing number of WT and mutant subunits indicated next to each curve) can be clearly seen. In *B*, the smooth red line superimposed on the data (shown in black) is the sum of five Boltzmann functions that correspond to different combinations of WT and mutant Kir6.2 in a tetramer. The value of protein ratio calculated by fitting the overall Grel-V curve is shown on the top. At 1:4 cDNA ratio, a protein ratio of 0.57:0.43 gives the best fit. At 1:1 cDNA ratio, a protein ratio of 0.83:0.17 gives the best fits (in blue), consistent with estimation from the Western blots and chemiluminescence surface expression assay shown in Fig.28.

Figure 31

A

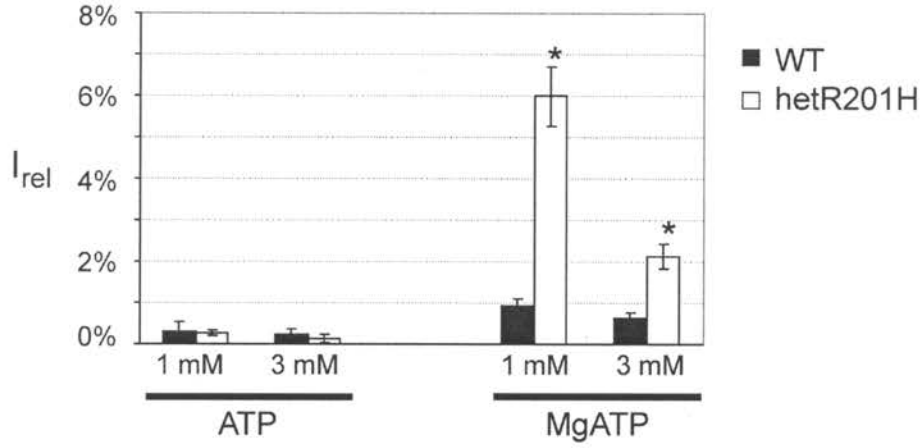

B

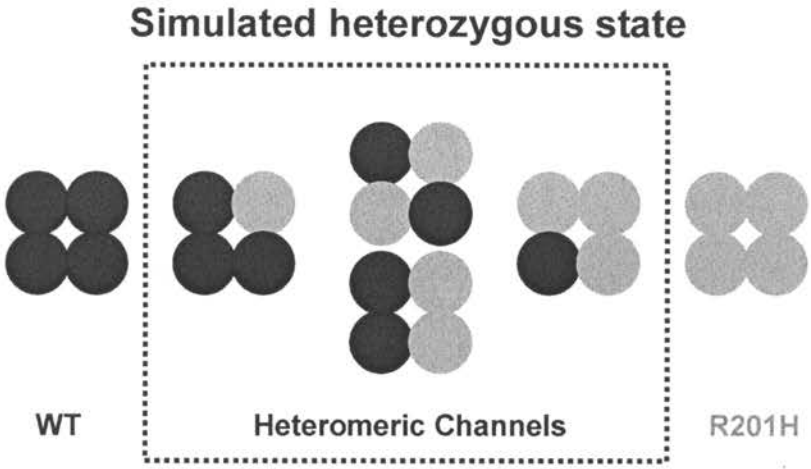

	WT	Heteromeric Channels			R201H
Fraction of total channel population:	0.4746	**0.39**	**0.119**	**0.016**	0.00083
Estimated number in a single β-cell:	380	**312**	**95**	**13**	~0

Lin et al. Figure 4

Fig. 31 Reduced sensitivity of hetR201H channels to physiological concentrations of MgATP. (A) Comparison of channel activity from WT and hetR201H channels in 1 or 3 mM ATP in the absence or presence of Mg^{2+} (MgATP). Currents were normalized to that observed in the absence of ATP (I_{rel}). (B) Schematic of the fraction of the different channel types expected when WT and R201H Kir6.2 are expressed at equal cDNA ratio (simulated heterozygous state) and the corresponding number of each type of channel expected in the plasma membrane of a single β-cell. Although homR201H channels are very active in physiological concentrations of MgATP (see Appendix Fig.35), they are unlikely to contribute to K_{ATP} conductance in β-cells since they are practically nonexistent in the heterozygous state. Rather, the overactivity of K_{ATP} channels seen in patients is likely due to heteromeric channels containing 1, 2,or 3 mutant subunits. Estimated fraction of individual channel populations (0, 1, 2, 3, or 4 mutants) in the total channel population is based on the WT: R201H protein ratio of 0.83 : 0.17 as shown in Fig.30B. The number of each type of channels in a single β-cell is calculated assuming the total number of K_{ATP} channels is 500 (a conservative over estimation based on data present in the literature) (Branstrom, Leibiger et al. 1998; Dunne, Cosgrove et al. 2004).

Figure 32

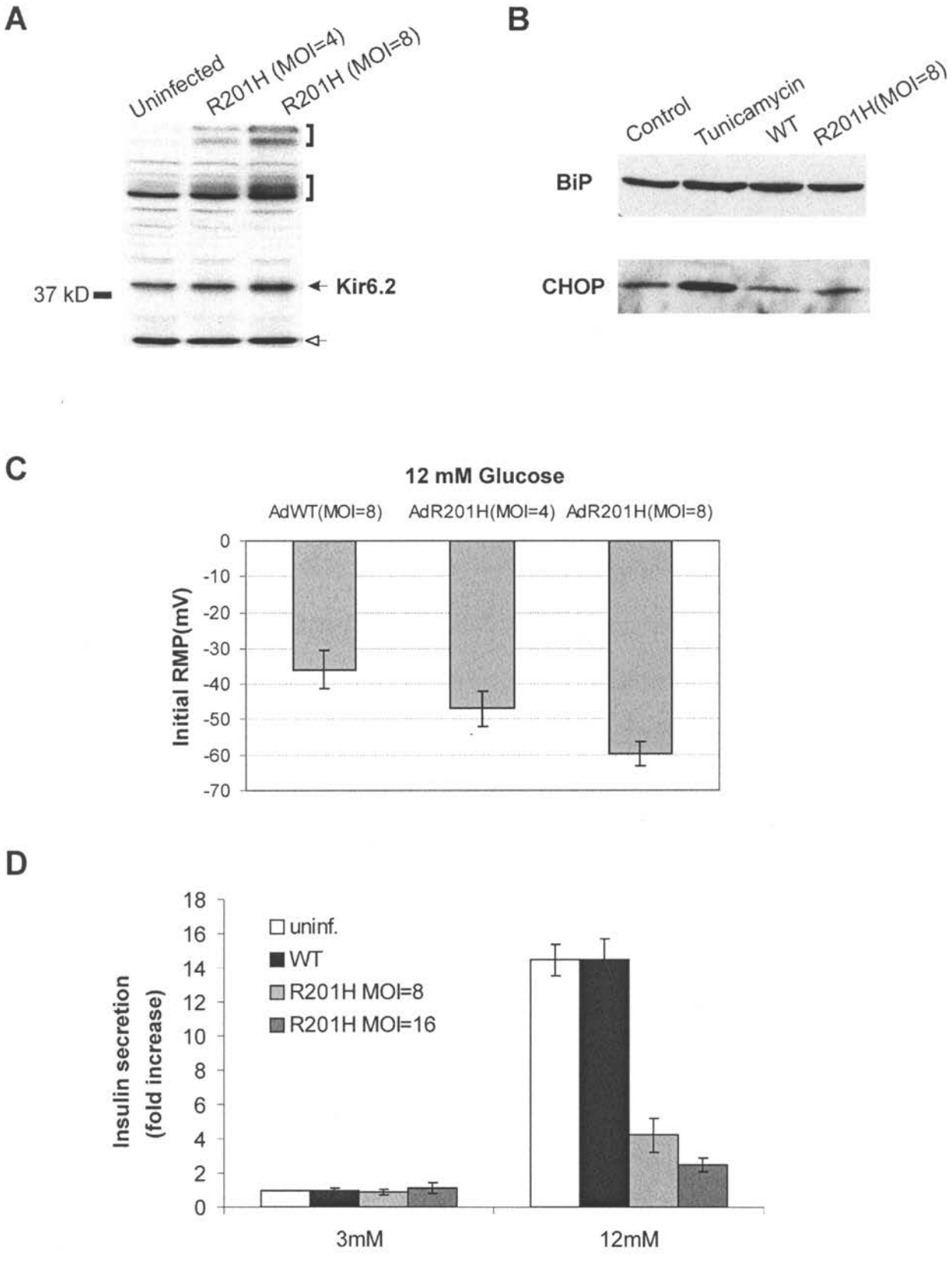

Lin et al., Figure 5

Fig. 32 Expression of R201H mutant Kir6.2 in INS-1 cells. (A) Western blots of endogenous Kir6.2 in uninfected INS-1 cells and endogenous as well as R201H Kir6.2 in cells infected with the R201H Kir6.2 virus. Shown is the full length of the blot where monomeric Kir6.2 is indicated by solid arrow and oligomeric Kir6.2 previously reported by us and others indicated by brackets (Zerangue, Malan et al. 2001; Yan, Lin et al. 2005). There are a number of nonspecific bands; a major one on the bottom is indicated by open arrow to show that equal amount of protein was loaded in each lane. (B) Comparison of BiP and CHOP protein levels in uninfected control cells and cells infected with WT or R201H Kir6.2 virus. Tunicamycin treated cells (1 μg/ml for 8 hours) were served as a positive control (see Fig.29). (C) The resting membrane potential (RMP) of INS-1 cells infected with WT Kir6.2 virus or R201H Kir6.2 virus at 12 mM glucose. (n = 25-39). The RMP of cells infected with WT Kir6.2 virus is similar to that of uninfected cells (not shown) (Lin, Yan et al. 2005), and is much more depolarized than cells infected with the R201H virus. Note the value shown is the initial RMP upon break-in. Previous studies have found that this value is similar to that obtained using perforated patch-clamp recording (Lin, Yan et al. 2005). (D) Insulin secretion in response to 12 mM glucose stimulus was greatly reduced in cells infected with the R201H Kir6.2 virus, whereas no difference was seen at basal level glucose (3 mM). Note the higher MOI used due to the higher cell density needed for insulin secretion assays.

Figure 33

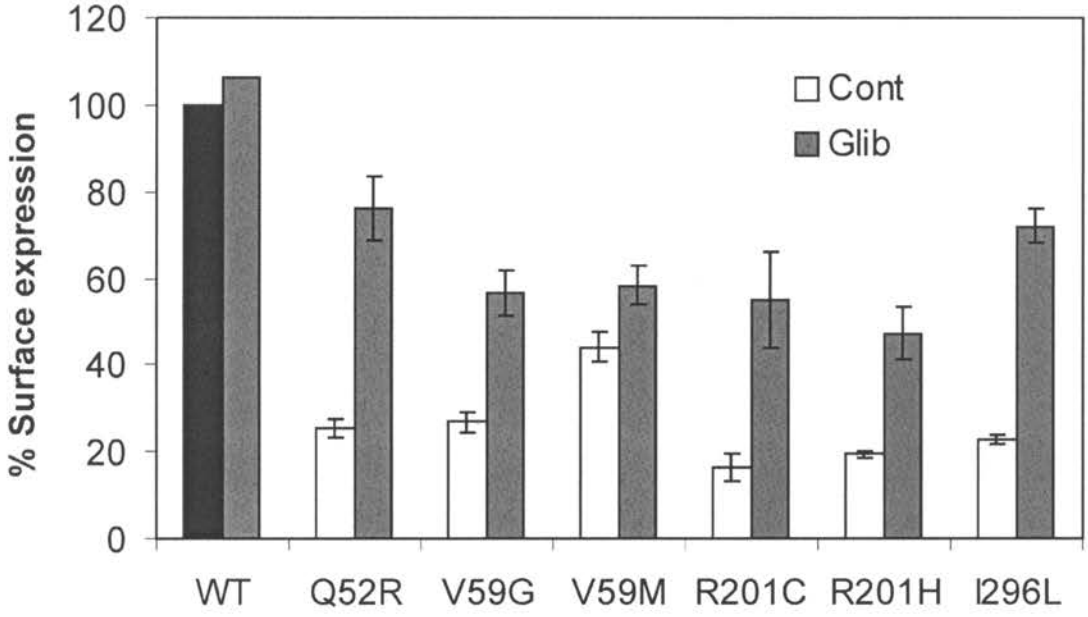

Lin et al., Figure 6

Fig. 33 Effects of sulfonylureas on expression of PNDM-causing mutant K_{ATP} channels. Surface expression of various PNDM mutant channels in cells treated with or without 5 μM glibenclamide for 24 hours was quantified by chemiluminescence assays. Glibenclamide treatment increased surface expression of all mutants to varying degrees. Each bar represents mean ± s.e.m. of 4-5 experiments.

APPENDIX

Figure 34

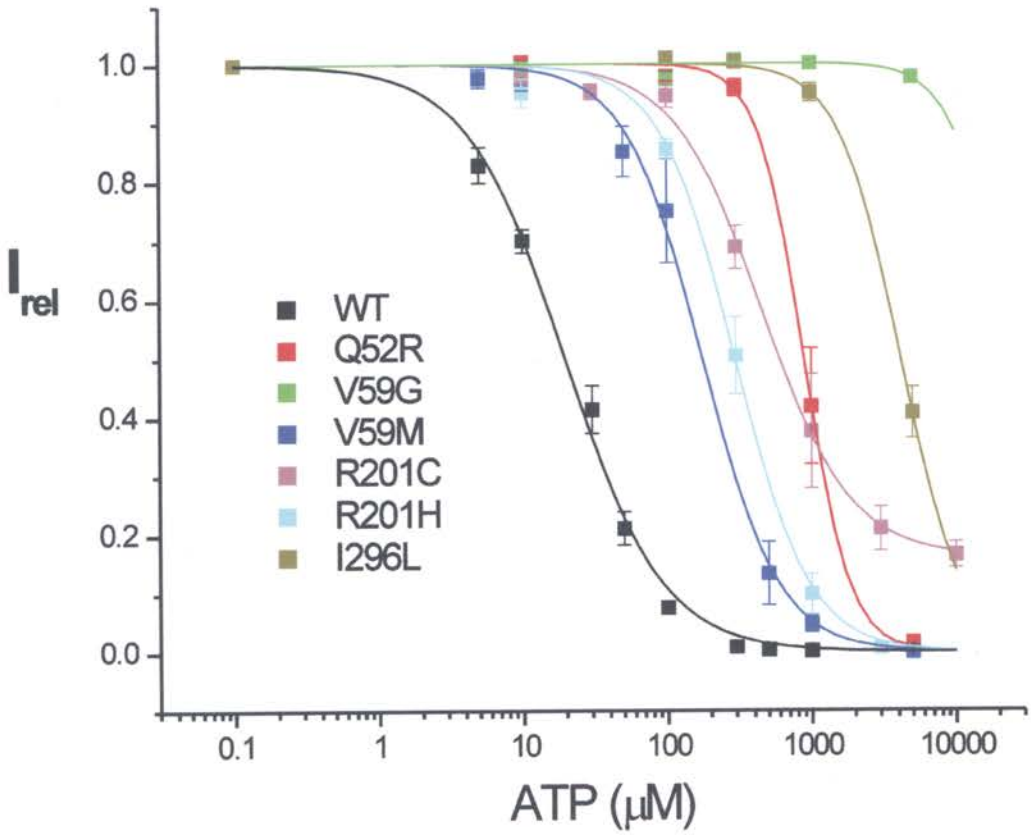

Lin et al. Appendix Figure 1

Fig.34 ATP response of WT and PNDM mutant channels

(A) ATP dose response curves in the absence of Mg^{2+}. Currents in different ATP concentrations were normalized to the current observed in the absence of ATP. Data points (n = 5-9) were fitted by the Hill equation: $I_{rel} = 1/(1+([ATP]/IC_{50})^H$. (B) The IC_{50} values for ATP obtained in this study are compared to those obtained from previous studies by others. Although the absolute values differ somewhat, the extent of ATP sensitivity reduction for most mutants is in general agreement, with the exception of Q52R. The IC_{50} of ATP for Q52R we obtained (889 μM) is substantially higher than that reported previously (84 μM from Proks *et al.* and 125 μM from Koster *et al.*). A notable difference between our experiments and those of others is that 1 mM EDTA was included in the bath solution during our inside-out patch-clamp recording. In earlier work, we have shown that EDTA nearly eliminates channel rundown, allowing for more accurate measurement of ATP sensitivity (Enkvetchakul, Loussouarn et al. 2000; Lin, Jia et al. 2003).

Table VII Comparison of IC_{50} ATP from this study and previous studies

Mutation	IC_{50} ATP from this study (μM); H = Hill coefficient	IC_{50} ATP from other studies (μM)	Phenotype
WT	15 (H = 1.5)	7 (1); 6 (2)	none
Q52R	889 (H = 2.8)	84 (1); 125 (2)	DEND
V59G	>10,000 (H = 3.7)	7,400 (1)	DEND
V59M	176 (H = 1.7)	58 (3); 16 (2)	Intermediate DEND
R201C	415 (H = 1.6)	106 (1)	PNDM/some DEND
R201H	296 (H = 1.7)	299 (4)	PNDM
I296L	4,200 (H =2.1)	3,400 (5); 771 (2)	DEND

The IC_{50} of ATP inhibition for the various homomeric PNDM mutant channels obtained in this study are compared to those obtained from previous studies (see reference cited following each value). In general, the values we obtained are somewhat higher than those reported previously, especially for the Q52R mutation. A notable difference between our experiments and those of others is that 1 mM EDTA was included in the bath solution during our inside-out patch-clamp recording. EDTA chelates residual Mg^{2+} and has been previously shown to eliminate channel rundown, thereby allowing for more stable current and accurate measurement of ATP sensitivity (Lin et al, 2003). Since channel rundown is known to lead to an increase in the apparent channel ATP sensitivity (Enkvetchakul et al., 2000), the higher IC_{50} values in the absence of rundown, as is the case in this study, are therefore expected. With the exception of V59M (see main text discussion on the role of channel expression in disease phenotype), the IC_{50} ATP from this study correlates quite well with the disease phenotype (also see MgATP sensitivity comparison in Appendix figure 36).

Figure 35

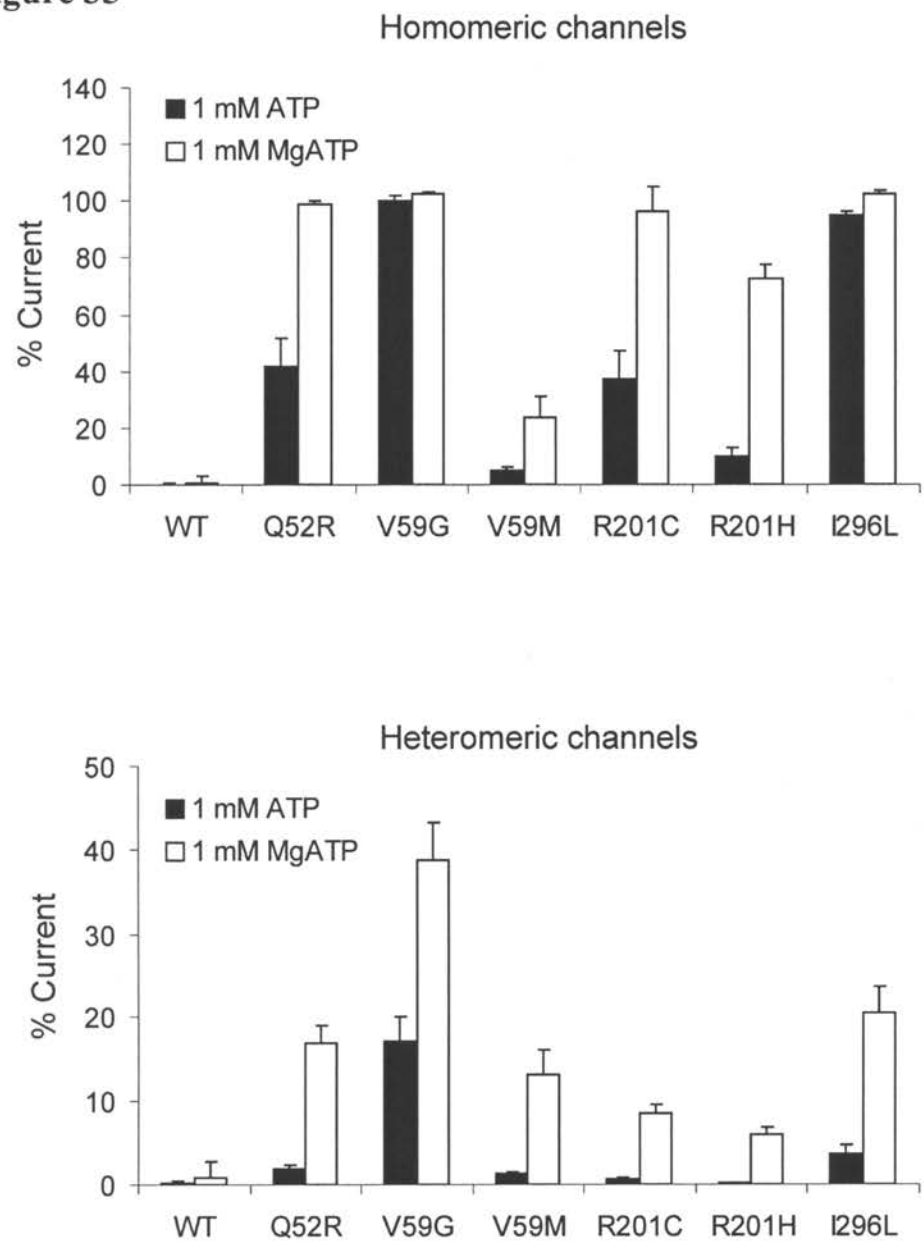

Lin et al. Appendix Figure 2

Fig.35 MgATP response of WT and PNDM mutant channels. Currents were normalized to that seen in the absence of ATP (K-INT solution).

Figure 36

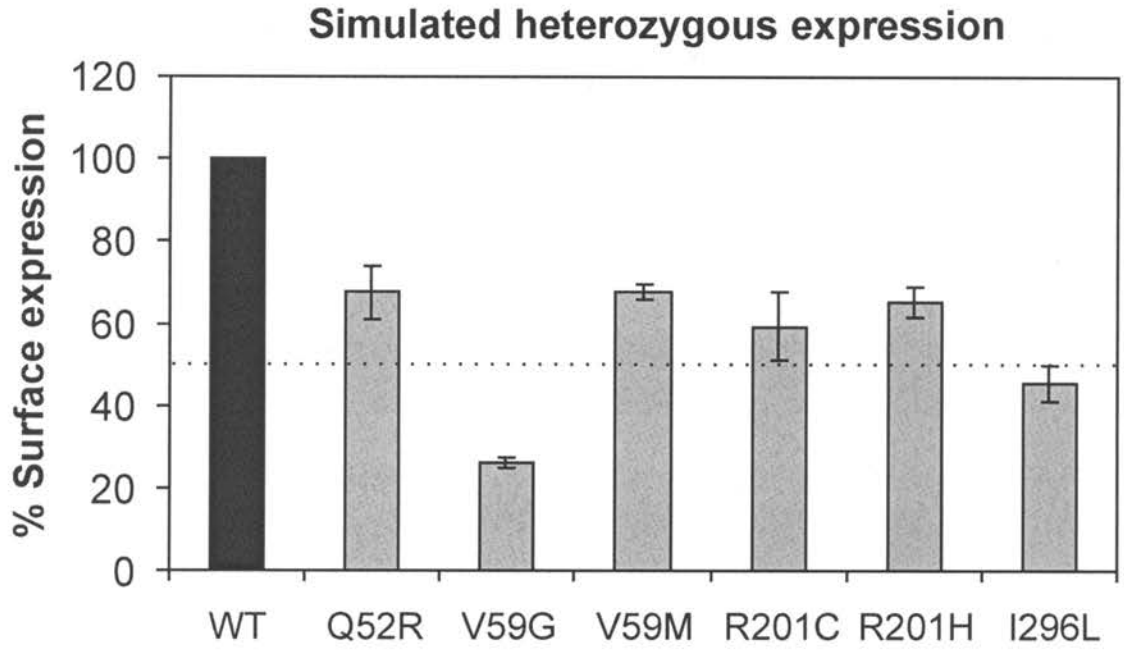

Lin et al. Appendix Figure 3

Fig.36 Channel expression level under simulated heterozygous state. To evaluate how mutations affect overall channel expression in the heterozygous state, we performed chemiluminescence assays in cells co-expressing WT and mutant Kir6.2 at 1:1 cDNA ratio. The overall channel expression level was also reduced in all mutations in simulated heterozygous state, with the reduction being mild (<50%) in Q52R, V59M, and R201C, and more severe (>50%) in V59G and I296L. The varying degrees of reduction seen in the different mutations indicate that the effects of mutations on channel biogenesis and expression may or may not be dominant.

CHAPTER FIVE

Correlating Structure to Function in Kir6.2 and SUR1

Yu-Wen Lin[1], Satoko Shimamura[1], Jillene Casey[1], Courtney MacMullen[2], Arupa Ganguly[2], Charles A. Stanley[2], and Show-Ling Shyng [1]

From the Center for Research on Occupational and Environmental Toxicology, Oregon Health & Science University, Portland, OR 97239,[1] and Division of Endocrinology/Diabetes, The Children's Hospital of Philadelphia, Philadelphia, Pennsylvania, 19104. [2]

The results described here are from studies carried out to elucidate the channel defects caused by a set of Kir6.2 and SUR1 mutations identified from CHI patients. Satoko Shimamura and Jillene Casey made most of the ratKir6.2 mutant cDNA constructs. I performed all the functional studies. These mutations were identified from Dr. Charles Stanley's lab. In the cysless project, I performed functional study on a SUR1construct that lacks all of the 16 intracellular cysteine residues that was made by Satoko Shimamura.

INTRODUCTION

The activity of pancreatic K_{ATP} channels regulates insulin secretion. As expected, mutations of K_{ATP} channels that lead to channel dysfunction result in insulin secretion disorders. These mutations provide unique tools to probe the structure-functional relationship of the channel protein. Recently we have obtained a set of novel Kir6.2 and SUR1 mutations identified from patients with congenital hyperinsulinism (CHI). As reviewed in Chapter 1, CHI is characterized by an excessive release of insulin despite severe hypoglycemia with loss of K_{ATP} channel function being the major underlying cause. I have conducted preliminary studies to characterize the molecular defects in K_{ATP} channels caused by these disease mutations.

Of the eight Kir6.2 mutations I examined, all mutants have reduced or lack of expression at the cell surface. In addition, some of them exhibit specific gating defects. Thus we conclude that the expression defect, gating defects or both are likely the main reason causing the disease. Sequence comparison with potassium channels whose structures have been solved revealed that the affected Kir6.2 residues are all located in structural features that have been proposed to play a role in gating. Our study provides functional confirmation of the importance of these structures in Kir6.2 gating and biogenesis.

Toward understanding the gating behavior of K_{ATP} channel, it is necessary to know how SUR1 couples Kir6.2 to regulate its function. To understand how SUR1 couples to Kir6.2 to regulate channel activity, it is important to address the structural region in SUR1 that undergo conformational change or that physically interact with

Kir6.2 during channel gating. In an effort to address this question, we also constructed and characterized a SUR1 lacking all its intracellular cysteine as a tool for future cysteine crosslinking experiments.

MATERIALS AND METHODS

Molecular biology

Rat Kir6.2 cDNA is in pCDNAI/Amp vector (a generous gift from Dr. Carol A. Vandenberg) and SUR1 in pECE. Point mutations of SUR1 were introduced into hamster FLAG-SUR1 cDNA in the pECE plasmid using the QuickChange site-directed mutagenesis kit (Stratagene). Epitope tag and mutations were confirmed by DNA sequencing. All SUR1 constructs are in the pECE vector. Mutant clones from two independent PCR reactions were analyzed to avoid false results caused by undesired mutations introduced by PCR

Western blotting and chemiluminescence assay

Cell surface expression level of the mutant channel was assessed by Western blot and by a quantitative chemiluminescence assay using a SUR1 that was tagged with a FLAG-epitope (DYKDDDDK) at the N-terminus (fSUR1), as described previously (Taschenberger, Mougey et al. 2002). COSm6 cells grown in 35 mm dishes were transfected with 0.4 μg rat Kir6.2 and 0.6 μg fSUR1 and lysed 48-72 hours post-transfection in 20 mM HEPES, pH 7.0/5 mM EDTA/150 mM NaCl/1% Nonidet P-40 (IGAPEL) with Complete^{TR} protease inhibitors (Roche Applied Science, Indianapolis, IN). Proteins in the cell lysate were separated by SDS/PAGE (7.5% for SUR1 and 12%

for Kir6.2), transferred to nitrocellulose membrane, and analyzed by incubation with appropriate primary antibodies followed by horseradish peroxidase (HRP)-conjugated secondary antibodies (Amersham Biosciences, Piscataway, NJ), and visualized by enhanced chemiluminescence (Super Signal West Femto; Pierce, Rockford, IL). The primary antibodies used are: M2 mouse monoclonal anti-FLAG antibody for fSUR1 (Sigma, St. Louis, MO) and rabbit polyclonal anti-Kir6.2 for Kir6.2 (from Santa Cruz Biotechnology, Santa Cruz, CA). For chemiluminescence assay, cells were fixed with 2% paraformaldehyde for 30 min at 4°C. Fixed cells were preblocked in PBS+0.1% BSA for 30 min, incubated in M2 anti-FLAG antibody (10 μg/ml) for an hour, washed 4x30 min in PBS+0.1% BSA, incubated in HRP-conjugated anti-mouse (Jackson, 1:1000 dilution) for 20 min, and washed again 4x30 min in PBS+0.1% BSA, all at room temperature. Chemiluminescence of each dish was quantified in a TD-20/20 luminometer (Turner Designs) following 15 sec incubation in Power Signal Elisa luminol solution (Pierce). All steps after fixation were carried out at room temperature.

Electrophysiology

Patch-clamp recordings were performed in the inside-out configuration as previously described. Briefly, COSm6 cells were tranfected with cDNA encoding WT or mutant channel proteins, as well as cDNA for the green fluorescent protein (GFP) to help identify positively transfected cells. Patch-clamp recordings were made 36-72 hours post-transfection. Micropipettes were pulled from non-heparinized Kimble glass (Fisher Scientific) with resistance typically ~1-2.5 M□. The bath (intracellular) and pipette (extracellular) solution (K-INT) had the following composition: 140 mM KCl, 10 mM K-HEPES, 1 mM K-EGTA, pH 7.3. ATP and ADP were added as the

potassium salt. For measuring ATP^{4-} sensitivity, 1 mM EDTA was included in K-INT to prevent channel rundown (Lin, Jia et al. 2003). All currents were measured at a membrane potential of -50 mV (pipette voltage = +50 mV) and inward currents shown as upward deflections. Data were analyzed using pCLAMP software (Axon Instrument). Off-line analysis was performed using Microsoft Excel programs. The MgADP or diazoxide response was calculated as the current in a K-INT solution containing either 0.1 mM ATP and 0.5 mM ADP or 0.1 mM ATP and 0.3 mM diazoxide (both with1 mM free Mg^{2+}), relative to that in plain K-INT solution.

RESULTS

Functional characterization of Kir6.2 mutants associated with CHI

The eight novel Kir6.2 mutations identified from CHI patients are A101D, G134A, R136L, G156R, D204E, P266L, R301H, and R301P; their positions are mapped onto the homologous KirBac1.1 structure (Figure 38). These mutations are all recessive homozygous in patients. Because loss of channel expression at cell surface could be a mechanism causing loss of channel function, we first assessed surface expression level of these mutants by western blotting and then by an immunochemistry-based chemiluminescence assay for further protein quantification. By co-expressing mutant Kir6.2 with SUR1 in COS cells, biochemical and immunological analyses found that all mutants have reduced or lack of expression at the cell surface: A101D being ~69%, G134A being ~1%, R136L being ~36%, G156R being ~72%, D204E being ~78%, P266L being ~8%, R301H being ~17% and R301P being ~5%, that of WT (Figure 39). Interestingly, the steady state level of Kir6.2 protein is decreased in

G134A, R136L, R301H and R301P; the decrease of steady state Kir6.2 protein might render the lower surface expression of octomeric channels. Next we performed functional studies to test the gating behavior of these mutant channels and found that four mutant channels (G134A, R136L, G156R and D204E) do not generate detectable currents, indicating that some mutants have severe gating defects though with reasonable surface expression (R136L, G156R and D204E).

Among these mutant channels, the A101D mutation has only slightly reduced surface expression, the disease may therefore be caused by gating defects. However, on further test of its response to ATP, PIP_2 and MgADP, I found the mutant channel to have WT-like response toward these regulators. Whether the slightly reduced surface expression is sufficient to give rise to the disease will need to be determined in the future by studying this mutation in insulin secreting cells.

For the P266L mutation, it has reduced surface expression but normal gating property suggesting reduced surface expression is likely the underlying mechanism for the disease (Figure 40).

Both R301H and R301P have very low surface expression; both also exhibit a gating defect characterized by rapid current decay in ATP free solution similar to the inactivation behavior described in chapter 2 (see Figure 40). Because R301H and R301P inactivated like what we have seen in our inactivation mutants, we hypothesize that the R301 residue might be located in the interface domain between two Kir6.2 subunits and that disrupting the interaction damages channel stability. Based on the homology structure of GIRK channel, three residues, E292, S212 and F250 are in close proximity to R301. We therefore mutated these residues to test whether similar channel

inactivation can be induced. Our data show that mutation of F250 to alanine resulted in channel inactivation whereas mutation of E292 or S212 to alanine had no effect, suggesting that F250 might be the interacting partner of R301 (Figure 41.) To seek further evidence for interaction between R301 and F250, we constructed double cysteine mutations F250C /R301C and reciprocal mutations F250R/R301F to test whether channel stability can be restored if the interaction of these two residues are rebuilt. However, neither double cysteine mutations nor reciprocal mutant channels generated any detectable current; therefore, identification of the residue that interacts with R301 to stabilize channel activity will require further effort.

For D204E, it has reasonable surface expression but no detectable channel activity. We tested whether coexpresion of D204E with WT Kir6.2 could rescue the mutant. I found that when D204E was coexpressed with WT at 1:1 ratio, the heterozygous channel displayed inactivation distinct from WT channels. These results suggest that the homozygous mutants must have a serious gating defect, possibly by locking the channel in the closed or inactivated state (Figure 40).

Functional characterization of SUR1 construct lacking all its intracellular cysteine

In understanding the gating behavior of K_{ATP} channel, a central question is how SUR1 couples to Kir6.2 to regulate its function. As mentioned earlier, SUR1 confers two important functions of the pore complex: hypersensitizing Kir6.2 to ATP inhibition and stimulating channel activity via its ATPase activity (i.e. conferring MgADP sensitivity).

Cysteine cross-linking is widely used to probe protein structure. We are interested in using this approach to map the regions of SUR1, in particular in the nucleotide binding folds, that undergo conformational change during gating. This approach can also be used to map the structural domains that physically interact with Kir6.2 subunit during channel gating. We therefore constructed a SUR1 mutant (cysless SUR1) that lacks all of its intracellular cysteine (see Figure 43). We plan to use this construct for cross-linking experiments to study interaction of introduced cysteine pairs at specific positions. The purpose of making this construct is to avoid cross-linking between endogenous cysteines and between engineered cysteines and endogenous cysteines. So far we have constructed this cysless SUR1 and characterized its nucleotide sensitivity. Although the channel is active in the absence of ATP and appears to have normal ATP sensitivity, it lacks MgADP response.

DISSCUSION

In this study, we have examined the surface expression and characterized the functional phenotype of eight novel Kir6.2 mutation identified from CHI patients. Many of these mutants, for example, G134A, P266L, R301H and R301P, do have much lower surface expression; the reduced surface expression is expected to cause loss of the channel function, thus CHI. Interestingly, G134A is the second glycine of the selectivity filter; mutation at this position might affect ion selectivity. Additionally, our data suggest the G134A mutation may cause defect in protein folding or protein stability since the steady state of Kir6.2 protein level was greatly reduced.

For mutants that have reasonable surface expression but no recordable channel activity (R136L, G156R and D204E), different mechanisms may explain the disease. For instance, R136 is located in the pore region and may alter the packing of the pore structure to causes loss of channel function. In this regard, it is interesting to note that a homologous residue in Kir2.1 has been proposed to form an ion pair to stabilize the pore structure (Yang et al., 1997).

For the G156R mutant, it has good surface expression but no channel activity. This G156 residue is located at an interesting position in the TM2 helix. It has been proposed that TM2 helix bends and opens its conductance pathway during channel opening (Doyle et al., 1998; Jiang et al, 2002a; 2002b). Two conserved glycines (upper glycine and lower glycine in Figure 42) located in TM2 helix among K channels have been postulated as the bending sites. In Kir6.2, G156 (upper glycine) and G165 (lower glycine) are these two glycines (Figure 42). Either glycine has been favored as the pivotal bending point in different K channels. Studies by Yi et al, Sadja et al and Jin et al. support the upper glycine as the bending site in GIRK channels (Yi et al, 2001; Sadja et al., 2001; Jin et al., 2002) while Jiang et al's structure modeling suggests the lower glycine is responsible for the MthK channel opening. (Jiang et al., 2002)

According to these studies, the G156A mutation may lock the channel in the close state if this glycine plays the pivotal role as the glycine hinge. To test which glycine in Kir6.2 is important during K_{ATP} channel gating, we functionally tested the mutant channel of G156P and G165P (See Figure 42). By substitution of a proline at either glycine, we hypothesize that the mutant channel might be constitutively active or insensitive to ATP inhibition by causing a kink in the TM2 helix. Our results show that

the G156P have small current level but this small current can be largely increased by application of ATP and subsequently removal of the ATP inhibition as shown in Figure 41. However, the refreshed current by ATP decayed quickly and remained unstable. In contrast, G165P channel generates good current and this current is insensitive to ATP inhibition. Our data suggest the lower glycine (G165) may cause a kink in Kir6.2 during channel opening for the G165P mutation renders the channel insensitive to ATP inhibition. Nevertheless, both glycines are critical for channel gating as evidenced by the altered gating behavior when they are mutated, but the detail mechanisms would require more mutagenesis work and electrophysiological analysis.

For the R301H and R301P mutants, both trafficking defects and gating defects could contribute to their loss of channel function and the gating defects might be due to disruption of intersubunit interactions. However, to validate this hypothesis, its subunit-subunit interacting partner will need to be identified.

Figure 37. Positions of Novel Kir6.2 mutations identified in patients with Permanent Neonatal Diabetes

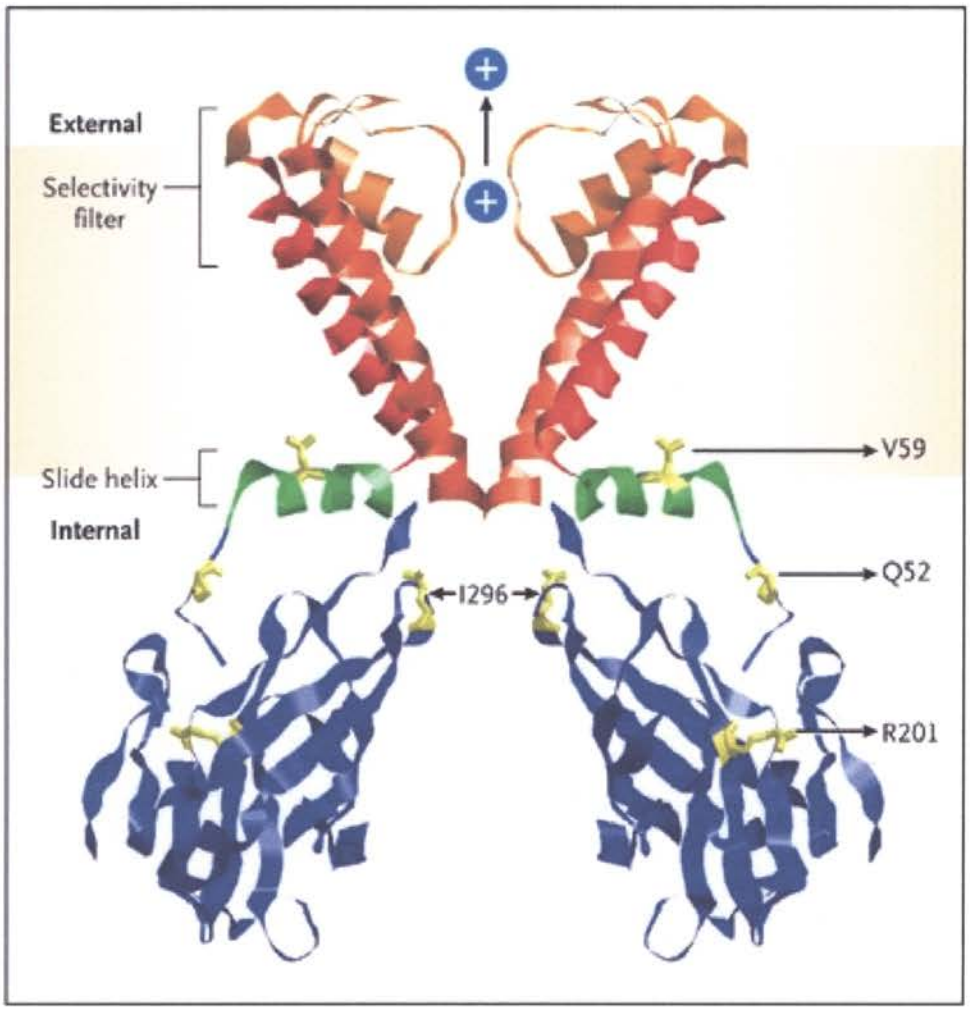

Gloyn AL. et al., 2004 NEJM

Figure 38. Positions of Novel Kir6.2 mutations identified from CHI patients

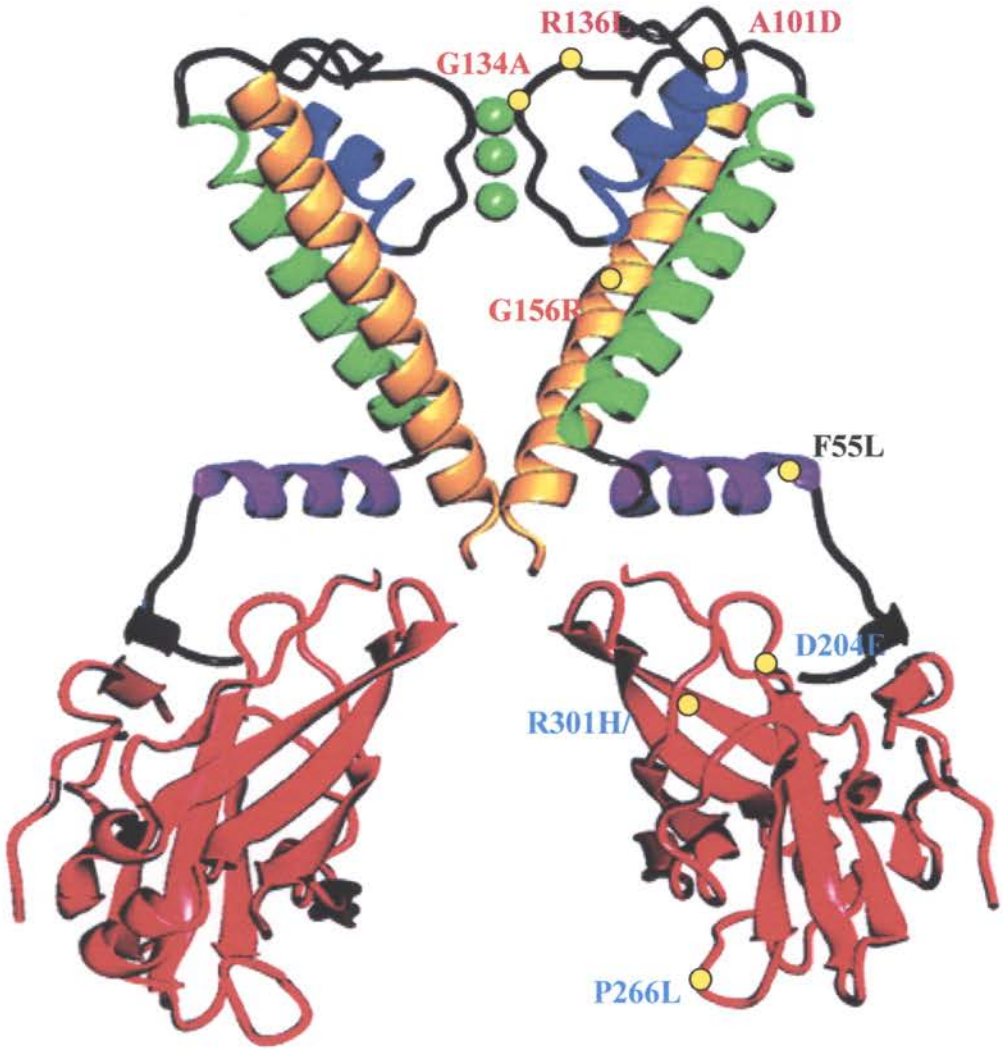

Kir6.2 mutations associated with CHI are mapped onto mGIRK1 structure. The residues located in the transmembrane regions are labeled in red while the residues located in the cytoplasmic domain are in cyan.

Kuo A. et al., Science.2003

Figure 39 Most Kir6.2 mutants have reduced their surface expression

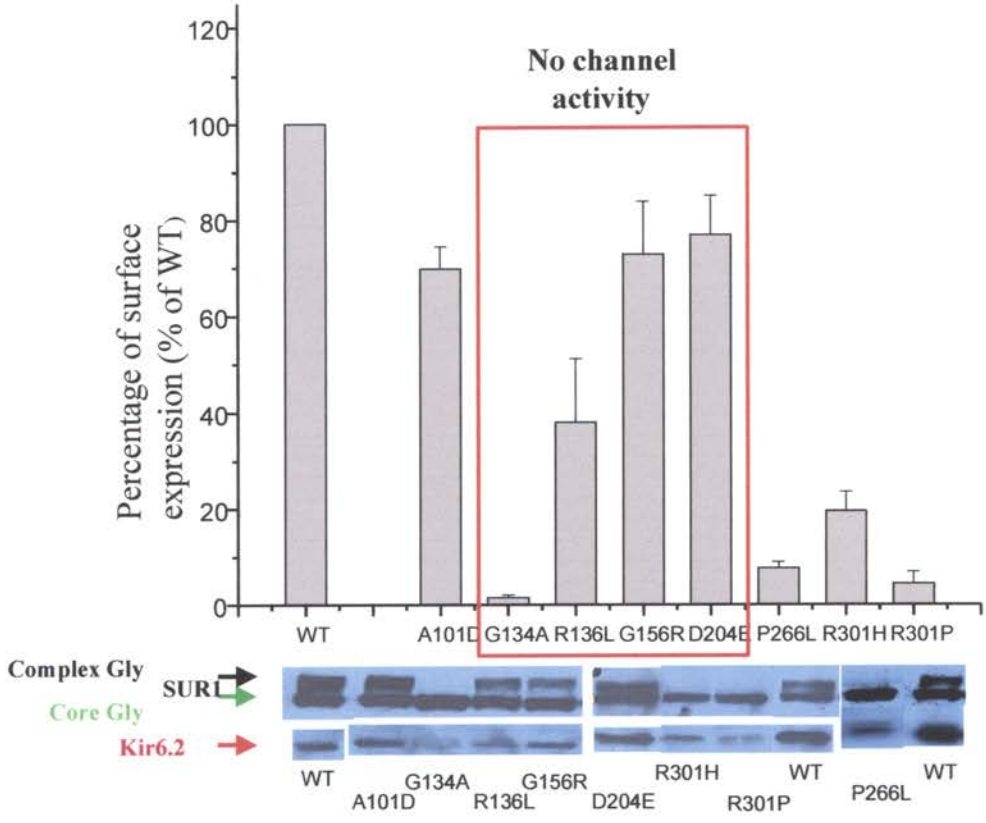

Top :The column chart shows results of quantification of surface expression among WT and various Kir6.2 mutants in COSm6 cells using chemiluminescence assays. These channels without any detectable current were labeled as well. . Expression level was normalized to that of WT channels. Each value is the average of 3-4 independent experiments. The error bar represents the stardard error of the mean (s.e.m.).
Bottom: Western blots of WT fSUR1 (upper panel) and WT or mutant Kir6.2 (lower panel) coexpressed in COSm6 cells. The complex-glycosylated form of fSUR1 is indicated by the solid arrow in black and the core-glycosylated form the green arrow. Note the upper band fSUR1 is reduced in some CHI mutants compared with WT, indicating reduced surface expression(G134A, R136L, G156R, R301H and R301P). In some mutants, reduced steady state Kir6.2 protein level was also apparent (G134A, R301H and R301P). The faint band right above monomeric Kir6.2 is nonspecific.

Figure 40 Functional characterizations of Kir6.2 mutants

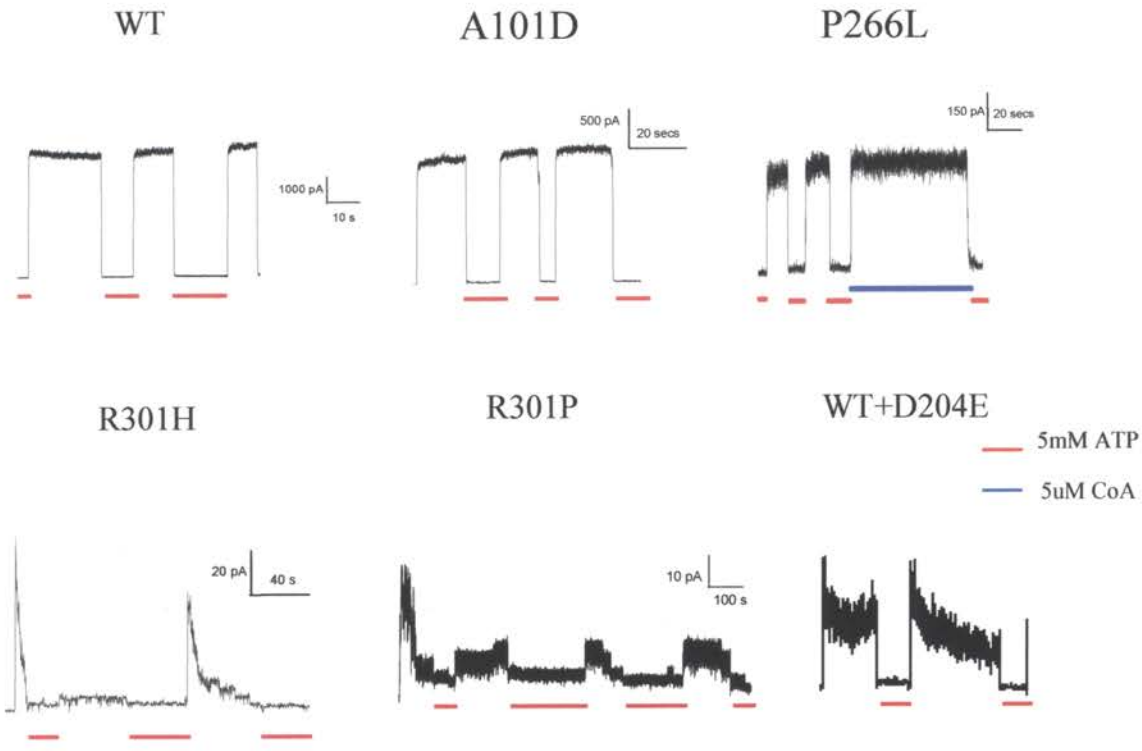

Representative inside-out patch-clamp recordings from cells expressing wild-type (WT), A101D, P266L, R301H, R301P or WT coexpressed with D204E as indicated. The applications of 5mMATP and 5μM oleoyl CoA are labeled in red and blue. All recordings were made at +50 mV pipette potential with symmetrical K-INT/EDTA solution on both sides of the membrane patch. Inward currents are shown as upward deflection. Some mutants, for example R301H, R301P and WT coexpressed with D204E show inactivation phenotype in ATP free solution.

Figure 41. Identification of the intersubunit-interacting partner of R301 residue

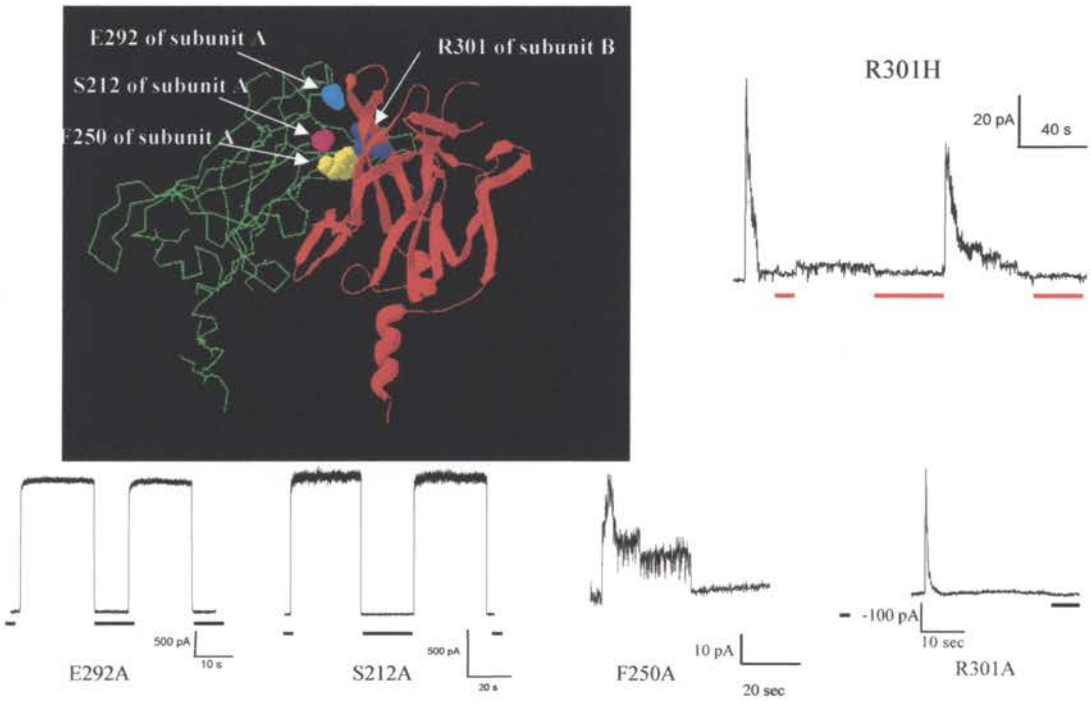

A simulated mGIRK structure was adopted to probe the interacting partner of R301 residue. In this model, E292, S212 and F250 from neighboring subunits are in close proximity with R301 in another subunit (Nishida and Mackinnon, 2002).
Representative inside-out patch-clamp recordings from cells expressing R301H, E292A, S212A, F250A and R301A. The applications of 5mMATP and 1mM ATP are labeled in red and black solid line. All recordings were made at +50 mV pipette potential with symmetrical K-INT/EDTA solution on both sides of the membrane patch. Inward currents are shown as upward deflection. F250A channels inactivated like R301A/R301H while E292A and S212A had stable current level.

Figure 42. Both upper glycine (G156) and lower glycine (G165) affect channel gating

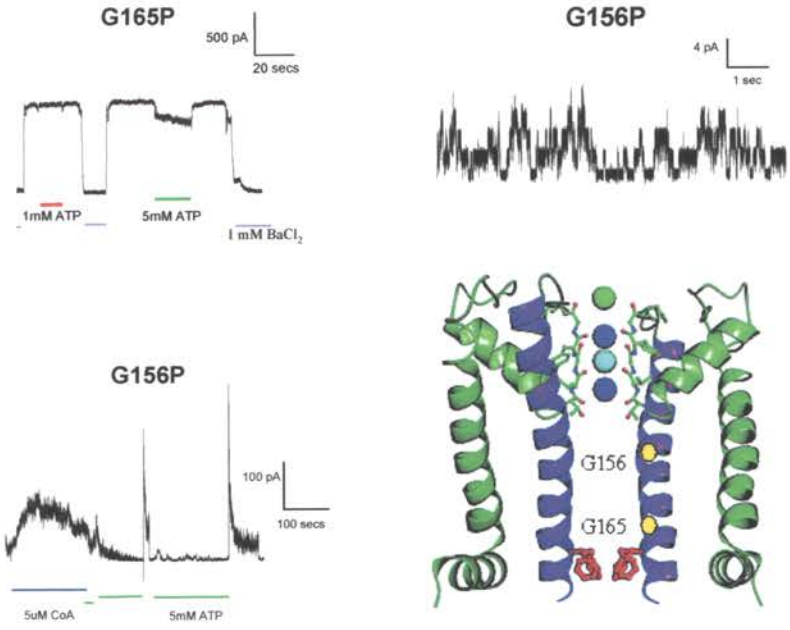

Conformation of the selectivity filter and the pore helices from KirBac1.1 structure is shown at the bottom right panel (Kuo et al., 2003). The inner helices are colored purple whereas the side chains of Phe^{168} blocking residues are colored red. G156 and G165 are mapped on one of the inner helices for their positions and are colored in yellow.
Representative inside-out patch-clamp recordings from cells expressing G156P and G165P are illustrated individually. The applications of 5mMATP and 1mM ATP are labeled in red and green line and 5μM oleoyl CoA in blue. Note that G165P has very low sensitivity to ATP inhibition and the zero current level was obtained by application of 1 mM barium chloride colored in purple. All recordings were made at +50 mV pipette potential with symmetrical K-INT/EDTA solution on both sides of the membrane patch. Inward currents are shown as upward deflection.

Figure 43. SUR1 with its intracellular cysteines

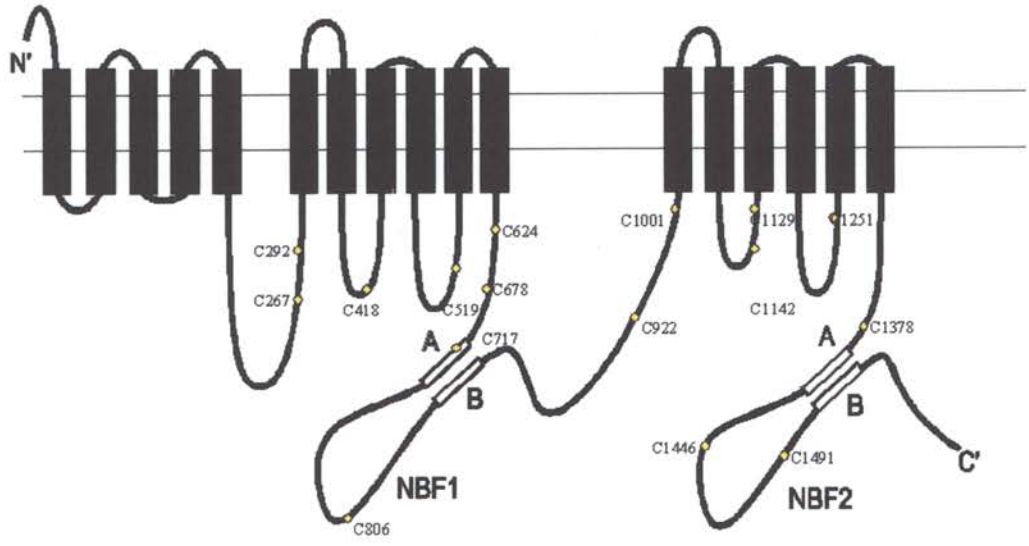

Transmembrane topology of SUR1 with two NBF domains. All 16 intracellular cysteines are indicated in yellow dots.

CONCLUSIONS AND FUTURE DIRECTIONS:

The work described in this dissertation improved our understanding of the structure-functional relationship in K_{ATP} channels in three aspects. First, our inter-subunit ion pair study in chapter two is the first to highlight the importance of subunit-subunit interaction between neighboring Kir6.2 in K_{ATP} channel gating. Our notion that subunit-subunit interaction is critical for gating is supported by the mGIRK and KirBac1.1 crystal structures and subsequent Kir6.2 structure modeling using mGIRK and KirBac1.1 as templates. In particular, in the mGIRK and KirBac1.1 structures the N and C termini from neighboring subunits interact, and in the simulated Kir6.2 tetramer structure the ATP docking site is at this N-C terminal interface, consistent with the possibility that ATP binding may change the subunit-subunit interaction to alter channel gating. The significance of intersubunit interactions has also been documented in other channels. For example, Zagotta's group has proposed that the intersubunit interaction (salts bridges in this case) in the C-terminal region affects gating of hyperpolarization-activated cyclic nucleotide-modulated (HCN) channels and cyclic nucleotide-gated (CNG) channels. (Craven and Zagotta, 2004). Additionally, Sun et al. showed that glutamate receptor desensitization is related to a change in the subunit-subunit interaction in the ligand-binding core. (Sun et al., 2002) Similar conclusions from Horning et al suggest a salt bridge in the dimer interface from AMPA receptor is involved in receptor desensitization (Horning and Mayer, 2004). Together these studies

support the dimer interface interactions as key structural elements involved in the gating of these channel/ receptor families.

Second, our results from the F55L study signify the critical role of the Kir6.2 slide helix in determining the intrinsic open probability of K_{ATP} channels and the importance of phospholipids and/or long chain acyl CoAs in setting the physiological activity of β-cell K_{ATP} channels. As research data show that the long chain CoA level is elevated in obese and Type II diabetes individuals, our finding raises the questions of how this change affects K_{ATP} channel activity and insulin secretion in these individuals and how composition of the dietary fat might reset/affect channel activity to affect insulin secretion. If fat has a significant effect on insulin secretion, is this a short-term effect like what we have observed in chapter 3 (Figure25C)? It would be interesting to know the answer.

Finally, our study from PNDM mutants demonstrates a surface expression defect of these mutants in addition to their gating defect. These novel findings implicate that the expression level of a mutation may play a role in determining disease severity. Interestingly, sulfonylureas significantly increase surface expression of a number of PNDM mutant channels, raising new questions about the use of these drugs in treatment of PNDM caused by Kir6.2 mutations. We learned a lesson that the heterozygous expression may not always follow the binomial distribution and the proportion of mutant protein incorporated into the channel complex expressed at the cell surface could determine the overall channel function.

Together, the studies carried out in this dissertation provide us some new ideas to further advance our knowledge in the regulation of K_{ATP} channel gating and

expression and the disease mechanism related to dysfunction of this channel.

Future Directions

In chapter two, we proposed that subunit-subunit interactions might play an important role during channel gating. To further test this hypothesis, it would be important to identify additional subunit-subunit interactions which when disrupted leads to gating defects. In this regard, we have continued this line of investigation by identifying potential interacting partners of naturally occurring disease Kir6.2 mutations that have already been shown to cause gating defects and that are localized to the subunit-subunit interface using homologous Kir6.2 structures as a guide. An example is described in the preliminary results presented in chapter five. Two mutations identified in patients with congenital hyperinsulinism, R301H and R301P, both cause K_{ATP} channel inactivation. R301 lies in the interface of two neighboring Kir6.2 subunits. To identify the interacting partner of R301, we have begun to mutate residues predicted to form chemical interactions with R301 according to the homologous mGIRK 1 structures. The reason we prefer the mGIRK for modeling the interacting partner is because KirBac1.1 channel is not a ligand-sensitive channel and might not be suitable as a template for subunit-subunit interactions. On the other hand, the channel modulating ligands for GIRK channels and K_{ATP} channels are quite different, thus the simulated model might not reflect the real conformation of Kir6.2 subunit. Although our functional data suggest that F250 is a promising residue interacting with R301, we encountered a problem of recording any detectable channel activity in the double cysteine or reciprocal mutants of F250 and R301 (F250C/R301C and F250R/R301F).

The null channel activity from double mutations might be due to exacerbated effect from one another since single mutation already causes severe inactivation. Alternately, this problem may be solved by switching the mutant clone from mouse to rat, which gives rise to much better expression thereby bigger currents in electrophysiological study. Finally, more detailed systematic studies of other potential interacting partners may also shed new light to the gating relevant subunit-subunit interactions.

In chapter three, we showed that the F55L mutation causes loss of channel function by reducing channel sensitivity to membrane phospholipids and/or long chain acyl CoAs. Significantly, we found that application of PIP_2 or long-chain CoA in the bath solution increased mutant channel activity to that seen in WT channels. An important future direction is to test whether increasing the levels of membrane phospohlipids and/or long chain acyl CoAs in insulin secreting cells (for example in the INS-1 cell line) expressing the F55L mutant Kir6.2 will rescue insulin secretion defect caused by this mutation. In addition, continued efforts in characterizing the gating defects in other novel Kir6.2 disease mutations are expected to shed new light to the structure-function relationship of K_{ATP} channels. For example, it is of great interest to know the role of each of the two glycines (G156 and G165) during K_{ATP} channel gating, a question that hasn't been pursued yet in the Kir6 family. Since the G156 mutant has reasonably good surface expression (72% of WT), the gating defect it causes is worth defining. Obtaining single channel data will be helpful to know which aspect of channel gating (fast or slow) is affected. My preliminary data from some single channel recordings on this particular mutant suggest that the intraburst flickerings may be

impaired. If confirmed, this would suggest that G156 is involved in fast gating. Also, comparison study between G156 and G165 with substitutions of various amino acids together with single channel analysis will help address this question.

In chapter four, our data provide strong evidence that the disease severity of PNDM is determined by the effect of a mutation on both channel gating and channel biogenesis. Sulfonylureas have been proposed as an alternative therapy in these PNDM patients to insulin injection. Given that our results show sulfonylureas not only affect the activity of mutant channels but can also increase surface expression of disease-causing mutation channels, it would be important to evaluate the overall effect of sulfonylurea on a given mutation. The INS-1 cell expression system we have established will be a very useful tool to screen for PNDM mutations appropriate for sulfonylurea therapy.

In the last chapter, I summarized our efforts so far in trying to understand how enzymatic activity at the nucleotide-binding fold of SUR1 is coupled to Kir6.2 to regulate channel activity. The disease-causing SUR1 mutations that I have shown to cause loss of channel regulation by MgADP are indicators of the structural regions that are involved in the functional crosstalk between SUR1 and Kir6.2. We can use this information to design recombinant SUR1 proteins fragments to study interaction domains in Kir6.2 and SUR1 using pull-down assays. Another approach to mapping interaction domains is to use cysteine cross-linking. For this, I have generated a SUR1 construct that lacks all cysteines in its cytoplasmic domain. By introducing cysteines

back to the construct at designated amino acid position, we will be able to address the questions of how and where SUR1 couples to Kir6.2 and regulate its gating. A potential problem of this construct is its lack of MgADP response, an important aspect of channel regulation. I have further tested the single cysteine mutants to identify cysteine residues that are important for the MgADP effect. Our results indicate that mutation of C678, C806 or C1251 individually reduced MgADP response; the complete lack of MgADP response in the cysless construct may come from the sum of each mutation. Interestingly, both C678 and C806 are located in the NBF1 domain while C1251 is located at N-terminus of the 16th TM, which is far from either NBD1 or NBD2, suggesting this region may be involved in the signal transduction post MgADP activation (see Figure 43). It is possible that we could substitute these three cysteines into different amino acids and generate a construct that retains MgADP response to over come this problem.

Reference

Aguilar-Bryan, L., Nichols, C. G., Wechsler, S. W., Clement, J. P. t., Boyd, A. E., 3rd, Gonzalez, G., Herrera-Sosa, H., Nguy, K., Bryan, J., and Nelson, D. A. (1995). Cloning of the beta cell high-affinity sulfonylurea receptor: a regulator of insulin secretion. Science 268, 423-426.

Aguilar-Bryan, L., Clement, J. P. t., Gonzalez, G., Kunjilwar, K., Babenko, A., and Bryan, J. (1998). Toward understanding the assembly and structure of KATP channels. Physiol Rev 78, 227-245.

Aguilar-Bryan, L., and J. Bryan. (1999). Molecular biology of adenosine triphosphate-sensitive potassium channels. Endocr Rev. 20:101-35.

Aguilar-Bryan, L., J. Bryan, et al. (2001). "Of mice and men: K(ATP) channels and insulin secretion." Recent Prog Horm Res 56: 47-68.

Alekseev, A. E., Kennedy, M. E., Navarro, B., and Terzic, A. (1997). Burst kinetics of co-expressed Kir6.2/SUR1 clones: comparison of recombinant with native ATP-sensitive K+ channel behavior. J Membr Biol 159, 161-168.

Alekseev, A. E., P. A. Brady, et al. (1998). "Ligand-insensitive state of cardiac ATP-sensitive K+ channels. Basis for channel opening." J Gen Physiol 111(2): 381-94.

Antcliff, J. F., S. Haider, et al. (2005). "Functional analysis of a structural model of the ATP-binding site of the K(ATP) channel Kir6.2 subunit." Embo J 24(2): 229-39.

Araki, E., S. Oyadomari, et al. (2003). "Impact of endoplasmic reticulum stress pathway on pancreatic beta-cells and diabetes mellitus." Exp Biol Med (Maywood) 228(10): 1213-7.

Ashcroft, F. M., Harrison, D. E., and Ashcroft, S. J. (1984). Glucose induces closure of single potassium channels in isolated rat pancreatic beta-cells. Nature 312, 446-448.

Ashcroft, F. M. (1988). "Adenosine 5'-triphosphate-sensitive potassium channels." Annu Rev Neurosci 11: 97-118.

Ashcroft, F. M. and F. M. Gribble (1998). "Correlating structure and function in ATP-sensitive K+ channels." Trends Neurosci 21(7): 288-94.

Ashcroft, F. M. and F. M. Gribble (1999). "ATP-sensitive K+ channels and insulin secretion: their role in health and disease." Diabetologia 42(8): 903-19.

Ashcroft, F. M. (2005). "ATP-sensitive potassium channelopathies: focus on insulin secretion." J Clin Invest 115(8): 2047-58.

Ayyagari, P. V., Harrell, L. E., Parsons, D. S., and Kolasa, K. (1996). Sympathetic sprouting reverses decreases in membrane-associated activity of protein kinase C following septohippocampal denervation of the rat hippocampus. Brain Res 708, 205-208.

Babenko, A. P., Samoilov, V. O., Kazantseva, S. T., and Shevchenko, Y. L. (1992). ATP-sensitive K(+)-channels in the human adult ventricular cardiomyocytes membrane. FEBS Lett 313, 148-150.

Babenko, A. P., Gonzalez, G., Aguilar-Bryan, L., and Bryan, J. (1998). Reconstituted human cardiac KATP channels: functional identity with the native channels from the sarcolemma of human ventricular cells. Circ Res 83, 1132-1143.

Babenko, A. P., Aguilar-Bryan, L., and Bryan, J. (1998). A view of sur/KIR6.X, KATP channels. Annu Rev Physiol 60, 667-687.

Babenko, A. P., Gonzalez, G., and Bryan, J. (1999). The tolbutamide site of SUR1 and a mechanism for its functional coupling to K(ATP) channel closure. FEBS Lett 459, 367-376.

Babenko, A. P., Gonzalez, G., and Bryan, J. (1999). Two regions of sulfonylurea receptor specify the spontaneous bursting and ATP inhibition of KATP channel isoforms. J Biol Chem 274, 11587-11592.

Babenko, A. P., Gonzalez, G., Aguilar-Bryan, L., and Bryan, J. (1999). Sulfonylurea receptors set the maximal open probability, ATP sensitivity and plasma membrane density of KATP channels. FEBS Lett 445, 131-136.

Babenko, A. P., Gonzalez, G., and Bryan, J. (1999). The N-terminus of KIR6.2 limits spontaneous bursting and modulates the ATP-inhibition of KATP channels. Biochem Biophys Res Commun 255, 231-238.

Baukrowitz, T., U. Schulte, D. Oliver, S. Herlitze, T. Krauter, S.J. Tucker, J.P. Ruppersberg, and B. Fakler. (1998). PIP2 and PIP as determinants for ATP inhibition of KATP channels. Science. 282:1141-4.

Baukrowitz, T., and B. Fakler. (2000). K(ATP) channels: linker between phospholipid metabolism and excitability. Biochem Pharmacol. 60:735-40.

Beguin, P., K. Nagashima, M. Nishimura, T. Gonoi, and S. Seino. (1999). PKA-mediated phosphorylation of the human K(ATP) channel: separate roles of Kir6.2 and SUR1 subunit phosphorylation. EMBO Journal. 18:4722-32.

Branstrom, R., I. B. Leibiger, et al. (1998). "Long chain coenzyme A esters activate the pore-forming subunit (Kir6. 2) of the ATP-regulated potassium channel." J Biol Chem 273(47): 31395-400.

Branstrom, R., C. A. Aspinwall, et al. (2004). "Long-chain CoA esters activate human pancreatic beta-cell KATP channels: potential role in Type 2 diabetes." Diabetologia 47(2): 277-83.

Bryan, J., and L. Aguilar-Bryan. (1997). The ABCs of ATP-sensitive potassium channels: more pieces of the puzzle. Curr Opin Cell Biol. 9:553-9.

Campbell, J. D., Sansom, M. S., and Ashcroft, F. M. (2003). Potassium channel regulation. EMBO Rep 4, 1038-1042.

Careaga, C.L., and J.J. Falke. (1992). Thermal motions of surface alpha-helices in the D-galactose chemosensory receptor. Detection by disulfide trapping. J Mol Biol. 226:1219-35.

Cartier, E. A., L. R. Conti, et al. (2001). "Defective trafficking and function of KATP channels caused by a sulfonylurea receptor 1 mutation associated with persistent hyperinsulinemic hypoglycemia of infancy." Proc Natl Acad Sci U S A 98(5): 2882-7.

Chan, K. W., H. Zhang, et al. (2003). "N-terminal transmembrane domain of the SUR controls trafficking and gating of Kir6 channel subunits." Embo J 22(15): 3833-43.

Chutkow, W. A., Simon, M. C., Le Beau, M. M., and Burant, C. F. (1996). Cloning, tissue expression, and chromosomal localization of SUR2, the putative drug-binding subunit of cardiac, skeletal muscle, and vascular KATP channels. Diabetes 45, 1439-1445.

Clement, J.P.t., K. Kunjilwar, G. Gonzalez, M. Schwanstecher, U. Panten, L. Aguilar-Bryan, and J. Bryan. (1997). Association and stoichiometry of K(ATP) channel

subunits. Neuron. 18:827-38.

Cohen, P. (1989). The structure and regulation of protein phosphatases. Annu Rev Biochem. 58:453-508.

Cole, S. P. (1992). The 1991 Merck Frosst Award. Multidrug resistance in small cell lung cancer. Can J Physiol Pharmacol 70, 313-329.

Collins, J. E. and J. V. Leonard (1984). "Hyperinsulinism in asphyxiated and small-for-dates infants with hypoglycaemia." Lancet 2(8398): 311-3.

Collins, J. E., J. V. Leonard, et al. (1990). "Hyperinsulinaemic hypoglycaemia in small for dates babies." Arch Dis Child 65(10): 1118-20.

Cook, D. L., L. S. Satin, et al. (1988). "ATP-sensitive K+ channels in pancreatic beta-cells. Spare-channel hypothesis." Diabetes 37(5): 495-8.

Crane, A. and L. Aguilar-Bryan (2004). "Assembly, maturation, and turnover of K(ATP) channel subunits." J Biol Chem 279(10): 9080-90.

Craven, K. B., and Zagotta, W. N. (2004). Salt bridges and gating in the COOH-terminal region of HCN2 and CNGA1 channels. J Gen Physiol 124, 663-677.

Cukras, C.A., I. Jeliazkova, and C.G. Nichols. (2002a). The role of NH(2)-terminal positive charges in the activity of inward rectifier K(ATP) channels. J Gen Physiol. 120:437-46.

Cukras, C.A., I. Jeliazkova, and C.G. Nichols. (2002b). Structural and functional determinants of conserved lipid interaction domains of inward rectifying kir6.2 channels. J Gen Physiol. 119:581-91.

Daut, J., Maier-Rudolph, W., von Beckerath, N., Mehrke, G., Gunther, K., and Goedel-Meinen, L. (1990). Hypoxic dilation of coronary arteries is mediated by ATP-sensitive potassium channels. Science 247, 1341-1344.

D'Hahan, N., Moreau, C., Prost, A. L., Jacquet, H., Alekseev, A. E., Terzic, A., and Vivaudou, M. (1999). Pharmacological plasticity of cardiac ATP-sensitive potassium channels toward diazoxide revealed by ADP. Proc Natl Acad Sci U S A 96, 12162-12167.

Diederichs, K., Diez, J., Greller, G., Muller, C., Breed, J., Schnell, C., Vonrhein, C., Boos, W., and Welte, W. (2000). Crystal structure of MalK, the ATPase subunit of the trehalose/maltose ABC transporter of the archaeon Thermococcus litoralis. Embo J 19, 5951-5961.

Doupnik, C. A., Davidson, N., and Lester, H. A. (1995). The inward rectifier potassium channel family. Curr Opin Neurobiol 5, 268-277.

Doyle, D.A., J. Morais Cabral, R.A. Pfuetzner, A. Kuo, J.M. Gulbis, S.L. Cohen, B.T. Chait, and R. MacKinnon. (1998). The structure of the potassium channel: molecular basis of K+ conduction and selectivity. Science. 280:69-77.

Drain, P., L. Li, et al. (1998). "KATP channel inhibition by ATP requires distinct functional domains of the cytoplasmic C terminus of the pore-forming subunit." Proc Natl Acad Sci U S A 95(23): 13953-8.

Drumm, M. L., Wilkinson, D. J., Smit, L. S., Worrell, R. T., Strong, T. V., Frizzell, R. A., Dawson, D. C., and Collins, F. S. (1991). Chloride conductance expressed by delta F508 and other mutant CFTRs in Xenopus oocytes. Science 254, 1797-1799.

Dunne, M. J., K. E. Cosgrove, et al. (2004). "Hyperinsulinism in infancy: from basic science to clinical disease." Physiol Rev 84(1): 239-75.

Edghill, E. L., A. L. Gloyn, et al. (2004). "Activating mutations in the KCNJ11 gene encoding the ATP-sensitive K+ channel subunit Kir6.2 are rare in clinically defined type 1 diabetes diagnosed before 2 years." Diabetes 53(11): 2998-3001.

Enkvetchakul, D., G. Loussouarn, E. Makhina, S.L. Shyng, and C.G. Nichols. (2000). The kinetic and physical basis of K(ATP) channel gating: toward a unified molecular understanding. Biophys J. 78:2334-48.

Enkvetchakul, D., Loussouarn, G., Makhina, E., and Nichols, C. G. (2001). ATP interaction with the open state of the K(ATP) channel. Biophys J 80, 719-728.

Enkvetchakul, D., and Nichols, C. G. (2003). Gating mechanism of KATP channels: function fits form. J Gen Physiol 122, 471-480.

Faivre, J. F., and Findlay, I. (1990). Action potential duration and activation of ATP-sensitive potassium current in isolated guinea-pig ventricular myocytes. Biochim Biophys Acta 1029, 167-172.

Fan, Z., and J.C. Makielski. (1997). Anionic phospholipids activate ATP-sensitive potassium channels. J Biol Chem. 272:5388-95.

Flynn, G. E., and Zagotta, W. N. (2001). Conformational changes in S6 coupled to the opening of cyclic nucleotide-gated channels. Neuron 30, 689-698.

Gaudet, R., and Wiley, D. C. (2001). Structure of the ABC ATPase domain of human TAP1, the transporter associated with antigen processing. Embo J 20, 4964-4972.

Glaser, B. (2000). "Hyperinsulinism of the newborn." Semin Perinatol 24(2): 150-63.

Gloyn, A. L., E. A. Cummings, et al. (2004a). "Permanent neonatal diabetes due to paternal germline mosaicism for an activating mutation of the KCNJ11 Gene encoding the Kir6.2 subunit of the beta-cell potassium adenosine triphosphate channel." J Clin Endocrinol Metab 89(8): 3932-5.

Gloyn, A. L., E. R. Pearson, et al. (2004b). "Activating mutations in the gene encoding the ATP-sensitive potassium-channel subunit Kir6.2 and permanent neonatal diabetes." N Engl J Med 350(18): 1838-49.

Gloyn, A. L., F. Reimann, et al. (2005). "Relapsing diabetes can result from moderately activating mutations in KCNJ11." Hum Mol Genet 14(7): 925-34.

Gordon, S.E., and W.N. Zagotta. (1995). Subunit interactions in coordination of Ni2+ in cyclic nucleotide-gated channels. Proc Natl Acad Sci U S A. 92:10222-6.

Gordon, S.E., M.D. Varnum, and W.N. Zagotta. (1997). Direct interaction between amino- and carboxyl-terminal domains of cyclic nucleotide-gated channels. Neuron. 19:431-41.

Gribble, F.M., S.J. Tucker, and F.M. Ashcroft. (1997). The essential role of the Walker A motifs of SUR1 in K-ATP channel activation by Mg-ADP and diazoxide. Embo J. 16:1145-52.

Gribble, F.M., P. Proks, B.E. Corkey, and F.M. Ashcroft. (1998a). Mechanism of cloned ATP-sensitive potassium channel activation by oleoyl-CoA. J Biol Chem. 273:26383-7.

Gribble, F.M., S.J. Tucker, T. Haug, and F.M. Ashcroft. (1998b). MgATP activates the beta cell KATP channel by interaction with its SUR1 subunit. Proc Natl Acad Sci U S A. 95:7185-90.

Gribble, F. M. and F. Reimann (2004). "Open to control--new hope for patients with neonatal diabetes." N Engl J Med 350(18): 1817-8.

Hattersley, A. T. and F. M. Ashcroft (2005). "Activating mutations in kir6.2 and neonatal diabetes: new clinical syndromes, new scientific insights, and new therapy." Diabetes 54(9): 2503-13.

He, Y., M. Ruiz, and J.W. Karpen. (2000). Constraining the subunit order of rod cyclic nucleotide-gated channels reveals a diagonal arrangement of like subunits. Proc Natl Acad Sci U S A. 97:895-900.

Henwood, M. J., A. Kelly, et al. (2005). "Genotype-phenotype correlations in children with congenital hyperinsulinism due to recessive mutations of the adenosine triphosphate-sensitive potassium channel genes." J Clin Endocrinol Metab 90(2): 789-94.

Hilgemann, D.W., and R. Ball. (1996). Regulation of cardiac Na+,Ca2+ exchange and KATP potassium channels by PIP2. Science. 273:956-9.

Hille, B. 2001. Ion Channels of Excitable Membranes. Sinauer, Sunderland, MA.

Hohmeier, H. E., H. Mulder, et al. (2000). "Isolation of INS-1-derived cell lines with robust ATP-sensitive K+ channel-dependent and -independent glucose-stimulated insulin secretion." Diabetes 49(3): 424-30.

Horenstein, J., D.A. Wagner, C. Czajkowski, and M.H. Akabas. (2001). Protein mobility and GABA-induced conformational changes in GABA(A) receptor pore-lining M2 segment. Nat Neurosci. 4:477-85.

Horning, M. S., and Mayer, M. L. (2004). Regulation of AMPA receptor gating by ligand binding core dimers. Neuron 41, 379-388.

Huang, C.L., S. Feng, and D.W. Hilgemann. (1998). Direct activation of inward rectifier potassium channels by PIP2 and its stabilization by Gbetagamma. Nature. 391:803-6.

Hung, L. W., Wang, I. X., Nikaido, K., Liu, P. Q., Ames, G. F., and Kim, S. H. (1998). Crystal structure of the ATP-binding subunit of an ABC transporter. Nature 396, 703-707.

Huopio, H., Reimann, F., Ashfield, R., Komulainen, J., Lenko, H. L., Rahier, J., Vauhkonen, I., Kere, J., Laakso, M., Ashcroft, F., and Otonkoski, T. (2000). Dominantly inherited hyperinsulinism caused by a mutation in the sulfonylurea receptor type 1. J Clin Invest 106, 897-906.

Huopio, H., S. L. Shyng, et al. (2002). "K(ATP) channels and insulin secretion disorders." Am J Physiol Endocrinol Metab 283(2): E207-16.

Inagaki, N., T. Gonoi, J.P.t. Clement, N. Namba, J. Inazawa, G. Gonzalez, L. Aguilar-Bryan, S. Seino, and J. Bryan. (1995). Reconstitution of IKATP: an inward rectifier subunit plus the sulfonylurea receptor. Science. 270:1166-70.

Inagaki, N., Gonoi, T., Clement, J. P., Wang, C. Z., Aguilar-Bryan, L., Bryan, J., and Seino, S. (1996). A family of sulfonylurea receptors determines the pharmacological properties of ATP-sensitive K+ channels. Neuron 16, 1011-1017.

Inagaki, N., T. Gonoi, and S. Seino. (1997). Subunit stoichiometry of the pancreatic beta-cell ATP-sensitive K+ channel. FEBS Lett. 409:232-6.

Inagaki, N., and Seino, S. (1998). ATP-sensitive potassium channels: structures, functions, and pathophysiology. Jpn J Physiol 48, 397-412.

Isacoff, E.Y., Y.N. Jan, and L.Y. Jan. (1990). Evidence for the formation of

heteromultimeric potassium channels in Xenopus oocytes. Nature. 345:530-4.

Isomoto, S., and Kurachi, Y. (1996). Molecular and biophysical aspects of potassium channels. Nippon Rinsho 54, 660-666.

Jiang, Y., Lee, A., Chen, J., Cadene, M., Chait, B. T., and MacKinnon, R. (2002). The open pore conformation of potassium channels. Nature 417, 523-526.

Jiang, Y., Lee, A., Chen, J., Cadene, M., Chait, B. T., and MacKinnon, R. (2002). Crystal structure and mechanism of a calcium-gated potassium channel. Nature 417, 515-522.

Jin, T., Peng, L., Mirshahi, T., Rohacs, T., Chan, K. W., Sanchez, R., and Logothetis, D. E. (2002). The (beta)gamma subunits of G proteins gate a K(+) channel by pivoted bending of a transmembrane segment. Mol Cell 10, 469-481.

John, S.A., J.N. Weiss, and B. Ribalet. (2001). Regulation of cloned ATP-sensitive K channels by adenine nucleotides and sulfonylureas: interactions between SUR1 and positively charged domains on Kir6.2. J Gen Physiol. 118:391-405.

John, S. A., J. N. Weiss, et al. (2003). Molecular mechanism for ATP-dependent closure of the K+ channel Kir6.2. J Physiol 552(Pt 1): 23-34.

Kantor, P. F., Coetzee, W. A., Carmeliet, E. E., Dennis, S. C., and Opie, L. H. (1990). Reduction of ischemic K+ loss and arrhythmias in rat hearts. Effect of glibenclamide, a sulfonylurea. Circ Res 66, 478-485.

Karpowich, N., Martsinkevich, O., Millen, L., Yuan, Y. R., Dai, P. L., MacVey, K., Thomas, P. J., and Hunt, J. F. (2001). Crystal structures of the MJ1267 ATP binding cassette reveal an induced-fit effect at the ATPase active site of an ABC transporter. Structure 9, 571-586.

Kerr, I. D. (2002). Structure and association of ATP-binding cassette transporter nucleotide-binding domains. Biochim Biophys Acta 1561, 47-64.

Klupa, T., E. L. Edghill, et al. (2005). "The identification of a R201H mutation in KCNJ11, which encodes Kir6.2, and successful transfer to sustained-release sulphonylurea therapy in a subject with neonatal diabetes: evidence for heterogeneity of beta cell function among carriers of the R201H mutation." Diabetologia.

Koster, J. C., B. A. Marshall, et al. (2000). "Targeted overactivity of beta cell K(ATP) channels induces profound neonatal diabetes." Cell 100(6): 645-54.

Koster, J. C., M. A. Permutt, et al. (2005). "Diabetes and Insulin Secretion: The ATP-Sensitive K+ Channel (KATP) Connection." Diabetes 54(11): 3065-72.

Koster, J. C., M. S. Remedi, et al. (2005). "ATP and Sulfonylurea Sensitivity of Mutant ATP-Sensitive K+ Channels in Neonatal Diabetes: Implications for Pharmacogenomic Therapy." Diabetes 54(9): 2645-54.

Krovetz, H.S., H.M. VanDongen, and A.M. VanDongen. (1997). Atomic distance estimates from disulfides and high-affinity metal- binding sites in a K+ channel pore. Biophys J. 72:117-26

Kubo, Y., Reuveny, E., Slesinger, P. A., Jan, Y. N., and Jan, L. Y. (1993). Primary structure and functional expression of a rat G-protein-coupled muscarinic potassium channel. Nature 364, 802-806.

Kuo, A., J. M. Gulbis, et al. (2003). Crystal structure of the potassium channel KirBac1.1 in the closed state. Science 300(5627): 1922-6.

Larsson, O., C. J. Barker, et al. (2000). Phosphatidylinositol 4,5-bisphosphate and ATP-sensitive potassium channel regulation: a word of caution. Diabetes 49(9): 1409-12.

Larsson, H.P., and F. Elinder. (2000). A conserved glutamate is important for slow inactivation in K+ channels. Neuron. 27:573-83.

Lawson, K. (2000). Potassium channel openers as potential therapeutic weapons in ion channel disease. Kidney Int 57, 838-845.

Light, P.E., C. Bladen, R.J. Winkfein, M.P. Walsh, and R.J. French. (2000). Molecular basis of protein kinase C-induced activation of ATP-sensitive potassium channels. Proc Natl Acad Sci U S A. 97:9058-63.

Lin, C. W., F. Yan, et al. (2005). Membrane Phosphoinositides Control Insulin Secretion Through Their Effects on ATP-Sensitive K+ Channel Activity. Diabetes 54(10): 2852-8.

Lin C.-W., Lin Y.-W., Yan F.-F., Casey J., Kochhar M., Pratt E.B. and Shyng S.-L. (2006). Kir6.2 mutations associated with neonatal diabetes reduce expression of K_{ATP} channels: implications in disease mechanism and sulfonylurea therapyDiabetes. (in press)

Lin, Y. W., T. Jia, et al. (2003). Stabilization of the Activity of ATP-sensitive Potassium Channels by Ion Pairs Formed between Adjacent Kir6.2 Subunits. J Gen Physiol 122(2): 225-37.

Lin, Y. W., MacMullen, C., Ganguly, A., Stanley, C. A., and Shyng, S. L. (2006). A novel KCNJ11 mutation associated with congenital hyperinsulinism reduces the

intrinsic open probability of beta-cell ATP-sensitive potassium channels. J Biol Chem 281, 3006-3012.

Lin, Y.F., Y.N. Jan, and L.Y. Jan. (2000). Regulation of ATP-sensitive potassium channel function by protein kinase A-mediated phosphorylation in transfected HEK293 cells. Embo J. 19:942-55.

Liou, H. H., Zhou, S. S., and Huang, C. L. (1999). Regulation of ROMK1 channel by protein kinase A via a phosphatidylinositol 4,5-bisphosphate-dependent mechanism. Proc Natl Acad Sci U S A 96, 5820-5825.

Liu, D.T., G.R. Tibbs, P. Paoletti, and S.A. Siegelbaum. (1998). Constraining ligand-binding site stoichiometry suggests that a cyclic nucleotide-gated channel is composed of two functional dimers. Neuron. 21:235-48.

Liu, G.X., P.J. Hanley, J. Ray, and J. Daut. (2001). Long-chain acyl-coenzyme A esters and fatty acids directly link metabolism to K(ATP) channels in the heart. Circ Res. 88:918-24.

Lopes, C.M., H. Zhang, T. Rohacs, T. Jin, J. Yang, and D.E. Logothetis. (2002). Alterations in Conserved Kir Channel-PIP(2) Interactions Underlie Channelopathies. Neuron. 34:933-44.

Loussouarn, G., Rose, T., and Nichols, C. G. (2002). Structural basis of inward rectifying potassium channel gating. Trends Cardiovasc Med 12, 253-258.

MacGregor, G.G., K. Dong, C.G. Vanoye, L. Tang, G. Giebisch, and S.C. Hebert. (2002). Nucleotides and phospholipids compete for binding to the C terminus of KATP channels. Proc Natl Acad Sci U S A. 99:2726-31.

Magge, S. N., S. L. Shyng, et al. (2004). Familial leucine-sensitive hypoglycemia of infancy due to a dominant mutation of the beta-cell sulfonylurea receptor. J Clin Endocrinol Metab 89(9): 4450-6.

Manning Fox, J. E., C. G. Nichols, et al. (2004). Activation of adenosine triphosphate-sensitive potassium channels by acyl coenzyme A esters involves multiple phosphatidylinositol 4,5-bisphosphate-interacting residues. Mol Endocrinol 18(3): 679-86.

Massa, O., D. Iafusco, et al. (2005). KCNJ11 activating mutations in Italian patients with permanent neonatal diabetes. Hum Mutat 25(1): 22-7.

Markworth, E., C. Schwanstecher, et al. (2000). ATP4- mediates closure of pancreatic beta-cell ATP-sensitive potassium channels by interaction with 1 of 4 identical sites. Diabetes 49(9): 1413-8.

Matsuo, M., S. Trapp, et al. (2000). Functional analysis of a mutant sulfonylurea receptor, SUR1-R1420C, that is responsible for persistent hyperinsulinemic hypoglycemia of infancy. J Biol Chem 275(52): 41184-91.

Matzaris, M., S.P. Jackson, K.M. Laxminarayan, C.J. Speed, and C.A. Mitchell. (1994). Identification and characterization of the phosphatidylinositol-(4, 5)- bisphosphate 5-phosphatase in human platelets. J Biol Chem. 269:3397-402.

Mikhailov, M. V., Campbell, J. D., de Wet, H., Shimomura, K., Zadek, B., Collins, R. F., Sansom, M. S., Ford, R. C., and Ashcroft, F. M. (2005). 3-D structural and functional characterization of the purified KATP channel complex Kir6.2-SUR1. Embo J 24, 4166-4175.

Miki, T., Iwanaga, T., Nagashima, K., Ihara, Y., and Seino, S. (2001). Roles of ATP-sensitive K+ channels in cell survival and differentiation in the endocrine pancreas. Diabetes 50 Suppl 1, S48-51.

Neher, E. and C. F. Stevens (1977). Conductance fluctuations and ionic pores in membranes. Annu Rev Biophys Bioeng 6: 345-81.

Nestorowicz, A., B. A. Wilson, et al. (1996). Mutations in the sulonylurea receptor gene are associated with familial hyperinsulinism in Ashkenazi Jews. Hum Mol Genet 5(11): 1813-22.

Nestorowicz, A., N. Inagaki, et al. (1997). A nonsense mutation in the inward rectifier potassium channel gene, Kir6.2, is associated with familial hyperinsulinism. Diabetes 46(11): 1743-8.

Nestorowicz, A., B. Glaser, et al. (1998). Genetic heterogeneity in familial hyperinsulinism. Hum Mol Genet 7(7): 1119-28.

Nichols, C. G., and Lederer, W. J. (1991). Adenosine triphosphate-sensitive potassium channels in the cardiovascular system. Am J Physiol 261, H1675-1686.

Nichols, C. G., Ripoll, C., and Lederer, W. J. (1991). ATP-sensitive potassium channel modulation of the guinea pig ventricular action potential and contraction. Circ Res 68, 280-287.

Nichols, C. G., Lederer, W. J., and Cannell, M. B. (1991). ATP dependence of KATP channel kinetics in isolated membrane patches from rat ventricle. Biophys J 60, 1164-1177.

Nichols, C. G., and Lederer, W. J. (1991). The mechanism of KATP channel inhibition by ATP. J Gen Physiol 97, 1095-1098.

Nichols, C.G., S.L. Shyng, A. Nestorowicz, B. Glaser, J.P.t. Clement, G. Gonzalez, L. Aguilar-Bryan, M.A. Permutt, and J. Bryan. (1996). Adenosine diphosphate as an intracellular regulator of insulin secretion. Science. 272:1785-7.

Nichols, C.G., and A.N. Lopatin. (1997). Inward rectifier potassium channels. Annu Rev Physiol. 59:171-91.

Nichols, C. G., and Cukras, C. A. (2001). K(ATP) channel regulators: balanced diets include carbohydrates, proteins, and fats. Circ Res 88, 849-851.

Nishida, M., and R. MacKinnon. (2002). Structural Basis of Inward Rectification. Cytoplasmic Pore of the G Protein-Gated Inward Rectifier GIRK1 at 1.8 A Resolution. Cell. 111:957-65.

Palmer, F.B., R. Theolis, Jr., H.W. Cook, and D.M. Byers. (1994). Purification of two immunologically related phosphatidylinositol-(4,5)- bisphosphate phosphatases from bovine brain cytosol. J Biol Chem. 269:3403-10.

Papazian, D.M., X.M. Shao, S.A. Seoh, A.F. Mock, Y. Huang, and D.H. Wainstock. (1995). Electrostatic interactions of S4 voltage sensor in Shaker K+ channel. Neuron. 14:1293-301.

Partridge, C. J., Beech, D. J., and Sivaprasadarao, A. (2001). Identification and pharmacological correction of a membrane trafficking defect associated with a mutation in the sulfonylurea receptor causing familial hyperinsulinism. J Biol Chem 276, 35947-35952.

Pascual, J.M., C.C. Shieh, G.E. Kirsch, and A.M. Brown. (1995). K+ pore structure revealed by reporter cysteines at inner and outer surfaces. Neuron. 14:1055-63.

Pegan, S., Arrabit, C., Zhou, W., Kwiatkowski, W., Collins, A., Slesinger, P. A., and Choe, S. (2005). Cytoplasmic domain structures of Kir2.1 and Kir3.1 show sites for modulating gating and rectification. Nat Neurosci 8, 279-287.

Phillips, L. R., Enkvetchakul, D., and Nichols, C. G. (2003). Gating dependence of inner pore access in inward rectifier K(+) channels. Neuron 37, 953-962.

Proks, P., Ashfield, R., and Ashcroft, F. M. (1999). Interaction of vanadate with the cloned beta cell K(ATP) channel. J Biol Chem 274, 25393-25397.

Proks, P., C. E. Capener, et al. (2001). Mutations within the P-loop of Kir6.2 modulate the intraburst kinetics of the ATP-sensitive potassium channel. J Gen Physiol 118(4): 341-53.

Proks, P., J. F. Antcliff, et al. (2004). Molecular basis of Kir6.2 mutations associated with neonatal diabetes or neonatal diabetes plus neurological features. Proc Natl Acad Sci U S A.

Proks, P., C. Girard, et al. (2005a). Functional effects of KCNJ11 mutations causing neonatal diabetes: enhanced activation by MgATP. Hum Mol Genet.

Proks, P., C. Girard, et al. (2005b). A gating mutation at the internal mouth of the Kir6.2 pore is associated with DEND syndrome. EMBO Rep 6(5): 470-5.

Quayle, J. M., Nelson, M. T., and Standen, N. B. (1997). ATP-sensitive and inwardly rectifying potassium channels in smooth muscle. Physiol Rev 77, 1165-1232.

Ribalet, B., S.A. John, and J.N. Weiss. (2000). Regulation of cloned ATP-sensitive K channels by phosphorylation, MgADP, and phosphatidylinositol bisphosphate (PIP(2)): a study of channel rundown and reactivation. J Gen Physiol. 116:391-410.

Riedel, M. J., P. Boora, et al. (2003). Kir6.2 polymorphisms sensitize beta-cell ATP-sensitive potassium channels to activation by acyl CoAs: a possible cellular mechanism for increased susceptibility to type 2 diabetes? Diabetes 52 (10): 2630-5.

Riedel, M. J., D. C. Steckley, et al. (2005). Current status of the E23K Kir6.2 polymorphism: implications for type-2 diabetes. Hum Genet 116(3): 133-45.

Riedel, M. J. and P. E. Light (2005). Saturated and cis/trans Unsaturated Acyl CoA Esters Differentially Regulate Wild-Type and Polymorphic {beta}-Cell ATP-Sensitive K+ Channels. Diabetes 54(7): 2070-9.

Romani, A. M. and A. Scarpa (2000). Regulation of cellular magnesium. Front Biosci 5: D720-34.

Sadja, R., Smadja, K., Alagem, N., and Reuveny, E. (2001). Coupling Gbetagamma-dependent activation to channel opening via pore elements in inwardly rectifying potassium channels. Neuron 29, 669-680.

Sagen, J. V., H. Raeder, et al. (2004). Permanent neonatal diabetes due to mutations in KCNJ11 encoding Kir6.2: patient characteristics and initial response to sulfonylurea therapy. Diabetes 53(10): 2713-8.

Salmeron, J., Hu, F. B., Manson, J. E., Stampfer, M. J., Colditz, G. A., Rimm, E. B., and Willett, W. C. (2001). Dietary fat intake and risk of type 2 diabetes in women. Am J Clin Nutr 73, 1019-1026.

Sato, N., F. Urano, et al. (2000). Upregulation of BiP and CHOP by the unfolded-protein response is independent of presenilin expression. Nat Cell Biol 2(12): 863-70.

Schroder, M. and R. J. Kaufman (2005). ER stress and the unfolded protein response. Mutat Res 569(1-2): 29-63.

Schulze, D., T. Krauter, et al. (2003). Phosphatidylinositol 4,5-bisphosphate (PIP2) modulation of ATP and pH sensitivity in Kir channels. A tale of an active and a silent PIP2 site in the N terminus. J Biol Chem 278(12): 10500-5.

Schulze, D., M. Rapedius, et al. (2003). Long-chain acyl-CoA esters and phosphatidylinositol phosphates modulate ATP inhibition of KATP channels by the same mechanism. J. Physiol 552(Pt 2): 357-67.

Sharma, N., A. Crane, et al. (2000). Familial hyperinsulinism and pancreatic beta-cell ATP-sensitive potassium channels. Kidney Int 57(3): 803-8.

Shapiro, M.S., and W.N. Zagotta. (2000). Structural basis for ligand selectivity of heteromeric olfactory cyclic nucleotide-gated channels. Biophys J. 78:2307-20.

Shield, J. P., Carradus, M., Stone, J. E., Hunt, L. P., Baum, J. D., and Pennock, C. A. (1995). Urinary heparan sulphate proteoglycan excretion is abnormal in insulin dependent diabetes. Ann Clin Biochem 32 (Pt 6), 557-560.

Shyng, S., T. Ferrigni, and C.G. Nichols. (1997a). Control of rectification and gating of cloned KATP channels by the Kir6.2 subunit. J Gen Physiol. 110:141-53.

Shyng, S., T. Ferrigni, and C.G. Nichols. (1997b). Regulation of KATP channel activity by diazoxide and MgADP. Distinct functions of the two nucleotide binding folds of the sulfonylurea receptor. J Gen Physiol. 110:643-54.

Shyng, S., and C.G. Nichols. (1997c). Octameric stoichiometry of the KATP channel complex. J Gen Physiol. 110:655-64.

Shyng, S.L., and C.G. Nichols. (1998a). Membrane phospholipid control of nucleotide

sensitivity of KATP channels. Science. 282:1138-41.

Shyng, S. L., T. Ferrigni, et al. (1998b). Functional analyses of novel mutations in the sulfonylurea receptor 1 associated with persistent hyperinsulinemic hypoglycemia of infancy. Diabetes 47(7): 1145-51.

Shyng, S.L., A. Barbieri, A. Gumusboga, C. Cukras, L. Pike, J.N. Davis, P.D. Stahl, and C.G. Nichols. (2000a). Modulation of nucleotide sensitivity of ATP-sensitive potassium channels by phosphatidylinositol-4-phosphate 5-kinase. Proc Natl Acad Sci U S A. 97:937-41.

Shyng, S.L., C.A. Cukras, J. Harwood, and C.G. Nichols. (2000b). Structural determinants of PIP(2) regulation of inward rectifier K(ATP) channels. J Gen Physiol. 116:599-608.

Singer, W.D., H.A. Brown, and P.C. Sternweis. (1997). Regulation of eukaryotic phosphatidylinositol-specific phospholipase C and phospholipase D. Annu Rev Biochem. 66:475-509.

Song, D.K., and F.M. Ashcroft. (2001). ATP modulation of ATP-sensitive potassium channel ATP sensitivity varies with the type of SUR subunit. J Biol Chem. 276:7143-9.

Smith, P. C., Karpowich, N., Millen, L., Moody, J. E., Rosen, J., Thomas, P. J., and Hunt, J. F. (2002). ATP binding to the motor domain from an ABC transporter drives formation of a nucleotide sandwich dimer. Mol Cell 10, 139-149.

Stanley, C. A. (2002). Advances in diagnosis and treatment of hyperinsulinism in infants and children. J Clin Endocrinol Metab 87(11): 4857-9.

Sun, Y., R. Olson, M. Horning, N. Armstrong, M. Mayer, and E. Gouaux. (2002).

Mechanism of glutamate receptor desensitization. Nature. 417:245-53.

Sigworth, F. J. (1980). The variance of sodium current fluctuations at the node of Ranvier. J Physiol 307: 97-129.

Tanabe, K., S.J. Tucker, M. Matsuo, P. Proks, F.M. Ashcroft, S. Seino, T. Amachi, and K. Ueda. (1999). Direct photoaffinity labeling of the Kir6.2 subunit of the ATP-sensitive K+ channel by 8-azido-ATP. J Biol Chem. 274:3931-3.

Tarasov, A., J. Dusonchet, et al. (2004). Metabolic Regulation of the Pancreatic Beta-Cell ATP-Sensitive K+ Channel: A Pas de Deux. Diabetes 53 Suppl 3: S113-22.

Taschenberger, G., A. Mougey, et al. (2002). Identification of a familial hyperinsulinism-causing mutation in the sulfonylurea receptor 1 that prevents normal trafficking and function of KATP channels. J Biol Chem 277(19): 17139-46.

Thomas, P. M., G. J. Cote, et al. (1995). Mutations in the sulfonylurea receptor gene in familial persistent hyperinsulinemic hypoglycemia of infancy. Science 268(5209): 426-9.

Trapp, S., Proks, P., Tucker, S. J., and Ashcroft, F. M. (1998). Molecular analysis of ATP-sensitive K channel gating and implications for channel inhibition by ATP. J Gen Physiol 112, 333-349.

Tucker, S.J., F.M. Gribble, C. Zhao, S. Trapp, and F.M. Ashcroft. (1997). Truncation of Kir6.2 produces ATP-sensitive K+ channels in the absence of the sulphonylurea receptor. Nature. 387:179-83.

Tucker, S.J., F.M. Gribble, P. Proks, S. Trapp, T.J. Ryder, T. Haug, F. Reimann, and F.M. Ashcroft. (1998). Molecular determinants of KATP channel inhibition by ATP.

Embo J. 17:3290-6.

Vaxillaire, M., C. Populaire, et al. (2004). Kir6.2 mutations are a common cause of permanent neonatal diabetes in a large cohort of French patients. Diabetes 53(10): 2719-22.

Walker, J. E., Saraste, M., Runswick, M. J., and Gay, N. J. (1982). Distantly related sequences in the alpha- and beta-subunits of ATP synthase, myosin, kinases and other ATP-requiring enzymes and a common nucleotide binding fold. Embo J 1, 945-951.

Wang, C., K. Wang, W. Wang, Y. Cui, and Z. Fan. (2002). Compromised ATP binding as a mechanism of phosphoinositide modulation of ATP-sensitive K(+) channels. FEBS Lett. 532:177-82.

Xiao, J., Zhen, X. G., and Yang, J. (2003). Localization of PIP2 activation gate in inward rectifier K+ channels. Nat Neurosci 6, 811-818.

Xie, L.H., M. Horie, and M. Takano. (1999). Phospholipase C-linked receptors regulate the ATP-sensitive potassium channel by means of phosphatidylinositol 4,5-bisphosphate metabolism. Proc Natl Acad Sci U S A. 96:15292-7.

Yamada, K., Ji, J. J., Yuan, H., Miki, T., Sato, S., Horimoto, N., Shimizu, T., Seino, S., and Inagaki, N. (2001). Protective role of ATP-sensitive potassium channels in hypoxia-induced generalized seizure. Science 292, 1543-1546.

Yamada, M., Ishii, M., Hibino, H., and Kurachi, Y. (2004). Mutation in nucleotide-binding domains of sulfonylurea receptor 2 evokes Na-ATP-dependent activation of ATP-sensitive K+ channels: implication for dimerization of

nucleotide-binding domains to induce channel opening. Mol Pharmacol 66, 807-816.

Yan, F., C. W. Lin, et al. (2004). Sulfonylureas correct trafficking defects of ATP-sensitive potassium channels caused by mutations in the sulfonylurea receptor. J Biol Chem 279(12): 11096-105.

Yan, F. F., C. W. Lin, et al. (2005). Role of ubiquitin-proteasome degradation pathway in biogenesis efficiency of {beta}-cell ATP-sensitive potassium channels. Am J Physiol Cell Physiol 289(5): C1351-9.

Yang, J., M. Yu, Y.N. Jan, and L.Y. Jan. (1997). Stabilization of ion selectivity filter by pore loop ion pairs in an inwardly rectifying potassium channel. Proc Natl Acad Sci U S A. 94:1568-72.

Yi, B. A., Lin, Y. F., Jan, Y. N., and Jan, L. Y. (2001). Yeast screen for constitutively active mutant G protein-activated potassium channels. Neuron 29, 657-667.

Yang, K., K. Fang, et al. (2005). Low temperature completely rescues the function of two misfolded K ATP channel disease-mutants. FEBS Lett 579(19): 4113-8.

Yuan, Y. R., Blecker, S., Martsinkevich, O., Millen, L., Thomas, P. J., and Hunt, J. F. (2001). The crystal structure of the MJ0796 ATP-binding cassette. Implications for the structural consequences of ATP hydrolysis in the active site of an ABC transporter. J Biol Chem 276, 32313-32321.

Zerangue, N., B. Schwappach, Y.N. Jan, and L.Y. Jan. (1999). A new ER trafficking signal regulates the subunit stoichiometry of plasma membrane K(ATP) channels. Neuron. 22:537-48.

Zerangue, N., and Jan, L. Y. (1998). G-protein signaling: fine-tuning signaling kinetics. Curr Biol 8, R313-316.

Zerangue, N., M. J. Malan, et al. (2001). Analysis of endoplasmic reticulum trafficking signals by combinatorial screening in mammalian cells. Proc Natl Acad Sci U S A 98(5): 2431-6.

Zingman, L. V., A. E. Alekseev, et al. (2001). Signaling in channel/enzyme multimers: ATPase transitions in SUR module gate ATP-sensitive K+ conductance. Neuron 31(2): 233-45.

Zhang, H., C. He, X. Yan, T. Mirshahi, and D.E. Logothetis. (1999). Activation of inwardly rectifying K+ channels by distinct PtdIns(4,5)P2 interactions. Nat Cell Biol. 1:183-8.

Zung, A., B. Glaser, et al. (2004). Glibenclamide treatment in permanent neonatal diabetes mellitus due to an activating mutation in Kir6.2. J Clin Endocrinol Metab 89(11): 5504-7.